

Fluid Dynamics and Viscosity in Strongly Correlated Fluids

THOMAS SCHÄFER

Department of Physics, North Carolina State University, Raleigh, NC 27695

Key Words Non-equilibrium physics, kinetic theory, effective field theory, holographic duality, heavy ion physics, quantum fluids.

Abstract We review the modern view of fluid dynamics as an effective low energy, long wavelength theory of many body systems at finite temperature. We introduce the concept of a nearly perfect fluid, defined by a ratio η/s of shear viscosity to entropy density of order \hbar/k_B or less. Nearly perfect fluids exhibit hydrodynamic behavior at all distances down to the microscopic length scale of the fluid. We summarize arguments that suggest that there is fundamental limit to fluidity, and we review the current experimental situation of measurements of η/s in strongly coupled quantum fluids.

CONTENTS

Fluid Dynamics	3
<i>Fluid Dynamics as an effective theory</i>	3
<i>Microscopic models of fluids: Kinetic Theory</i>	6
<i>Matching and Kubo relations</i>	8
<i>Microscopic models of fluids: Holography</i>	9
<i>Viscosity bounds</i>	11
Non-relativistic Fluids	13
<i>The unitary Fermi gas</i>	13
<i>Flow and viscosity</i>	14
Relativistic Fluids	16
<i>The quark gluon plasma</i>	16
<i>Flow, higher moments of flow, and viscosity</i>	18
Frontiers	22
<i>Transport coefficients</i>	22
<i>Quasi-particles</i>	22
<i>Viscosity bound</i>	23
<i>Other strongly correlated fluids</i>	23
<i>Equilibration at strong and weak coupling</i>	23
<i>Anomalous hydrodynamics</i>	23

Endnotes: Fluid Dynamics	24
<i>Hydrodynamic variables</i>	24
<i>Mass current, momentum density, and relativistic fluids</i>	24
<i>Second order fluid dynamics</i>	25
<i>Second order relativistic fluid dynamics</i>	26
<i>Hydrodynamics as an effective field theory</i>	27
<i>Conserved charges in kinetic theory</i>	28
<i>Linearized collision operator</i>	28
<i>Knudsen expansion</i>	30
<i>Linear response and general covariance</i>	31
<i>Fluctuations and the “breakdown” of second order fluid dynamics</i>	32
<i>Strong coupling results</i>	34
<i>Spectral function and quasi-normal modes</i>	36
<i>Dimensionless ratios: η/s or η/n?</i>	39
Endnotes: Nonrelativistic fluids	40
<i>Transport properties of the dilute Fermi gas</i>	40
<i>Spectral function at unitarity</i>	42
<i>Nonrelativistic AdS/CFT correspondence</i>	43
<i>Nonrelativistic scaling flows</i>	44
<i>Corona and ballistic limit</i>	46
<i>Transient fluid dynamics and the kinetic limit</i>	48
Endnotes: Relativistic fluids	49
<i>Transport properties of the quark gluon plasma</i>	49
<i>Scaling flows, from Bjorken to Gubser</i>	50
<i>From kinetics to hydrodynamics in relativistic heavy ion collisions</i>	51
<i>Knudsen number scaling</i>	52
<i>Sensitivity to the relaxation time</i>	53
Endnotes: Frontiers	54
<i>The role of the AdS/CFT correspondence</i>	54
<i>Puzzles and challenges</i>	55

παντα ρει (everything flows)

Heraclitus

The mountains flowed before the Lord.

Prophet Deborah, Judges, 5:5

1 Fluid Dynamics

1.1 Fluid Dynamics as an effective theory

Fluid dynamics is often described as a consequence of applying Newton's laws to a continuous deformable medium. However, the ideas underlying fluid dynamics are much more general. Fluid dynamics describes classical and quantum liquids, gases, and plasmas. It accounts for the low energy properties of magnetic materials, liquid crystals, crystalline solids, supersolids, and many other systems. Indeed, fluid dynamics is now understood as an effective theory for the long-distance, long-time properties of any material [1, 2]. The only requirement for the applicability of fluid dynamics is that the system relaxes to approximate local thermodynamic equilibrium on the time scale of the observation. This idea is captured by the two quotations above: In principle everything behaves as a fluid, but in some systems observing fluid dynamic behavior may require divine patience [3].

Fluid dynamics is based on the observation that there are two basic time scales associated with the behavior of a many body system. The first is a microscopic time scale τ_{fluid} that characterizes the rate at which a generic disturbance relaxes. In a typical molecular liquid this rate is governed by the collision rate between molecules. The second time scale τ_{diff} is associated with the relaxation of conserved charges¹. Because conserved charges cannot relax locally, but rather have to decay by diffusion or collective motion, this time increases with the length scale λ of the disturbance, $\tau_{diff} \sim \lambda$. Fluid dynamics is based on the separation of scales $\tau_{fluid} \ll \tau_{diff}$, and $\omega_{fluid} = \tau_{fluid}^{-1}$ can be viewed as the breakdown scale of fluid dynamics as an effective theory.

In a simple non-relativistic fluid the conserved charges are the mass density ρ , the momentum density $\vec{\pi}$, and the energy density \mathcal{E} . The momentum density can be used to define the fluid velocity, $\vec{u} = \vec{\pi}/\rho$. By Galilean invariance the energy density can then be written as the the sum of the internal energy density and kinetic energy density, $\mathcal{E} = \mathcal{E}_0 + \frac{1}{2}\rho u^2$. The conservation laws are²

$$\frac{\partial \rho}{\partial t} = -\vec{\nabla} \cdot \vec{\pi}, \quad (1)$$

$$\frac{\partial \pi_i}{\partial t} = -\nabla_j \Pi_{ij}, \quad (2)$$

$$\frac{\partial \mathcal{E}}{\partial t} = -\vec{\nabla} \cdot \vec{j}^\epsilon. \quad (3)$$

For these equations to close we have to specify constitutive relations for the stress tensor Π_{ij} and the energy current \vec{j}^ϵ . Since fluid dynamics is an effective long wavelength theory we expect that the currents can be systematically expanded in gradients of the hydrodynamic variables ρ , \vec{u} and \mathcal{E}_0 . In the case of the stress tensor the leading, no-derivative, terms are completely fixed by rotational symmetry and Galilean invariance. We have

$$\Pi_{ij} = \rho u_i u_j + P \delta_{ij} + \delta \Pi_{ij}, \quad (4)$$

where $P = P(\rho, \mathcal{E}_0)$ is the equation of state and $\delta\Pi_{ij}$ contains gradient terms. The approximation $\delta\Pi_{ij} = 0$ is known as ideal fluid dynamics. Ideal fluid dynamics is time reversal invariant and the entropy is conserved. If gradient terms are included then time reversal invariance is broken and the entropy increases. We will refer to $\delta\Pi_{ij}$ as the dissipative stresses. At first order in the gradient expansion $\delta\Pi_{ij}$ can be written as $\delta\Pi_{ij} = -\eta\sigma_{ij} - \zeta\delta_{ij}\langle\sigma\rangle$ with

$$\sigma_{ij} = \nabla_i u_j + \nabla_j u_i - \frac{2}{3}\delta_{ij}\langle\sigma\rangle, \quad \langle\sigma\rangle = \vec{\nabla} \cdot \vec{u}. \quad (5)$$

This expression contains two transport coefficients, the shear viscosity η and the bulk viscosity ζ . The energy current is given by $\vec{j}^\epsilon = \vec{u}w + \delta\vec{j}^\epsilon$, where $w = P + \mathcal{E}$ is the enthalpy. At leading order in the gradient expansion $\delta j_i^\epsilon = u_j \delta\Pi_{ij} - \kappa \nabla_i T$, where κ is the thermal conductivity. The second law of thermodynamics implies that η, ζ and κ must be positive.

We can now establish the expansion parameter that controls the fluid dynamic description. We first note that the ideal stress tensor contains two terms, which are related to the pressure P and the inertial stress $\rho u_i u_j$. The relative importance of these two terms is governed by the Mach number $Ma = v/c_s$, where $c_s^2 = (\partial P)/(\partial \rho)_{\bar{s}}$ is the speed of sound and $\bar{s} = s/n$ is the entropy per particle. Flows with $Ma \sim 1$ are termed compressible, and flows with $Ma \ll 1$ incompressible. We are most interested in expanding systems, which are certainly compressible.

The validity of hydrodynamics requires that dissipative terms are small relative to ideal terms. We will focus on the role of shear viscosity, because it is the dominant source of dissipation in the systems considered here, and because both ζ and κ can become zero in physically realizable limits. In particular, ζ vanishes in a scale invariant fluid like the unitary gas, and κ vanishes in a relativistic fluid with zero baryon chemical potential like the pure gluon plasma. In the case $Ma \sim 1$ the expansion parameter is

$$Re^{-1} = \frac{\eta \nabla u}{\rho u^2} = \frac{\eta}{\rho u L}, \quad (6)$$

where Re is the Reynolds number and L is a characteristic length scale of the flow. Before continuing we briefly comment on incompressible flows. The expansion parameter in this case is Ma^2/Re . Flows with $Ma \ll 1$ and $Re^{-1} \ll 1$ are nearly ideal, turbulent flows. The regime $Ma^2/Re \ll 1$ but $Re^{-1} \gtrsim 1$ is that of very viscous flow. Today interest in very viscous flow is often related to classical fluids in confined geometries. A typical example is the problem of bacterial swimming [4].

We note that Re^{-1} can be written as

$$Re^{-1} = \frac{\eta}{\hbar n} \times \frac{\hbar}{m u L}, \quad (7)$$

where both factors are dimensionless. The first factor is solely a property of the fluid, and the second factor characterizes the flow. For a typical classical flow the second factor is much smaller than one, and the validity of fluid dynamics places no constraints on $\eta/(\hbar n)$. For the types of experiments that are explored in Sects. 2 and 3 the second factor is of order one, and the applicability of fluid dynamics requires $\eta \lesssim \hbar n$. We note that in relativistic flows the inertial term is $\Pi_{ij} = s T u_i u_j$, and the analogous requirement is $\eta \lesssim \hbar s/k_B$. We refer to fluids that satisfy this condition as nearly perfect fluids [5, 6, 7, 8], and show that nearly perfect fluids exhibit hydrodynamic behavior on remarkably short length and time scales, comparable to microscopic scales such as the inverse

temperature or the inverse Fermi wave vector. Throughout this review, we use units in which $\hbar = k_B = 1$.

The long wavelength expansion can be extended beyond the first order in gradients of the hydrodynamic variables^{3,4}. The classical higher order equations are known as Burnett and super-Burnett equations [9,10]. Explicit forms of second order terms based on kinetic theory were derived by Grad in the non-relativistic case [11], and by Israel, Stewart and others for relativistic fluids [12]. Historically, these theories have not been used very frequently. One reason is that the effects are not very large. In the case of the Navier-Stokes equation dissipative terms can exponentiate and alter the motion qualitatively, even if at any given time gradient corrections are small. A simple example is a collective oscillation of a fluid, see Sect. 2.2. Without viscosity the mode cannot decay, but if dissipation is present the motion is exponentially damped. Typically, second order terms do not exponentiate, and the gain in accuracy from including higher order terms is frequently offset by uncertainties in higher order transport coefficients or the need for additional boundary conditions.

The second reason that higher order theories are infrequently used is that the classical equations at second order are unstable to short-wavelength perturbations. In relativistic fluid dynamics problems with acausality and instability already appear at the Navier-Stokes level. These difficulties are not fundamental: Fluid dynamics is an effective theory, and unstable or acausal modes occur outside the domain of validity of the theory. It is nevertheless desirable to construct schemes that have second or higher order accuracy and satisfy causality and stability requirements. A possible solution is to promote the dissipative currents to hydrodynamic variables and postulate a set of relaxation equations for these quantities. Consider the dissipative stress tensor and define $\pi_{ij} = \delta\Pi_{ij}$. The relaxation equation for π_{ij} is

$$\tau_R \dot{\pi}_{ij} = -\pi_{ij} - \eta\sigma_{ij} + \dots, \quad (8)$$

where \dots contains second order terms such as $(\nabla \cdot u)\sigma_{ij}$ and $\sigma_{ik}\sigma_{kj}$. To second order accuracy this equation is equivalent to $\delta\Pi_{ij} = -\eta\sigma_{ij} + \tau_R\eta\dot{\sigma}_{ij} + \dots$, which is part of the standard Burnett theory. Physically, equ. (8) describes the relaxation of the dissipative stresses to the Navier-Stokes form. The resulting equations are stable and causal, and the sensitivity to higher order gradients can be checked by varying second order coefficients like τ_R [13].

Equ. (8) was first proposed by Maxwell as a model for very viscous fluids [14]. Cattaneo observed that relaxation equations can be used to restore causality and studied a relaxation model in the context of Fourier's law $\delta\vec{j}^\epsilon = -\kappa\vec{\nabla}T$ [15, 16]. Relaxation equations were derived from kinetic theory by Müller [17], Israel and Stewart [18], and others. To achieve the expected scaling of second order terms with Re^{-2} it is important to include a full set of second order terms that respect the symmetries of the theory. This problem was addressed for relativistic scale invariant fluids by Baier et al. [19], and in the non-relativistic case by Chao et al. [20].

It is well known that the low energy expansion in effective field theories⁵ is not a simple power series in the expansion parameter ω/Λ . Quantum fluctuations lead to non-analytic terms. In the case of fluid dynamics $\Lambda = \omega_{fluid}$ and non-analyticities arise due to thermal fluctuations of the hydrodynamic variables. As a consequence the dissipative currents $\delta\Pi_{ij}$ and $\delta\vec{j}^\epsilon$ contain not only gradient terms but also stochastic contributions. The magnitude of the stochastic terms is

determined by fluctuation-dissipation theorems. We have

$$\langle \Pi_{ij}(t, \vec{x}) \Pi_{kl}(t', \vec{x}') \rangle = 2\eta T \left(\delta_{ik} \delta_{jl} + \delta_{il} \delta_{jk} - \frac{2}{3} \delta_{ij} \delta_{kl} \right) \delta(t - t') \delta(\vec{x} - \vec{x}'), \quad (9)$$

$$\langle j_i^\epsilon(t, \vec{x}) j_j^\epsilon(t', \vec{x}') \rangle = 2\kappa T^2 \delta_{ij} \delta(t - t') \delta(\vec{x} - \vec{x}'), \quad (10)$$

where $\langle \cdot \rangle$ denotes a thermal average and we have neglected bulk viscosity. A calculation of the response function in stochastic fluid dynamics shows that the hydrodynamic expansion contains non-analyticities that are smaller than the Navier-Stokes term, but larger than second order terms [21, 22]. This implies that, strictly speaking, the second order theory is only consistent if stochastic terms are included. Some studies of fluctuating fluid dynamics have been performed [23], but in particle and nuclear physics this problem has only recently attracted interest [24].

1.2 Microscopic models of fluids: Kinetic Theory

Within fluid dynamics the equation of state and the transport coefficients are parameters that have to be extracted from experiment. If a more microscopic description of the fluid is available then we can compute these parameters in terms of more fundamental quantities. The simplest microscopic description of a fluid is kinetic theory. Kinetic theory is itself an effective theory that describes the long distance behavior of an underlying classical or quantum many-body system. It is applicable whenever there is a range of energies and momenta in which the excitations of the fluid are long-lived quasi-particles. Kinetic theory can be used to relate properties of these quasi-particles, their masses, lifetimes, and scattering cross sections, to the equation of state and the transport coefficients. Kinetic theory can also be used to extend the description of collective effects such as sound or macroscopic flow into the regime where fluid dynamics breaks down.

The basic object in kinetic theory is the quasi-particle distribution function $f_p(\vec{x}, t)$. Hydrodynamic variables can be written as integrals of f_p over $d\Gamma = d^3p/(2\pi)^3$. For example, the off-diagonal component of the stress tensor is given by

$$\Pi_{ij}(\vec{x}, t) = \int d\Gamma_p p_i v_j f_p(\vec{x}, t), \quad (i \neq j), \quad (11)$$

where $\vec{v} = \vec{\nabla}_p E_p$ is the quasi-particle velocity. Similar expressions exist for other conserved currents⁶. The equation of motion for $f_p(\vec{x}, t)$ is the Boltzmann equation

$$\left(\frac{\partial}{\partial t} + \vec{v} \cdot \vec{\nabla}_x + \vec{F} \cdot \vec{\nabla}_p \right) f_p(\vec{x}, t) = C[f_p], \quad (12)$$

where $\vec{F} = -\vec{\nabla}_x E_p$ is the force and $C[f_p]$ is the collision term. By taking moments of the Boltzmann equation we can derive the conservation laws (1-3). In order to extract the constitutive relations we have to assume that the distribution function is close to the equilibrium distribution $f_p(\vec{x}, t) = f_p^0(\vec{x}, t) + \delta f_p(\vec{x}, t)$, and that gradients of $f_p(\vec{x}, t)$ are small. The equilibrium distribution can be expressed in terms of the conserved charges or, more conveniently, in terms of the corresponding intensive quantities μ, T and \vec{u} . We find

$$f_p^0(\vec{x}, t) = \frac{1}{\exp[\beta(E_p - \vec{u} \cdot \vec{p} - \mu)] \pm 1}, \quad (13)$$

where $\beta = 1/T$, the \pm sign corresponds to fermions and bosons, respectively, and β, μ, \vec{u} are functions of \vec{x} and t .

To identify the expansion parameter we have to understand the scales involved in the collision term. If $\delta f_p \ll f_p^0$ we can use $C[f_p^0] = 0$ to linearize the collision term. The linearized collision term is a hermitean, negative semi-definite, operator that can be expanded in terms of its eigenvalues and eigenvectors⁷. We refer to the inverse eigenvalues as collision times. In order to solve the Boltzmann equation we have to invert the collision term. At long times we can therefore approximate the collision term by the longest collision time τ_0 and write

$$C[f_p^0 + \delta f_p] \simeq -\frac{\delta f_p}{\tau_0}, \quad (14)$$

where we have used the fact that at late times δf_p is dominated by its projection on the lowest eigenvector. Equ. (14) is known as the BGK (Bhatnagar-Gross-Krook) or relaxation time approximation [25]. We can define a mean free path by $l_{mfp} = \tau_0 \bar{v}$ where $\bar{v} = \langle v^2 \rangle^{1/2}$. The expansion parameter for the gradient expansion is given by the Knudsen number

$$Kn = \frac{l_{mfp}}{L} \quad (15)$$

where $L \sim \nabla^{-1}$ as in equ. (6). The systematic determination of the constitutive equation via an expansion in Kn is called the Chapman-Enskog expansion [26]. We find, for example,

$$\eta = \frac{1}{3} n l_{mfp} \bar{p}, \quad (16)$$

and $\tau_R = \tau_0 = \eta/P$ [26, 20]. In order to estimate the Reynolds number we can use $Ma = u/c_s \sim 1$. In kinetic theory we find $c_s^2 = \frac{5}{9} \langle v^2 \rangle$ and $Kn \sim Re^{-1}$. The Knudsen expansion is equivalent to the Reynolds number expansion in fluid dynamics⁸.

Fluid dynamics corresponds to the long time behavior of kinetic theory. It is also interesting to examine the short time behavior. Consider the response of the fluid to an external shear strain h_{xy} with frequency ω and wave number k . The solution of the Boltzmann equation is of the form

$$\delta f_p(\omega, k) = \frac{1}{2T} \frac{-i\omega p_x v_y}{-i\omega + i\vec{v} \cdot \vec{k} + \tau_0^{-1}} f_p^0 h_{xy}. \quad (17)$$

This result can be used to compute the spectral function of correlators of conserved currents. For $k = 0$ the term $(-i\omega + \tau_0^{-1})$ in the denominator of equ. (17) leads to a Lorentzian shape of the spectral function, which is a signature of the presence of quasi-particles. The spectral function also provides information about the breakdown of kinetic theory for large ω and k . There is no intrinsic scale in the Boltzmann equation other than the collision time τ_0 which sets the scale for the hydrodynamic expansion. The high energy scale is set by matching the Boltzmann equation to the equation of motion for a non-equilibrium Green function in quantum field theory [27]. Instead of matching these equations explicitly, we can compare the kinetic spectral functions in equ. (17) to the spectral functions in quantum field theory, see Sect. 2.1. The result shows that the breakdown scale is $\omega_{micro} \sim T$. This scale should be compared to the hydrodynamic scale $\omega_{fluid} \sim \tau_0^{-1} \sim P/\eta$. For a typical fluid these scales are well separated, but for a nearly perfect fluid the two scales are comparable. At least parametrically, in a nearly perfect fluid there is no room for kinetic theory, that means there is no regime in which kinetic theory is more accurate than fluid dynamics.

The collision term is determined by the quasi-particle cross section σ , and a rough estimate of the mean free path is given by $l_{mfp} = 1/(n\sigma)$. Using equ. (16) we find $\eta \sim \bar{p}/\sigma$. This result has two interesting consequences:

1. The viscosity of a dilute gas is independent of its density. The physical reason for this behavior is that viscosity is determined by the rate of momentum diffusion. The number of particles is proportional to n , but the mean free path scales as $1/n$. As a result, the diffusion rate is constant. Maxwell was so surprised by this result that he tested it by measuring the damping rate of a torsion pendulum in a sealed container as a function of the air pressure [28, 29]. He confirmed that η is not a function of P at fixed T . Of course, if the air is very dilute then $l_{mfp} > L$ and the hydrodynamic description breaks down. In this limit, known as the Knudsen regime, damping is proportional to pressure.
2. The result $\eta \sim 1/\sigma$ also implies that viscosity of a weakly coupled gas is very large. This is counter-intuitive because we think of viscosity as friction between fluid layers. Consider a fluid sheared between two parallel plates in the xz plane. The force per unit area is

$$\frac{F}{A} = \eta \nabla_y u_x. \quad (18)$$

We naively expect this force to grow with the strength of the interaction. Our intuition is shaped by very viscous fluids, for which viscosity is indeed determined by force chains and solid friction. This expectation is not entirely inappropriate, because the word viscosity is derived from the Latin word for mistletoe, *viscum album*.

1.3 Matching and Kubo relations

In the case of kinetic theory we can derive the equations of fluid dynamics from the underlying microscopic theory. In more complicated cases, for example if the short distance description is a strongly coupled field theory, this may not be possible. In that case we can rely on the fact that fluid dynamics is a general long distance effective theory, and compute the transport coefficients based on the idea of matching. Matching expresses the requirement that in the regime of validity of the effective theory, correlation functions must agree with correlators in the microscopic theory. Consider the retarded correlation function of the stress tensor

$$G_R^{xyxy}(\omega, \mathbf{k}) = -i \int dt \int d^3x e^{i\omega t - i\vec{k}\cdot\vec{x}} \Theta(t) \langle [\Pi^{xy}(t, \vec{x}), \Pi^{xy}(0, 0)] \rangle. \quad (19)$$

In linear response theory this function controls the stress induced by an external strain. In fluid dynamics $\Pi_{xy} \simeq \rho u_x u_y$ and we can compute the correlation function from linearized hydrodynamics and fluctuation relations. We find⁹

$$G_R^{xyxy}(\omega, k) = P - i\eta\omega + \tau_R\eta\omega^2 - \frac{\kappa_R}{2}k^2 + O(\omega^3, \omega k^2), \quad (20)$$

where τ_R is the relaxation time defined in equ. (8) and κ_R is another second order transport coefficient [22]. Equ. (20) implies the Kubo relation

$$\eta = - \lim_{\omega \rightarrow 0} \lim_{k \rightarrow 0} \frac{d}{d\omega} \text{Im} G_R^{xyxy}(\omega, \vec{k}). \quad (21)$$

This equation can be applied to field theory, on the basis of equ. (19) and the microscopic definition of the stress tensor. This method is used to compute transport coefficients on the lattice, in both relativistic and non-relativistic field theories [30, 31, 32, 33, 34, 35]. The difficulty with using Kubo's formula is that imaginary time Monte Carlo simulations do not provide direct access to correlation functions for real frequencies. Measuring the shear viscosity requires analytic continuation of imaginary time data, which leads to uncertainties that are difficult to quantify. We note that some transport coefficients, like the parameter κ_R in equ. (20) can be measured directly from imaginary time data.

Equation (20) confirms that the expansion parameter of the hydrodynamic expansion is ω/ω_{fluid} with $\omega_{fluid} \simeq P/\eta \simeq \tau_R^{-1}$. Note that fluctuations introduce non-analytic¹⁰ terms at order $\omega^{3/2}$ [21, 22]. This is a breakdown of the gradient expansion, but not a breakdown of hydrodynamics. For example, at second order in the low energy expansion the $\omega^{3/2}$ term is completely determined by η and P , and the relaxation time τ_R can be extracted by matching $G_R(\omega)$ to the low energy expansion in fluid dynamics.

1.4 Microscopic models of fluids: Holography

Kinetic theory provides explicit theoretical realizations of weakly coupled fluids. Holographic dualities and the AdS/CFT correspondence have led to controlled realizations of strongly coupled fluids. The basic idea originated from the study of black holes. It had been known for some time that black holes have entropy, and that the process of a perturbed black hole settling down to a stationary configuration bears some resemblance to dissipative relaxation in fluids. Indeed, it was shown that one can assign a shear viscosity and electric conductivity to the “stretched horizon”, an imaginary surface that hovers just above the event horizon [36].

These ideas were made precise in the context of the AdS/CFT correspondence [37], see the reviews [38, 39, 40, 41]. In the simplest case one considers a Schwarzschild black hole embedded in five dimensional Anti-de-Sitter (AdS₅) space. The full spacetime has additional compact dimensions, which are required by string theory but play no role in our discussion. Black holes in AdS₅ do not evaporate and the black hole is in thermal equilibrium. This means that the rate of Hawking radiation balances the amount of energy falling back into the black hole. Based on its causal structure we can view AdS₅ as having a “boundary” which is four-dimensional Minkowski space. Matter on the boundary is in thermal equilibrium with the black hole spacetime.

The AdS/CFT correspondence asserts that the boundary is described by an ordinary quantum field theory, and that the correlation functions of this field theory have a dual description in terms of boundary correlation functions of a gravitational theory in the bulk. The correspondence is simplest if the boundary theory is strongly coupled and contains a large number N of degrees of freedom. In this case the bulk theory is simply classical Einstein gravity. The partition function of the boundary quantum field theory (QFT) is

$$Z_{QFT}[J_i] = \exp(-S[\phi_i|_{\partial M} = J_i]) , \quad (22)$$

where J_i is a set of sources in the field theory, S is the gravitational action, ϕ_i is a dual set of fields in the gravitational theory, and ∂M is the boundary of AdS_5 . The fields ϕ_i satisfy classical equations of motions subject to boundary conditions on ∂M .

The original construction involves a black hole in AdS₅ and is dual to a relativistic fluid governed by a generalization of QCD known as $\mathcal{N} = 4$ super Yang-Mills theory. This theory is considered in the limit of a large number of colors N_c . The gravitational theory is Einstein gravity with additional matter fields that are not relevant here. The AdS₅ black hole metric is

$$ds^2 = \frac{(\pi TR)^2}{u} (-f(u)dt^2 + d\vec{x}^2) + \frac{R^2}{4u^2 f(u)} du^2, \quad (23)$$

where \vec{x}, t are Minkowski space coordinates, and u is a “radial” coordinate where $u = 1$ is the location of the black hole horizon and $u = 0$ is the boundary. T is the temperature, R is the AdS radius, and $f(u) = 1 - u^2$. In the boundary theory the metric couples to the stress tensor $\Pi_{\mu\nu}$. Correlation functions of the stress tensor can be found by linearizing the bulk action around the AdS₅ solution, $g_{AB} = g_{AB}^0 + \delta g_{AB}$, where $A, B = 1, \dots, 5$. Small oscillations of the off-diagonal strain δg_x^y are particularly simple. We consider harmonic dependence on the Minkowski coordinates $\delta g_x^y = \phi_k(u) e^{ikx - i\omega t}$. Fluctuations are governed by the wave equation

$$\phi_k''(u) - \frac{1+u^2}{uf(u)} \phi_k'(u) + \frac{\omega^2 - k^2 f(u)}{(2\pi T)^2 u f(u)^2} \phi_k(u) = 0. \quad (24)$$

This differential equation has two linearly independent solutions. The retarded correlation function corresponds to picking a solution that is purely infalling at the horizon [38]. For small (or very large) ω, k this solution can be found analytically [42, 43]. $G_R(\omega, k)$ is computed by inserting the solution into the Einstein-Hilbert action, and then computing the variation with respect to the boundary value of δg_x^y . The result¹¹ is of the form given in equ. (20) with [44, 19]

$$P = \frac{sT}{4}, \quad \eta = \frac{s}{4\pi}, \quad \tau_R = \frac{2 - \log(2)}{2\pi T}. \quad (25)$$

Note that in the case of a relativistic fluid η is naturally expressed in units of the entropy density s , not the density n . This is because a relativistic fluid need not have a conserved particle number. As a rough comparison we can use the fact that for a weakly interacting relativistic gas $s/n = 3.6$. We observe that the AdS/CFT correspondence describes a very good fluid. In particular, $\eta/s < 1$ and $\tau_R \sim T^{-1}$. This is a remarkable result because the AdS/CFT correspondence has provided the first reliable theoretical description of a nearly perfect fluid.

There are many aspects of the strongly coupled fluid that can be studied using AdS/CFT:

1. The spectral function¹² $\eta(\omega) = -\frac{1}{\omega} \text{Im} G_R(\omega)$ does not show evidence for quasi-particles [43, 45]. Instead of a Lorentzian of width $1/\tau_R$ one finds a smooth function that interpolates between the hydrodynamic limit $\eta(0) = \eta$ and the high frequency limit $\eta(\omega) \sim \omega^3$. Because of non-renormalization theorems, the $\omega \rightarrow \infty$ limit is given by the correlation function in free field theory.
2. The relaxation time can be written as $\tau_R = c\eta/P$ with $c = (2 - \log(2))/2 \simeq 0.65$. This value can be compared to the Israel-Stewart result $\tau_R = 1.5\eta/P$. We observe that the relaxation time is very short, but in units of η/P it is only a factor of 2.3 smaller than kinetic theory would predict. The AdS/CFT correspondence has also been used to compute other second order transport coefficients [19].
3. The validity of the hydrodynamic expansion is controlled by the location of the poles of $G_R(\omega)$ in the complex ω plane. The hydrodynamic pole of the shear correlator is located

at $\omega \simeq iD_\eta k^2$, where $D_\eta = \eta/(sT)$ is the momentum diffusion constant. Non-hydrodynamic poles correspond to so-called quasi-normal modes of the linearized Einstein equations. These quasi-normal modes come in complex conjugate pairs and are located at a minimum distance of order T from the real axis [46]. This observation confirms that the expansion parameter in a nearly perfect fluid is ω/T .

4. Using the AdS/CFT correspondence one can study the approach to equilibrium in great detail. For initial conditions that lead to Bjorken flows the approach to hydrodynamics is very rapid. After the quasi-normal modes are damped, on time scales on the order of $(\tau T) \lesssim 1$, the Navier-Stokes description is very accurate, even though non-equilibrium contributions to the pressure can be large [47, 48]. This phenomenon is sometimes referred to as rapid “hydrodynamization”.
5. Heller et al. studied the large order behavior of the hydrodynamic expansion for a Bjorken-like flow. They found that the gradient expansion is an asymptotic series, and that the radius of convergence is zero [49]. The coefficients of high order terms, and the leading singularity in the Borel plane, are governed by the lowest quasi-normal mode. We note that this phenomenon is unrelated to the non-analytic terms in the expansion mentioned above. The calculation is performed in the large N_c limit of the field theory, so non-analytic terms in the gradient expansion are suppressed [50]. Heller et al. speculate that the large order behavior is analogous to the factorial divergence of large orders of perturbation theory in quantum field theory.

Finally, we note that one can directly derive the equation of fluid dynamics by promoting the parameters that label the near horizon metric to hydrodynamic variables [51]. Solving the resulting Einstein equations order-by-order in gradients provides an alternative derivation of the second order transport coefficients discussed above. This method provides a general connection between solutions of the Einstein equation and the Navier-Stokes equation, referred to as the fluid-gravity correspondence [52].

1.5 Viscosity bounds

The AdS/CFT correspondence provides an explicit, albeit somewhat theoretical, example of a nearly perfect fluid, leading to two questions: Can nearly perfect fluids be realized in the laboratory, and is there a fundamental limit to fluidity? We address the first question in Sects. 2 and 3 below. There are several arguments that the answer to the second question is affirmative. We summarize these arguments here:

Uncertainty relation [5]: Kinetic theory predicts that $\eta = \frac{1}{3}nl_{mpf}\bar{p}$, and that low viscosity corresponds to a short mean free path. However, the uncertainty relation suggests that the product of the mean free path and the mean momentum cannot become arbitrarily small. Using $l_{mpf}\bar{p} \gtrsim 1$ implies $\eta/n \gtrsim 1/3$. This argument was originally presented in the context of relativistic fluids. In these systems the inverse Reynolds number is given by $\eta/(s\tau T)$. Using the entropy per particle of a weakly interacting relativistic Bose gas, $s/n = 3.6$, we get $\eta/s \gtrsim 0.09$.

There are several issues with this argument. First, it is based on the application of kinetic theory in a regime where there are no well-defined quasi-particles and the theory is not applicable. Second, there is no obvious reason that the entropy per particle cannot be much larger than the free-gas

value¹³ [53]. Finally, a bound on transport coefficients related to the uncertainty relation was first proposed by Mott in connection with electric conductivity [54]. A minimal conductivity implies that the metal-insulator transition must be continuous. However, this prediction is known to be false. Continuous metal-insulator transitions have been observed [55], and the physical mechanism of these transitions can be understood in terms of Anderson localization.

Holographic dualities [6]: The value $\eta/s = 1/(4\pi)$ is obtained in the strong coupling limit of a large class of holographic theories. These theories are characterized by the fact that the dual gravitational description involves the Einstein-Hilbert action [56,38,57]. Kovtun, Son, and Starinets (KSS) conjectured that the strong coupling result is an absolute lower bound for the ratio η/s in all fluids,

$$\frac{\eta}{s} \geq \frac{1}{4\pi} \quad (26)$$

This idea is a significant step forward compared to the argument based on the uncertainty relation. The value $1/(4\pi)$ is the result of a reliable calculation. Holographic dualities explain why the relevant quantity is η/s , and they account for the difference between momentum and charge diffusion. The diffusion constant goes to zero in the strong coupling limit [58,59,60], whereas the ratio η/s remains finite.

However, holographic theories exist that provide counterexamples to the KSS conjecture [61,62]. Finite coupling corrections increase the ratio η/s , but there are cases in which calculable finite N_c corrections lower η/s . In terms of the dual description these theories correspond to gravitational theories that contain a certain higher derivative correction to the Einstein-Hilbert action known as the Gauss-Bonnet term [63]. Although this result rules out the KSS conjecture, there are compelling arguments for a weaker version of the viscosity bound. Given that the violation of the KSS bound can be related to the Gauss-Bonnet term one has to study constraints on the Gauss-Bonnet coefficient λ_{GB} . It was found that large values of λ_{GB} lead to violations of causality. For the class of theories that are known to violate the KSS bound causality implies the slightly weaker bound $\eta/s \geq \frac{16}{25} \frac{1}{4\pi}$ [64]. It seems likely that this is not the final word from holographic dualities. Generalizations of Gauss-Bonnet gravity, so-called Lovelock theories, have been studied [65], and lower values of η/s may be possible.

Fluctuations [21,22]: Shear viscosity is related to momentum diffusion, and $\eta/s = 0$ would imply that mean free path for momentum transport is zero. However, in fluid dynamics momentum can also be carried by collective modes such as sound and shear waves. Indeed, if the viscosity is small this process becomes more efficient because the damping rate of sound and shear modes is small. This observation suggests that the physical viscosity of the fluid cannot be zero.

This argument can be made more precise using the low energy expansion of hydrodynamic correlation functions. Fluctuations not only contribute to non-analytic terms in $G_R(\omega)$, but they also correct the polynomial terms that determine the transport coefficients. The retarded shear stress correlator in a relativistic fluid is of the form $G_R(\omega) = P + \delta P + i\omega(\eta + \delta\eta) + \dots$ where δP is a correction to the pressure and

$$\eta + \delta\eta = \eta + \frac{17}{120\pi^2} \frac{\Lambda_K D_\eta s^2 T^3}{\eta^2}. \quad (27)$$

is the physical viscosity. Here, Λ_K is the breakdown momentum of the hydrodynamic description and $D_\eta = \eta/(sT)$ is the momentum diffusion constant. The gradient expansion requires $\Lambda_K D_\eta \lesssim 1$.

We observe that $\delta\eta \sim 1/\eta^2$, so the physical viscosity cannot become arbitrarily small. The bound for η/s depends on the equation of state. For a quark gluon plasma $\eta/s \gtrsim 0.1$ [21], and in a non-relativistic Fermi gas $\eta/s \gtrsim 0.2$ [22].

The bound is interesting, because it sheds some light on what is special about shear viscosity. The stress tensor is quadratic in the fluid velocity and has a leading order, non-linear coupling to shear waves. Other currents do not have non-linear mode couplings at leading order. The bound is not universal, but it is complementary to the holographic bounds in the sense that it only operates at finite N , whereas the holographic bounds are rigorous at infinite N .

It is difficult to summarize the situation regarding the proposed viscosity bounds. There is strong evidence that viscosity is different from other transport coefficients. We can find systems for which bulk viscosity, conductivity, or diffusion constants vanish, but there are physical effects, the universality of the graviton coupling in holographic theories, and the universality of the stress tensor in stochastic fluid dynamics, that make it difficult to find scenarios in which the shear viscosity vanishes. The precise value of the bound is not known, but empirically the value $\eta/s = 1/(4\pi)$ found in simple holographic theories is a good approximation for the viscosity of the best quantum fluids that can be studied in the laboratory as discussed further below.

2 Non-relativistic Fluids

2.1 The unitary Fermi gas

In the following two sections we describe theoretical and experimental results regarding the transport properties of the two best fluids that have been studied in the laboratory [7]. These two fluids are ultracold atomic Fermi gases magnetically tuned to a Feshbach resonance, and the quark gluon plasma produced in relativistic heavy ion collisions at the relativistic heavy ion collider (RHIC) in Brookhaven, New York, and the large hadron collider (LHC) at CERN in Geneva, Switzerland.

Ultracold Fermi gases are composed of atoms with half-integer total spin. Experiments focus on alkali atoms such as ${}^6\text{Li}$. These atoms can be confined in all-optical or magneto-optical traps. We concentrate on systems in which two hyperfine states are macroscopically occupied. Because the density and temperature are very low details of the atomic interaction and the atomic structure are not resolved, and the two hyperfine states can be described as the two components of a point-like non-relativistic spin 1/2 fermion. The fermions are governed by the effective Lagrangian

$$\mathcal{L} = \psi^\dagger \left(i\partial_0 + \frac{\vec{\nabla}^2}{2m} \right) \psi - \frac{C_0}{2} (\psi^\dagger \psi)^2. \quad (28)$$

The coupling constants C_0 is related to the s -wave scattering length a . At low temperature and density neither higher partial waves nor range corrections are important. The two-body s -wave scattering matrix is

$$\mathcal{M} = \frac{4\pi}{m} \frac{1}{1/a + iq}, \quad (29)$$

where q is the relative momentum. The precise relation between C_0 and a depends on the regularization scheme. In dimensional regularization $C_0 = 4\pi a/m$. In the limit of weak coupling this result follows from the Born approximation.

Of particular interest is the “unitarity” limit $a \rightarrow \infty$. In this limit the system has no dimensionful parameters and the theory is scale invariant [66]. The scattering amplitude behaves as $1/(iq)$, which saturates the s -wave unitarity bound. The two-body wave function scales as $1/r$ and the many body system is strongly correlated even if the density is low. Experimentally, the unitarity limit can be studied using magnetically tuned Feshbach resonances [67, 68].

We note that even at unitarity the dilute Fermi gas has well-defined quasi-particles if the temperature is large. The average scattering amplitude scales as $\sigma \sim \langle q^{-2} \rangle \sim \lambda_{dB}^2$, where $\lambda_{dB} \sim (mT)^{-1/2}$ is the thermal wave length. In the high temperature limit the average cross section is small, and the collisional width of a fermion quasi-particle is $\Gamma \sim zT$ [69], where $z = (n\lambda^3)/2 \ll 1$ is the fugacity. In this regime the shear viscosity can be computed using kinetic theory¹⁴. The result is [70, 71]

$$\eta = \frac{15}{32\sqrt{\pi}}(mT)^{3/2}. \quad (30)$$

As expected, the viscosity is independent of density and increases with temperature. The ratio η/n scales as $1/z$ and is parametrically large. We also find $\eta/s \sim 1/(z \log(1/z))$.

In the regime $z \gtrsim 1$ the unitary gas is strongly coupled. At $z \sim 12$ the system undergoes a phase transition to a superfluid [72]. In the superfluid phase the $U(1)$ symmetry of the effective Lagrangian equ. (28) is spontaneously broken, and at low temperature there is a well defined bosonic quasi-particle related to the $U(1)$ Goldstone mode. Momentum diffusion due to Goldstone modes can be studied using kinetic theory, and we find $\eta \sim T^{-5}$ [73]. Combined with equ. (30) this result indicates that the viscosity has a minimum in the vicinity of the critical temperature. In this regime there are no reliable calculations of transport properties, but T-matrix calculations suggest that η/n reaches a value of about 0.5 [74]. We note that at T_c the entropy per particle is very close to one. Lower values of the shear viscosity, $\eta/s \simeq 0.2$, have been found in quantum Monte Carlo calculations [35].

In kinetic theory the viscosity spectral function has a Lorentzian line shape with width $\tau_R^{-1} = P/\eta$ [75]. In the strongly coupled regime the shape of the spectral function is not known, but one can determine the asymptotic behavior¹⁵ for $\omega \rightarrow \infty$ as well as the frequency sum rule. The sum rule is given by [76, 74]

$$\frac{2}{\pi} \int d\omega \left[\eta(\omega) - \frac{\mathcal{C}}{15\pi\sqrt{m\omega}} \right] = \frac{2}{3} \mathcal{E}, \quad (31)$$

where \mathcal{C} is a short distance coefficient known as the contact density, which measures the strength of short range correlations [77], and the subtraction term inside the integral corresponds to the high frequency tail of the spectral function [78]. In the high temperature limit $\mathcal{C} = 4\pi n^2 \lambda_{dB}^2$, and one can check that the high frequency tail smoothly matches kinetic theory for $\omega \sim T$. We can now identify the relevant scales that limit the fluid dynamic and kinetic descriptions, $\omega_{fluid} \sim zT$ and $\omega_{micro} \sim T$. For $z \ll 1$ we find the expected hierarchy of scales, but in the strongly correlated regime both scales are comparable, and new theoretical methods are needed¹⁶.

2.2 Flow and viscosity

Fluid dynamics can be observed in experiments that involve releasing the gas from a deformed trap. In typical experiments the trap corresponds to a harmonic confinement potential $V = \frac{1}{2}m(\omega_{\perp}^2 x_{\perp}^2 + \omega_z^2 z^2)$ with an aspect ratio $\omega_{\perp}/\omega_z \sim (20 - 30)$. In hydrostatic equilibrium pressure gradients along

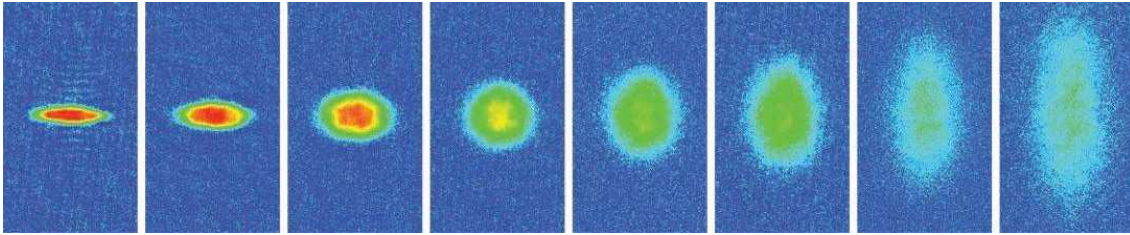


Figure 1: Expansion of a dilute Fermi gas at unitarity [79]. The cloud contains $N \simeq 1.5 \cdot 10^5$ ${}^6\text{Li}$ atoms at a temperature $T \simeq 8\mu\text{K}$. The figure shows a series of false color absorption images taken between $t = (0.1 - 2.0)$ ms. The scale of the images is the same. The axial size of the cloud remains nearly constant as the transverse size is increasing.

the transverse direction are much larger than pressure gradients along the longitudinal direction. Hydrodynamic evolution after the gas is released converts this difference into different expansion velocities, and during the late stages of the evolution the cloud is elongated along the transverse direction, see Fig. 1. The observation of this effect led to the discovery of nearly perfect fluidity in ultracold gases [79]. Shear viscosity counteracts the differential acceleration and leads to a less deformed final state. The shear viscosity can be measured by studying the time evolution of the cloud radii [80, 81].

An alternative approach is based on recapturing the gas after release from the trap, which excites a transverse breathing mode. Hydrodynamic behavior can be verified by measuring the frequency of the collective mode. In an ideal fluid $\omega = \sqrt{10/3}\omega_{\perp}$, whereas in a weakly collisional gas $\omega = 2\omega_{\perp}$ [82, 83]. The transition from ballistic behavior in the weak coupling limit to hydrodynamic behavior in the unitary gas has been observed experimentally [84, 85]. In the hydrodynamic regime damping of collective modes is governed by dissipative terms. The rate of energy dissipation is

$$\dot{E} = - \int d^3x \left\{ \frac{1}{2} \eta(x) (\sigma_{ij})^2 + \zeta(x) \langle \sigma \rangle^2 + \frac{\kappa(x)}{T} (\vec{\nabla} T)^2 \right\}. \quad (32)$$

At unitarity the system is scale invariant and the bulk viscosity is predicted to vanish [86, 66]. This prediction was experimentally verified in [87]. Thermal conductivity does not contribute to damping because the gas is isothermal. As a consequence the damping rate is a measure of shear viscosity.

Both the expansion and the collective mode experiments involve approximate scaling flows¹⁷. The motion is analogous to the Hubble flow in cosmology, and to the Bjorken expansion of a quark gluon plasma (QGP). Consider the Euler equation for the acceleration of an ideal fluid, $\vec{u} \simeq -\vec{\nabla} P/\rho = -\vec{\nabla} \mu/m$, where we have used the Gibbs-Duhem relation $dP = nd\mu$. Because the external potential is harmonic, the chemical potential is harmonic, too. As a consequence the velocity field is linear, and the cloud expands in a self-similar fashion. Because the fluid velocity is linear the shear stress σ_{ij} is spatially constant and the rate of dissipation is sensitive to the spatial integral of $\eta(x)$

$$\langle \eta \rangle = \int d^3x \eta(x). \quad (33)$$

Using measurements of the trap integrated entropy we can extract the ratio $\langle \eta \rangle / \langle s \rangle$. This analysis

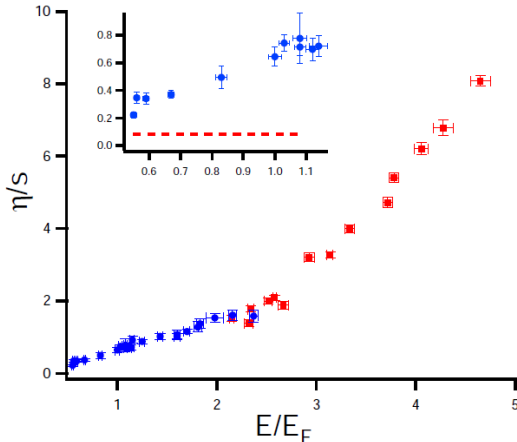


Figure 2: Measurements of η/s in the dilute Fermi gas at unitarity by use of collective modes (blue circles) and elliptic flow (red squares), from [81]. The data are shown as a function of the total energy of the clouds in units of E_F , the energy of a zero temperature Fermi gas with the same number of particles. At high temperature E/E_F is proportional to temperature. Note that η/s in the plot refers to a ratio of trap integrated quantities, $\langle\eta\rangle/\langle s\rangle$.

was originally performed in [88, 89]. A more recent analysis that combines collective mode data at low T with expansion data at high T is shown in Fig. 2 [81]. The high temperature data matches expectations from kinetic theory¹⁸. The viscosity drops with T and the ratio of trap averages reaches $\langle\eta\rangle/\langle s\rangle \lesssim 0.4$.

It is clearly desirable to unfold these measurements and determine local values of η/s . The main difficulty is a reliable treatment of the low density corona. In this regime η is independent of density and the integral in equ. (33) is ill defined, signaling the breakdown of fluid dynamics in the dilute region. The problem also appears if one applies the Navier-Stokes equation to an expanding gas cloud. In the dilute regime η is not a function of density and the viscous stresses $\eta\sigma_{ij}$ are independent of position, implying that although ideal stresses propagate with the speed of sound, viscous stresses propagate with infinite speed. As discussed in Sect. 1.1 this problem can be solved by including a finite relaxation time [90, 80]. In the low density regime the viscous relaxation time $\tau_R \simeq \eta/(nT)$ is large. Because the dissipative stresses are zero initially, taking a finite relaxation time into account suppresses the contribution of the corona¹⁹. A schematic version of this idea was used in Cao et al. [81], but a more systematic treatment is needed.

3 Relativistic Fluids

3.1 The quark gluon plasma

The QGP is a hot and dense systems of quarks and gluons governed by the QCD Lagrangian

$$\mathcal{L} = -\frac{1}{4}G_{\mu\nu}^a G_{\mu\nu}^a + \sum_f \bar{q}_f (i\gamma^\mu D_\mu - m_f) q_f, \quad (34)$$

where $G_{\mu\nu}^a = \partial_\mu A_\nu^a - \partial_\nu A_\mu^a + gf^{abc}A_\mu^b A_\nu^c$ is the QCD field strength tensor, g is the coupling constant and f^{abc} are the $SU(3)$ structure constants. The covariant derivative acting on the quark fields is $iD_\mu q = (i\partial_\mu + gA_\mu^a \frac{\lambda^a}{2})q$ and m_f is the quark mass. At the temperature scale probed in RHIC or LHC experiments the three light flavors, up, down, and strange, are thermally populated, whereas the heavy flavors, mainly charm and bottom, are produced in hard collisions and can serve as probes of the medium.

Asymptotic freedom implies that at very high temperature the QGP can be described in terms of quark and gluon quasi-particles. A typical gluon has a thermal momentum of order T . Soft gluons with momenta much lower than T are modified by the interaction with hard particles. As a consequence, electric gluons acquire a Debye screening mass $m_D \sim gT$. In perturbation theory there is no static screening of magnetic fields, but magnetic gluons are dynamically screened for momenta greater than $(m_D^2 \omega)^{1/3}$, where ω is the frequency. The static magnetic sector of QCD is non-perturbative even if the temperature is very large. Confinement in three-dimensional pure gauge theory generates a mass scale of order $g^2 T$. This mass scale determines the magnetic screening scale in the QGP, $m_M \sim g^2 T$.

Perturbation theory in the quark gluon plasma is based on the separation of scales $m_M \ll m_D \ll T$. Strict perturbation theory in g works only for very low values of the coupling constant, $g \lesssim 1$ [91]. However, quasi-particle models that rely on the separation of scales describe the thermodynamics of the plasma quite well, even for temperatures close to the phase transition to a hadronic gas [92].

The dispersion relation for the bosonic modes in the plasma evolves smoothly from quasi-gluons with masses $m \sim m_D$ at momenta $q \gtrsim gT$ to collective oscillations, plasmons, at low q . The energy of the plasmon in the limit $q \rightarrow 0$ is $\omega_P = m_D/\sqrt{3}$, and the plasmon width is $\Gamma \sim g^2 T$ [93]. The calculation of the collisional width of quasi-particles with momenta of order T is a complicated, non-perturbative problem, but the width remains parametrically small, $\Gamma \sim g^2 \log(1/g)T$ [94].

Momentum diffusion is controlled by binary scattering between quarks and gluons. The cross section is proportional to g^4 , and the IR divergence due to the exchange of massless gluons is regulated by dynamic screening. As a consequence the shear viscosity scales as $\eta \sim T^3/(g^4 \log(1/g))$. A detailed calculation²⁰ in $N_f = 3$ QCD gives [95, 96, 97]

$$\eta = \frac{kT^3}{g^4 \log(\mu^*/m_D)}, \quad (35)$$

where $k = 106.67$. The scale inside the logarithm is sensitive to bremsstrahlung processes such as $gg \rightarrow ggg$. Arnold et al. found $\mu^* = 2.96T$ [96, 97]. The time scale for momentum diffusion is $\eta/(sT) \sim 1/(g^4 \log(1/g)T)$. This scale is parametrically large, but the precise value is very sensitive to the coupling constant. In $N_f = 3$ QCD we get $\eta/s \simeq 9.2/(g^4 \log(1/g))$. Using $g \simeq 2$, which corresponds to $\alpha_s \simeq 0.3$, and $\log(1/g) \gtrsim 1$ we conclude that $\eta/s \lesssim 0.6$.

At $T \simeq 150$ MeV the quark gluon plasma undergoes a crossover transition to a hadronic resonance gas [98, 99]. The resonance gas is strongly coupled, but as the temperature is reduced further the system evolves to a weakly coupled gas of mostly pions, kaons, and nucleons. The viscosity of a pion gas is parametrically large, $\eta/s \sim (f_\pi/T)^4$, where $f_\pi \simeq 93$ MeV is the pion decay constant [100]. Similar to the arguments in the case of cold Fermi gases we therefore expect that η/s has a minimum in the vicinity of T_c . In this regime the only reliable theoretical approach is lattice gauge theory. As in the case of non-relativistic fermions the calculations are difficult because one has to

extract the viscosity spectral function from imaginary time data. In the case of pure gauge theory Meyer finds $\eta/s = 0.102(56)$ at $T = 1.24T_c$ and $\eta/s = 0.134(33)$ at $T = 1.65T_c$ [31].

Useful constraints on the spectral function are provided by sum rules. Romatschke and Son showed that [101]

$$\frac{2}{\pi} \int d\omega [\eta(\omega) - \eta_{T=0}(\omega)] = \frac{2}{5} \mathcal{E}, \quad (36)$$

where $\eta_{T=0}(\omega)$ is the spectral function at zero temperature. The high frequency behavior can be studied in perturbation theory. We find $\eta(\omega) \sim \omega^3$ at both zero and non-zero temperature. Finite temperature effect were studied in [102,103]. We note that in non-relativistic theories the tail of the spectral function is determined by short range correlations, whereas in a relativistic theory the high frequency behavior is determined by the gg and $q\bar{q}$ continuum. In kinetic theory the shape of the spectral function at small frequency is a Lorentzian with a width proportional to $1/\eta$. The lattice calculation in [31] does not find a quasi-particle peak, but the resolution is insufficient to draw a final conclusions. A spectral function that is broadly consistent with the existence of quasi-particles was observed in a study of the electric conductivity of the quark gluon plasma [104].

3.2 Flow, higher moments of flow, and viscosity

Experimental information about transport properties of the quark gluon plasma comes from the observation of hydrodynamic flow in heavy ion collisions at collider energies [105,106]. Several observations support the assumption that heavy ion collisions create a locally thermalized system:

1. The overall abundances of produced particles is described by a simple thermal model that depends on only two parameters, the temperature T and the baryon chemical potential μ at freezeout [107,108].
2. For transverse momenta $p_\perp \lesssim 2$ GeV the spectra dN/d^3p of produced particles follow a modified Boltzmann distribution characterized by the freezeout temperature and a collective radial expansion velocity [109,105]. Radial flow manifests itself in the fact that the spectra of heavy hadrons, which acquire a larger momentum boost from the collective expansion, have a larger apparent temperature than the spectra of light hadrons.
3. In non-central collisions the azimuthal distribution of produced particles shows a strong anisotropy termed elliptic flow [110,105]. Elliptic flow represents the collective response of the quark gluon plasma to pressure gradients in the initial state, which in turn are related to the geometry of the overlap region of the colliding nuclei, see Fig. 3.

Analysis of the azimuthal distribution is the main tool for constraining the shear viscosity of the plasma. We define harmonics of the particle distribution

$$p_0 \frac{dN}{d^3p} \Big|_{p_z=0} = v_0(p_T) \left(1 + 2v_1(p_T) \cos(\phi - \Psi_1) + 2v_2(p_T) \cos(2\phi - \Psi_2) + \dots \right), \quad (37)$$

where p_z is the longitudinal (beam) direction, p_T is the transverse momentum, and ϕ is the angle relative to the impact parameter direction. The coefficient v_2 is known as elliptic flow, and the higher moments are termed triangular, quadrupolar, etc. flow. The angles Ψ_i are known as flow angles. Substantial elliptic flow, reaching about $v_2(p_T = 2 \text{ GeV}) \simeq 20\%$ in semi-central collisions,

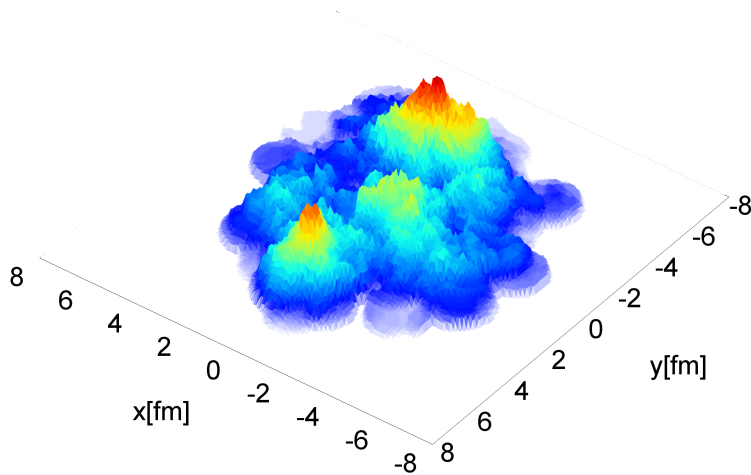


Figure 3: Initial energy density in a Au+Au collision at RHIC from the Monte-Carlo KLN model, see [111,112]. This model include the effects from the collision geometry, fluctuations in the initial position of the nucleons inside the nucleus, and non-linear gluon field evolution. More sophisticated versions of the model also include quantum fluctuations of the gluon field.

was discovered in the early RHIC data [113,114] and confirmed at the LHC [115]. More recently, it was realized that fluctuations in the initial energy density generates substantial higher harmonics, including odd Fourier moments such as v_3 [116], and fluctuations of the flow angles relative to the impact parameter plane [117].

Viscosity tends to equalize the radial flow velocity and suppress elliptic flow and higher flow harmonics. An estimate of the relevant scales can be obtained from simple scaling solutions of fluid dynamics²¹. The simplest solution of this type was proposed by Bjorken, who considered a purely longitudinal expansion [118]. Bjorken assumed that the initial entropy density is independent of rapidity, and that the subsequent evolution is invariant under boosts along the z axis. The Bjorken solution provides a natural starting point for more detailed numerical and analytical studies [105, 119]. Bjorken flow is characterized by a flow profile of the form $u_\mu = \gamma(-1, 0, 0, u_z) = (-t/\tau, 0, 0, z/\tau)$, where $\gamma = (1 - u_z^2)^{1/2}$ is the boost factor and $\tau = (t^2 - z^2)^{1/2}$ is the proper time. This velocity field solves the relativistic Navier-Stokes equation. Energy conservation then determines the evolution of the entropy density. We find

$$-\frac{\tau}{s} \frac{ds}{d\tau} = 1 - \frac{4}{3} \frac{\eta}{sT\tau}, \quad (38)$$

where we have neglected bulk viscosity. In ideal hydrodynamics $s \sim T^3$ and $T \sim 1/\tau^{1/3}$. The validity of the gradient expansion requires that the viscous correction is small [5]

$$\frac{\eta}{s} \ll \frac{3}{4}(T\tau). \quad (39)$$

It is usually assumed that in the QGP η/s is approximately constant. For the Bjorken solution $T\tau \sim \tau^{2/3}$ increases with time, and equ. (39) is most restrictive during the early stages of the

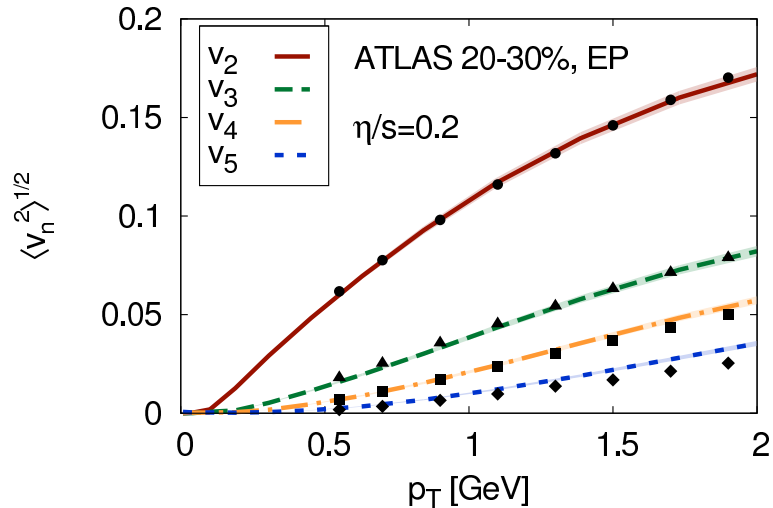


Figure 4: Fourier coefficients v_2, \dots, v_5 of the azimuthal charged particle distribution as a function of the transverse momentum p_T measured in $Pb + Pb$ collisions at the LHC [120] The lines show a hydrodynamic analysis performed using $\eta/s = 0.2$ [121].

evolution. Using an equilibration time $\tau_0 = 1$ fm and an initial temperature $T_0 = 300$ MeV gives $\eta/s \lesssim 0.6$. We conclude that fluid dynamics can be applied to heavy ion collisions only if the QGP behaves as a nearly perfect fluid.

At late time the expansion becomes three dimensional and $T\tau$ is independent of time. The fluid is composed of hadronic resonances that have cross sections that reflect hadronic sizes and are approximately independent of energy. In that case $\eta \sim T/\sigma$. Using $s \sim T^3$ and $T \sim 1/\tau$ we find that the dissipative correction $\eta/(sT\tau)$ increases with proper time as τ^2 . This result shows that fluid dynamics also breaks down at late times. At RHIC and LHC energies the duration of the fluid dynamic phase is 5-10 fm/c, depending on collision energy and geometry. We note that in contrast to the situation in heavy ion collisions there is no freeze-out in the cold atomic gas experiments. At unitarity the mean cross section increases as the temperature drops, and the fluid parameter $\eta/(nT\tau)$ is approximately constant during the evolution.

In heavy ion collisions we can observe only the final distribution of hadrons. In principle one could imagine reconstructing azimuthal harmonics of the stress tensor from the measured particle distribution, but doing so would require very complete coverage and particle identification, and it has not been attempted. In any case, hadrons continue to interact after the fluid freezes out, and some rearrangement of momentum takes place. This means that we need a prescription for converting hydrodynamic variables to kinetic distribution functions. What is usually done is that on the freezeout surface the conserved densities in fluid dynamics are matched²² to kinetic theory [122].

In ideal fluid dynamics the distribution functions are Bose-Einstein or Fermi-Dirac distributions characterized by the local temperature and fluid velocity. Viscosity modifies the stress tensor, and via matching to kinetic theory this modification changes the distribution functions f_p . The value of η/s constrains only the $p_i v_j$ moment of the distribution function. The full distribution function can

be reconstructed only if the collision term is specified. Using the BGK collision term one obtains a very simple formula for the leading correction δf_p

$$\delta f_p = \frac{1}{2T^3} \frac{\eta}{s} f_0 (1 \pm f_0) p_\alpha p_\beta \sigma^{\alpha\beta}, \quad (40)$$

where the \pm sign refers to Bose/Fermi distributions. This result is a reasonable approximation to more microscopic theories [96]. The shift in the distribution function leads to a modification of the single particle spectrum. In the case of the Bjorken expansion and at large p_T we find

$$\frac{\delta(dN)}{dN_0} = \frac{1}{3\tau_f T_f} \frac{\eta}{s} \left(\frac{p_T}{T_f} \right)^2, \quad (41)$$

where dN_0 is the number of particles produced in ideal fluid dynamics, $\delta(dN)$ is the dissipative correction, and τ_f is the freezeout time. In a system with strong longitudinal expansion viscous corrections tend to equalize the momentum flow by pushing particles to higher p_T . Because the single particle distribution enters into the denominator of v_2 this effect tends to suppress v_2 at large p_T . The effect from the numerator, dissipative corrections due to the $\cos(2\phi)$ component of the radial flow, act in the same direction [123]. What is important is that corrections to the spectrum are controlled by the same parameter $\eta/(s\tau T)$ that governs the derivative expansion in fluid dynamics²³. This reflects the fact that in the regime in which kinetic theory can be matched to fluid dynamics we have $Kn \sim Re^{-1}$.

We obtain several simple predictions that have been confirmed by experiment [124]: Dissipative corrections increase with p_T , they are larger in small systems that freeze out earlier, and they are larger for higher harmonics that are more sensitive to gradients of the radial flow profile. Quantitative predictions that provide not only bounds on η/s but also reliable measurements of transport properties of the plasma require a number of ingredients [125]:

1. An initial state model that incorporates the nuclear geometry and fluctuations in the initial energy deposition. The simplest possibility is a Monte-Carlo implementation of the Glauber model [126], but some calculations also include saturation effects, quantum fluctuations of the initial color field, and pre-equilibrium evolution of the initial field [121]. Alternatively, one may try to describe the pre-equilibrium stage using kinetic theory [127, 128] or the AdS/CFT correspondence [129]. At the end of the initial stage the stress tensor is matched to fluid dynamics.
2. Second order dissipative fluid dynamics in 2+1 (boost invariant) or 3+1 dimensions. Calculations must include checks to ensure insensitivity to poorly constrained second order transport coefficients²⁴ and a realistic equation of state (EOS). A realistic EOS has to match lattice QCD results at high temperature, and a hadronic resonance gas below T_c [130]. The resonance gas EOS must allow for chemical non-equilibrium effects below the chemical freezeout temperature $T_{chem} \simeq T_c$.
3. Kinetic freezeout and a kinetic afterburner. At the kinetic freezeout temperature the fluid is converted to hadronic distribution functions. Ideally, these distribution functions are evolved further using a hadronic cascade [131, 132], but at a minimum one has to include feed-down from hadronic resonance decays.

Initial estimates of η/s from the RHIC data have been obtained in [133, 134, 135]. A more recent analysis of LHC data is shown in Fig. 4 [121]. The authors found $\eta/s \simeq 0.2$ at the LHC, and $\eta/s \simeq 0.12$ from a similar analysis of RHIC data. Similar results were obtained by other authors. Song et al. reported an average value of $\eta/s \simeq (0.2-0.24)$ at the LHC and $\eta/s \simeq 0.16$ at RHIC [136]. Luzum and Ollitrault tried to constrain the allowed range of η/s , obtaining $0.07 \leq \eta/s \leq 0.43$ at RHIC [137]. Given the complexity of the analysis, uncertainties are difficult to quantify. A survey of the main sources of error in the determination of η/s can be found in [138]. Interestingly, the extracted values of η/s are lower at RHIC than they are at the LHC, as one would expect based on asymptotic freedom. We emphasize, however, that given the uncertainties it is too early to make this statement with high confidence.

4 Frontiers

In absolute units the shear viscosity of the ultracold Fermi gas and the quark gluon plasma differ by more than 25 orders of magnitude [7]. The approximate universality of η/s in strongly coupled fluids, and the near agreement with the value predicted by the AdS/CFT correspondence in the strong coupling limit of a large class of field theories is quite remarkable²⁵. Much work remains to be done in order to determine to what extent this observation can be made precise, and what it implies about the structure of strongly correlated quantum systems. In this outlook we can only give a very brief summary of some of these issues.

4.1 Transport coefficients

There is an ongoing effort to map out the full density and temperature dependence of η/s in both the ultracold gases and the quark gluon plasma, and to determine other transport coefficients, like the bulk viscosity and diffusion coefficients. There are a number of experimental puzzles that remain to be addressed²⁶. In the case of heavy ion collisions, nearly ideal flow is even more pervasive than one would expect. Strong flow is also observed in photons, electrons from heavy quark decays, and hadrons emitted in high-multiplicity $p + Pb$ collisions at LHC energies, see [139] for a recent summary and original references. In the case of cold atomic gases we now have very accurate data for the dependence of $\langle \eta \rangle$ on the total energy of the cloud [140]. These data have not been unfolded. It was observed that the scaling of $\langle \eta \rangle$ with the total energy is remarkably simple, $\langle \eta \rangle / \langle n \rangle \sim aE + bE^3$ for all energies above the critical point, but the origin of this scaling behavior is not understood.

4.2 Quasi-particles

We would like to understand whether nearly perfect fluidity, $\eta/s \sim 1/(4\pi)$, necessarily implies the absence of quasi-particles, as is the case in the AdS/CFT correspondence. The most direct way to study this issue is to determine the spectral function. Since the only local probe of the stress tensor is the graviton, this will likely require numerical studies. We are also interested in pushing weak coupling descriptions into the regime where the quasi-particle picture breaks down, for example by using the renormalization group.

4.3 Viscosity bound

Whether there is a fundamental lower limit for η/s is unknown. Part of the issue may well be that we need to define more carefully what we mean by a fluid, and that we need to understand how these defining characteristics are reflected in microscopic theories. We would also like to know what kinds of theories have holographic duals, and what aspects of the field theory lead to the emergence of certain universal features, such as a shear viscosity to entropy density ratio that saturates the holographic bound $\eta/s = 1/(4\pi)$.

4.4 Other strongly correlated fluids

In addition to the two fluids discussed in this review several other systems may be of interest. One interesting class is two dimensional fluids, for example the electron gas in graphene [141], and the so-called strange metal phase of the high T_c superconductors [142].

4.5 Equilibration at strong and weak coupling

Empirical evidence suggests that equilibration in heavy ion collisions takes place on a very short time scale, $\tau_{eq} \sim 1$ fm. Rapid equilibration is natural in holographic theories [47], but it is difficult to make contact with asymptotic freedom and the well-established theory and phenomenology of parton distribution functions. Understanding equilibration in weak coupling is a complicated problem that involves many competing scales, and even establishing the parametric dependence of the equilibration time on α_s is difficult, see [143] for a recent overview.

4.6 Anomalous hydrodynamics

Several novel hydrodynamic effects have been discovered in recent years. An example is the chiral magnetic effect. Topological charge fluctuations in the initial state of a heavy ion collision, combined with the magnetic field generated by the highly charged ions, can manifest themselves in electric charge fluctuations in the final state [144]. This effect is now understood as part of a broader class of anomalous hydrodynamic effects [145]. Anomalous transport coefficients were originally discovered in the context of holographic dualities in [146], and interpreted using general arguments based on fluid dynamics in [147].

Acknowledgments: This work was supported in parts by the US Department of Energy grant DE-FG02-03ER41260. We would like to acknowledge useful discussions with Peter Arnold, Harvey Meyer, Guy Moore, Dam Son, Derek Teaney, and John Thomas.

Endnotes

1 Fluid dynamics

1.1 Fluid dynamics as an effective theory

1. *Hydrodynamic variables:* In addition to the conserved charges there are two more classes of hydrodynamics variables, Goldstone modes associated with spontaneously broken global symmetries, and order parameters near second order phase transitions. The simplest example of a Goldstone mode is the phase of the order parameter in a superfluid. In the dilute Fermi gas discussed in Sect. 2 the order parameter is $\langle\psi\psi\rangle = \rho e^{i\varphi}$. The low energy effective theory can be expressed in terms of gradients of φ . The corresponding hydrodynamic variable is the superfluid velocity $\vec{u}_s = (\vec{\nabla}\varphi)/m$. The hydrodynamic description of the superfluid then involves two velocity fields, the normal velocity \vec{u}_n and the superfluid velocity \vec{u}_s . The momentum density can be written as $\vec{\pi} = \rho_n\vec{u}_n + \rho_s\vec{u}_s$, where $\rho = \rho_n + \rho_s$ is the total mass density of the fluid. The theory of superfluid (two fluid) hydrodynamics was developed by Landau and Khalatnikov [148]. A new ingredient in hydrodynamic theories involving broken symmetries is the role of non-trivial commutation relations between the order parameter and the conserved charges. These commutators are implemented in fluid dynamics as non-trivial Poisson brackets [149], which constrain the equation for the Goldstone modes.

In QCD chiral symmetry is broken and in the limit that quarks are massless the pion is a Goldstone mode. The hydrodynamic theory of pions is described in [150, 151], but the theory is of somewhat limited value because the mass of the pion, $m_\pi \simeq 135$ MeV, is comparable to the breakdown scale of hydrodynamics.

Near a continuous phase transition fluctuations of the order parameter are large and the magnitude of the order parameter also becomes a hydrodynamic variable. Hydrodynamic theories near a second order phase transition can be classified according to the symmetries of the order parameter, and possible non-trivial Poisson brackets. The resulting theories are known as model A-J in the classification of Hohenberg and Halperin [152]. The superfluid transition in the cold Fermi gas is described by model F, which also governs the lambda point in liquid Helium. A possible tri-critical point in QCD can be analyzed in terms of model H [153], which also describes the endpoint of the liquid-gas transition in water.

2. *Mass current, momentum density, and relativistic fluids:* In equ. (1,2) we have used that the mass current $\vec{j}_\rho = \rho\vec{u}$, which appears in the conservation law $\partial_t\rho = -\vec{\nabla}\cdot\vec{j}_\rho$, is equal to the momentum density, $\vec{\pi}$. This identification follows from very general arguments [154]. It implies that there are no diffusive terms in the mass current, and provides an important constraint for quasi-particle theories, see equ. (59).

In relativistic hydrodynamics there need not be a conserved particle number current. In this case the fluid four velocity u_μ is defined in terms of the energy current. In particular, we define u_μ to be the velocity of the frame in which the ideal stress tensor is diagonal. The ideal stress tensor is

$$\Pi_{\mu\nu} = (\mathcal{E} + P)u_\mu u_\nu + P g_{\mu\nu}, \quad (42)$$

where we use the convention $u^2 = -1$. More formally, we can define u^μ through the condition

$u^\mu \Pi_{\mu\nu} = \mathcal{E} u_\nu$. This relation implies that the energy current in the rest frame does not receive any dissipative corrections, $\Pi_{0i} = 0$. The energy and momentum conservation laws are expressed through the relation $\nabla^\mu T_{\mu\nu} = 0$. We can split this equation into longitudinal and transverse parts using the projectors

$$\Delta_{\mu\nu}^{\parallel} = -u_\mu u_\nu, \quad \Delta_{\mu\nu} = g_{\mu\nu} + u_\mu u_\nu. \quad (43)$$

The longitudinal and transverse projections of $\nabla^\mu T_{\mu\nu} = 0$ can be viewed as the equation of energy (or entropy) conservation and the relativistic Euler equation, respectively. We get

$$\nabla^\mu (s u_\mu) = 0, \quad D u_\mu = -\frac{1}{\mathcal{E} + P} \nabla_\mu^\perp P, \quad (44)$$

where $D = u^\mu \nabla_\mu$ and $\nabla_\mu^\perp = \Delta_{\mu\nu} \nabla^\nu$.

There are two basic possibilities for defining the fluid velocity in a theory with a conserved particle current n_μ , such as the baryon current in QCD. The first option, called the Landau frame, is to define the fluid velocity in terms of the energy current. In this case there are dissipative corrections to the baryon current

$$n_\mu = n u_\mu + \delta n_\mu, \quad (45)$$

where, at leading order in the gradient expansion, δn_μ is related to the thermal conductivity [154]. This choice is convenient in the relativistic domain, but the non-relativistic limit is somewhat subtle. The other option, known as the Eckardt frame, corresponds to defining the fluid velocity in terms of the particle current. In this case n_μ is non-diffusive, and the energy current contains dissipative corrections, in particular the thermal conductivity.

3. Second order fluid dynamics: The most general form of the stress tensor of a non-relativistic scale invariant fluid at second order in the gradient expansion was determined in [20]. The result is

$$\begin{aligned} \delta \Pi_{ij} = & -\eta \sigma_{ij} + \eta \tau_R \left[g_{ik} \dot{\sigma}_j^k + u^k \nabla_k \sigma_{ij} + \frac{2}{3} \langle \sigma \rangle \sigma_{ij} \right] + \lambda_1 \sigma_{\langle i}^k \sigma_{j \rangle k} + \lambda_2 \sigma_{\langle i}^k \Omega_{j \rangle k} \\ & + \lambda_3 \Omega_{\langle i}^k \Omega_{j \rangle k} + \gamma_1 \nabla_{\langle i} T \nabla_{j \rangle} T + \gamma_2 \nabla_{\langle i} P \nabla_{j \rangle} P + \gamma_3 \nabla_{\langle i} T \nabla_{j \rangle} P \\ & + \gamma_4 \nabla_{\langle i} \nabla_{j \rangle} T + \gamma_5 \nabla_{\langle i} \nabla_{j \rangle} P + \kappa_R R_{\langle ij \rangle}. \end{aligned} \quad (46)$$

Here, $\mathcal{O}_{\langle ij \rangle} = \frac{1}{2}(\mathcal{O}_{ij} + \mathcal{O}_{ji} - \frac{2}{3} g_{ij} \mathcal{O}^k_k)$ denotes the symmetric traceless part of a tensor \mathcal{O}_{ij} , $\Omega_{ij} = \nabla_i u_j - \nabla_j u_i$ is the vorticity tensor, and R_{ij} is the Ricci tensor. This term vanishes in flat space, but it is needed to establish the general form of the response function even in flat space, see equ. (76). We note that equ. (46) contains 10 second order transport coefficients. This number is larger than the number of second order coefficients in the Burnett equation [10], despite the fact that we have imposed conformal symmetry. This is related to the fact that the Burnett equations were derived from kinetic theory, and that some transport coefficients allowed by the symmetries vanish in this framework.

For phenomenological applications it is useful to rewrite the second order equations as a relaxation equation for the viscous stress $\pi_{ij} \equiv \delta \Pi_{ij}$. For this purpose we use the first order relation $\pi_{ij} = -\eta \sigma_{ij}$ and rewrite equ. (46) as

$$\pi_{ij} = -\eta \sigma_{ij} - \tau_R \left[g_{ik} \dot{\pi}_j^k + V^k \nabla_k \pi_{ij} + \frac{5}{3} \langle \sigma \rangle \pi_{ij} \right] \quad (47)$$

$$+ \frac{\lambda_1}{\eta^2} \pi_{\langle i}{}^k \pi_{j \rangle k} - \frac{\lambda_2}{\eta} \pi_{\langle i}{}^k \Omega_{j \rangle k} + \lambda_3 \Omega_{\langle i}{}^k \Omega_{j \rangle k} + \dots,$$

where \dots refers to the terms proportional to γ_i and κ_R . Note that this reformulation is not unique, and that it does not represent a formal improvement over the second order equations. Theories of this type can be derived in kinetic theory, and they can be used to restore causality and stability for perturbations of all wavelengths, not just wavelengths longer than the inverse breakdown scale of the hydrodynamic description.

It is interesting to study the physical meaning of the different terms in equ. (47). We begin with the term proportional to τ_R . Consider a non-zero strain σ_{ij} which arises at time $t = 0$. For simplicity assume the local rest frame and vanishing bulk stress $\langle \sigma \rangle$. Then the stress tensor is $\pi_{ij} = -\eta \sigma_{ij} (1 - \exp(-t/\tau_R))$, which shows that τ_R is the time scale for dissipative stresses to relax to the Navier-Stokes value. The relaxation time also ensures that the front of a shear wave propagates with a finite speed, see equ. (149). In a periodically driven system τ_R determines the phase lag between the strain σ_{ij} and the stress π_{ij} . Note that the dissipated energy is proportional to $\sigma_{ij} \pi_{ij}$, and a non-zero phase lag reduces the amount of energy dissipated by viscous stresses.

The terms proportional to λ_i describe non-linearities in the stress-strain relation. Consider a fluid moving in the x direction sheared between two parallel plates in the xz plane. The first order term $\pi_{ij} = -\eta \sigma_{ij}$ describes Newton's law of friction, $F_x/A = \eta \nabla_y u_x$. At second order we also find a normal force, $F_y/A = -\lambda_1 (\nabla_y u_x)^2$. The λ_2 term describes the coupling between shear and vorticity, and the λ_3 term implies that in a rotating fluid confined in a cylindrical container there is a normal force on the walls of the container. We note that this force is not dissipative.

4. Second order relativistic fluid dynamics: In relativistic fluid dynamics we define the shear tensor $\sigma^{\mu\nu}$ using the projection operator $\Delta_{\mu\nu}$. We have

$$\sigma^{\mu\nu} = \Delta^{\mu\alpha} \Delta^{\nu\beta} \left(\nabla_\alpha u_\beta + \nabla_\beta u_\alpha - \frac{2}{3} \eta_{\alpha\beta} \nabla \cdot u \right). \quad (48)$$

Note that in rest frame of the fluid this expression reduces to the non-relativistic result. At second order in the gradient expansion the stress tensor of a scale invariant fluid is [19]

$$\begin{aligned} \delta\Pi^{\mu\nu} &= -\eta\sigma^{\mu\nu} + \eta\tau_R \left[\langle D\sigma^{\mu\nu} \rangle + \frac{1}{3} \sigma^{\mu\nu} (\nabla \cdot u) \right] \\ &+ \lambda_1 \sigma^{\langle\mu}{}_\lambda \sigma^{\nu\rangle\lambda} + \lambda_2 \sigma^{\langle\mu}{}_\lambda \Omega^{\nu\rangle\lambda} + \lambda_3 \Omega^{\langle\mu}{}_\lambda \Omega^{\nu\rangle\lambda} + \kappa_R \left[R^{\langle\mu\nu\rangle} - 2u_\alpha u_\beta R^{\alpha\langle\mu\nu\rangle\beta} \right], \end{aligned} \quad (49)$$

where $D = u \cdot \nabla$ and $\mathcal{O}^{\langle\mu\nu\rangle} = \frac{1}{2} \Delta^{\mu\alpha} \Delta^{\nu\beta} (\mathcal{O}_{\alpha\beta} + \mathcal{O}_{\beta\alpha} - \frac{2}{3} \Delta^{\mu\nu} \Delta^{\alpha\beta} \mathcal{O}_{\alpha\beta})$ denotes the transverse traceless part of $\mathcal{O}^{\alpha\beta}$. The relativistic vorticity tensor is $\Omega^{\mu\nu} = \frac{1}{2} \Delta^{\mu\alpha} \Delta^{\nu\beta} (\partial_\alpha u_\beta - \partial_\beta u_\alpha)$, and $R_{\mu\nu\alpha\beta}$ is the Riemann tensor. We note that the number of terms is smaller than in the non-relativistic case. This is related to the fact that without a conserved baryon current the number of independent hydrodynamical variables is smaller. We also note that the numerical coefficient in front of $\sigma_{\mu\nu} (\nabla \cdot u)$ is different. This is due to the difference between relativistic and non-relativistic scale transformations. To second order accuracy the stress tensor is equivalent to the relaxation equation

$$\pi^{\mu\nu} = -\eta\sigma^{\mu\nu} - \tau_R \left[\langle D\pi^{\mu\nu} \rangle + \frac{4}{3} \pi^{\mu\nu} (\nabla \cdot u) \right] \quad (50)$$

$$+ \frac{\lambda_1}{\eta^2} \pi^{\langle \mu}{}_{\lambda} \pi^{\nu \rangle \lambda} - \frac{\lambda_2}{\eta} \pi^{\langle \mu}{}_{\lambda} \Omega^{\nu \rangle \lambda} + \lambda_3 \Omega^{\langle \mu}{}_{\lambda} \Omega^{\nu \rangle \lambda} + \kappa_R \left[R^{\langle \mu \nu \rangle} - 2u_{\alpha} u_{\beta} R^{\alpha \langle \mu \nu \rangle \beta} \right],$$

where $\pi^{\mu\nu} = \delta\Pi^{\mu\nu}$ is the dissipative contribution to the stress tensor.

5. *Hydrodynamics as an effective field theory:* Can hydrodynamics be formulated not only as an effective theory, but as an effective field theory? The standard response is that this is not possible [155], because dissipative effects cannot be described by a local lagrangian. There are, however, at least a few situations in which hydrodynamics can be reformulated as an effective field theory. The simplest case is the non-dissipative flow of a superfluid at zero temperature, see [156, 157, 158]. The basic observation is that if one implements the full Galilean (or Lorentz) and gauge invariance of the microscopic theory then the effective action of the Goldstone mode will necessarily contain the non-linear terms needed to recover the equations of fluid mechanics. Consider the dilute Fermi gas in the superfluid phase, see Sect. 2.1. The effective lagrangian for the Goldstone mode φ is

$$\mathcal{L} = P(X), \quad X = \mu - \partial_0 \varphi - \frac{(\vec{\nabla} \varphi)^2}{2m}, \quad (51)$$

where $P(\mu)$ is the pressure and μ is the chemical potential. The form of the variable X is determined by $U(1)$ and Galilean invariance, and the relation $\mathcal{L} = P(X)$ ensures that we obtain the correct thermodynamic potential for constant fields $X = \mu$. Note that equ. (51) is the leading term in a low energy expansion where we treat $\nabla \varphi \sim O(1)$ but $\nabla^2 \varphi \ll \nabla \varphi$ [158]. This expansion is useful because it respects Galilean and $U(1)$ symmetry exactly order by order in the low energy expansion, and as a consequence it is equivalent to superfluid hydrodynamics.

Expanding equ. (51) in powers of $(\partial\varphi)/\mu$ reproduces the conventional low energy expansion of the effective field theory for the Goldstone mode. We find, in particular, that the velocity of the Goldstone mode is the speed of sound,

$$\mathcal{L} = \frac{f^2}{2} \left[(\partial_0 \varphi)^2 - c_s^2 (\vec{\nabla} \varphi)^2 + \dots \right], \quad (52)$$

with $f^2 = (\partial n)/(\partial \mu)$ and $c_s^2 = (\partial P)/(\partial \rho)$. Note that for the dilute Fermi gas at unitarity dimensional analysis implies that $P(\mu) \sim m^{3/2} \mu^{5/2}$.

We can write equ. (51) in terms of hydrodynamic variables by introducing the superfluid velocity $\vec{v}_s = (\vec{\nabla} \varphi)/m$. The equation of motion for the field φ leads to

$$\partial_0 \bar{n} + \frac{1}{m} \vec{\nabla} \cdot (\bar{n} \vec{\nabla} \varphi) = 0, \quad (53)$$

where we have defined $\bar{n} = P'(X)$. Equ. (53) is the continuity equation for the current $\vec{j} = \bar{n} \vec{u}_s$. We can derive a second equation by using the identity $dP = n d\mu$. We get

$$\partial_0 \vec{u}_s + \frac{1}{2} \vec{\nabla} u_s^2 = -\frac{1}{m} \vec{\nabla} \mu. \quad (54)$$

which is the Euler equation in a superfluid. We note that higher derivative corrections to equ. (51) correspond to non-dissipative higher order terms in the equations of fluid dynamics. Next-to-leading order (NLO) terms have been determined [159]. They lead to non-linearities in the dispersion law for sound waves, and to corrections to the equation of hydrostatic equilibrium in small systems.

A different situation in which the fluid dynamic expansion can be written as an effective field theory is the systematic calculation of retarded correlation functions including noise and dissipation [160, 161, 162, 163, 164]. We can write the effective action as a functional integral over the noise, the hydrodynamic variables, and suitable Lagrange multipliers that enforce the linearized equations of motion. This representation can be used to derive a set of Feynman rules for the retarded correlation functions. The diagrammatic approach is particularly powerful as a method for computing non-analytic terms in the correlation function induced by thermal fluctuations, see Fig. 5 and equ. (85).

More recent ideas about hydrodynamics and effective field theory can be found in [165, 166, 167].

1.2 Models of fluids: Kinetic theory

6. *Conserved charges in kinetic theory:* For completeness we give the complete definition of the conserved charges in non-relativistic kinetic theory. We have

$$\rho(\vec{x}, t) = \int d\Gamma_p m f_p(\vec{x}, t) \quad (55)$$

$$\vec{j}_\rho(\vec{x}, t) = \int d\Gamma_p m \vec{v} f_p(\vec{x}, t), \quad (56)$$

$$\Pi_{ij}(\vec{x}, t) = \int d\Gamma_p p_i v_j f_p(\vec{x}, t) + \delta_{ij} \left(\int d\Gamma_p E_p f_p(\vec{x}, t) - \mathcal{E}(\vec{x}, t) \right), \quad (57)$$

where $\vec{v} = \vec{\nabla}_p E_p$ and \mathcal{E} is the energy density. Note that in equilibrium we view E_p and \mathcal{E} as functions of the thermodynamic variables, but in kinetic theory we must consider these quantities as functionals of the distribution function f_p . In a weakly interacting gas we have $E_p = p^2/(2m)$ and $\mathcal{E} = \int d\Gamma_p E_p f_p$, but in general these relations are modified by interactions. The dependence of \mathcal{E} and E_p on f_p is constrained by conservation laws. Momentum conservation requires [27, 69]

$$E_p = \frac{\delta \mathcal{E}}{\delta f_p}, \quad (58)$$

and the equality of the mass current \vec{j}_ρ and the momentum density $\vec{\pi}$ implies that

$$\int d\Gamma_p m \vec{v} f_p = \int d\Gamma_p \vec{p} f_p. \quad (59)$$

These conditions are quite non-trivial to satisfy. Microscopic theories that are consistent with the constraints are discussed in [27, 69, 168]. The condition given in equ. (58) also holds in relativistic theories, see [169]. Another difficulty in constructing quasi-particle models of the thermodynamic properties of the many-body system is to find an explicit expression for $\mathcal{E}[f_p]$. This problem can be avoided by focusing on the enthalpy

$$\mathcal{E} + P = \int d\Gamma_p \left(\frac{1}{3} \vec{v} \cdot \vec{p} + E_p \right) f_p(\vec{x}, t). \quad (60)$$

The same observation applies to relativistic theories. In a relativistic fluid we can use $\mathcal{E} + P = sT$ (for $\mu = 0$) to construct a quasi-particle model for the entropy density.

7. *Linearized collision operator:* The relaxation of hydrodynamic variables near equilibrium is determined by the linearized collision term. We write the distribution function as $f_p = f_p^0(1 +$

χ_p/T) where f_p^0 is the equilibrium distribution, see equ. (13). The linearized collision operator corresponding to binary $2 \rightarrow 2$ is scattering is $C[f_p] \equiv (f_p^0/T)C_L[\chi_p]$ with

$$C_L[\chi_{p1}] = - \int \left(\prod_{i=2}^4 d\Gamma_i \right) w(1, 2; 3, 4) f_{p2}^0 [\chi_{p1} + \chi_{p2} - \chi_{p3} + \chi_{p4}] . \quad (61)$$

The transition rate $w(1, 2; 3, 4)$ is given by

$$w(1, 2; 3, 4) = (2\pi)^4 \delta^3 \left(\sum_i \vec{p}_i \right) \delta \left(\sum_i E_i \right) |\mathcal{M}|^2 , \quad (62)$$

and \mathcal{M} is the scattering amplitude. The scattering amplitude for low energy s -wave scattering is given in equ. (29). We can define an inner product for distribution functions

$$\langle \chi | \psi \rangle = \int d\Gamma_p f_p^0 \chi_p \psi_p . \quad (63)$$

Detailed balance and the symmetries of the transition rate imply that C_L is a hermitean, negative semi-definite operator. Zero eigenvalues of C_L correspond to the conservation laws for particle number, momentum, and energy, $\chi_i^{(0)} \sim 1, \vec{p}, E_p$. In the space orthogonal to the zero modes C_L can be written as

$$C_L = - \sum_i \frac{|\chi_i\rangle\langle\chi_i|}{\tau_i} . \quad (64)$$

The BGK (or relaxation time) model is based on the assumption that that the collision term, or, more accurately, its inverse, is dominated by the longest collision time,

$$C_L \simeq - \frac{|\chi_0\rangle\langle\chi_0|}{\tau_0} \simeq - \frac{1}{\tau_0} . \quad (65)$$

Here, we also assume that C_L acts on a distribution function that has a large component along χ_0 . This is a reasonable approximation at late times.

Near the hydrodynamic limit the left hand side of the Boltzmann equation can be expanded in derivatives of the hydrodynamic variables T, μ, \vec{u} . This is known as the Chapman-Enskog expansion [26]. The linearized Boltzmann equation is of the form

$$|X\rangle = C_L|\psi\rangle , \quad (66)$$

where the driving term X arises from the gradient expansion and ψ_p is the off-equilibrium distribution induced by the external stress. Consider a distribution $f^0(T, \mu, \vec{u})$ describing a pure shear flow $u_y(x)$. We find

$$\left(\frac{\partial}{\partial t} + \vec{v} \cdot \vec{\nabla}_x + \vec{F} \cdot \vec{\nabla}_p \right) f^0(T, \mu, u_y(x)) = - \frac{f^0}{T} v_x p_y \nabla_x u_y , \quad (67)$$

and $X = v_x p_y \nabla_x u_y \equiv X_0 \nabla_x u_y$. Using the definition of the stress tensor in kinetic theory, equ. (57), we get

$$\eta = - \frac{1}{T} \langle X_0 | \psi_0 \rangle = \frac{1}{T} \langle X_0 | (-C_L^{-1}) | X_0 \rangle , \quad (68)$$

where we have defined $\psi = \psi_0 \nabla_x u_y$ and used the linearized Boltzmann equation. This result shows that the shear viscosity is positive. We can also establish a variational bound on η . The Cauchy-Schwarz inequality implies

$$\eta \geq \frac{\langle X_0 | \psi_{var} \rangle^2}{\langle \psi_{var} | (-C_L) | \psi_{var} \rangle}, \quad (69)$$

which is valid for any variational distribution function $|\psi_{var}\rangle$. We note that this is not a fundamental bound for η . Instead, equ. (69) provides a bound on η in the context of a given collision term and quasi-particle dispersion relation. Similar bounds can be derived for other transport coefficients. Finally, we note that in the BGK approximation the solution of the Boltzmann equation is given by $|\psi_0\rangle = -\tau_0 |X_0\rangle$. Equation (68) then leads to the simple result $\eta = \tau_0 P$. Using $P = nT$ and $\langle mv^2 \rangle = 3T$ we can write this as $\eta = \frac{1}{3} n l_{mfp} \bar{p}$. More systematic calculations of η are based on expanding ψ_{var} in a complete set of polynomials $L^{(k)}(x)$,

$$\psi_{var}(\vec{p}) = p_x p_y \sum_{k=0}^{N-1} c_k L^{(k)} \left(\frac{p^2}{mT} \right). \quad (70)$$

and truncate the expansion at order N . A convenient choice in non-relativistic kinetic theory is the set of generalized Laguerre (Sonine) polynomials [170]. This expansion typically converges rapidly. The result for η given in equ. (30) is based on using $N = 1$, but higher order corrections are known to be quite small, on the order of 2% [171].

8. Knudsen expansion: The Chapman-Enskog method provides an expansion of δf_p in the Knudsen number $Kn = l_{mfp}/L$. This expansion corresponds to the gradient expansion in hydrodynamics. Schematically, $\delta f_p = \delta f_p^1 \tau_0 (\nabla u) + \delta f_p^2 \tau_0^2 (\nabla^2 u) + \dots$, where τ_0 is the relaxation time and ∇u is a shorthand for derivatives of the hydrodynamic variables. The first term, δf_p^1 determines the viscosity and thermal conductivity, the second term determines second order transport coefficients, and so on. Each of these term has an expansion in powers of the density of the gas. In the case of the shear viscosity

$$\eta = \eta_0 \left[1 + \eta_1 (n \lambda_{dB}^3) + \eta_2 (n \lambda_{dB}^3)^2 + \dots \right], \quad (71)$$

where n is the density and λ_{dB} is the de Broglie wave length. Note that η_1 may contain terms of order l_{mfp}/λ_{dB} , but not terms of order l_{mfp}/L . Higher order terms in the density arise from a number of sources. The first is that the Boltzmann equation for the single particle distribution arises from truncating a set of classical or quantum equations for N -body distribution functions [170,27]. At leading order in the density the Boltzmann equation only contains two-body collisions, but at higher order it also includes collisions between three and more particles. The second source of corrections is the density expansion of the equation of state and the quasi-particle properties. In the case of the equation of state, the resulting expression is the well known virial expansion.

It was found that the expansion in density breaks down at the level of four-body collisions, and that resummation beyond effects already summed by the Boltzmann equation is required [172]. This leads to the appearance of terms that are logarithmic in the density, and to a breakdown of the Knudsen expansion. The latter can be traced to hydrodynamic modes, and is equivalent to the appearance of non-analytic terms in the gradient expansion.

In relativistic theories $n\lambda_{dB}^3 \sim 1$ and the only expansion parameter is the coupling constant. The structure of the perturbative expansion is not well understood. Only the heavy quark diffusion constant has been determined beyond leading order in the coupling constant [173]. The shear viscosity has been determined beyond leading logarithmic accuracy, i.e. the numerical coefficient inside the logarithm of g was computed [97].

Finally, we note that it was recently argued that one can organize kinetic theory in terms of separate power series expansion in Re^{-1} and Kn [174]. This corresponds to a situation where we view the Israel-Stewart model (or similar relaxation schemes) not only as practical implementation of second order hydrodynamics, but as resummed hydrodynamic theories that can be used in cases where the inverse Reynolds number is not small.

1.3 Matching and Kubo relations

9. Linear response and general covariance: In order to study linear response we have to couple the stress tensor Π_{ij} (or $\Pi_{\mu\nu}$ in the relativistic theory) to an external tensor field. From the symmetries of the stress tensor it is clear that this tensor transforms like the metric. We can therefore perform the analysis by considering fluid dynamics in a curved background. There is a large amount of literature on relativistic fluid dynamics in curved space [175]. The method can be extended to non-relativistic fluid dynamics using the formalism developed in [158]. Consider a three-dimensional metric $g_{ij}(t, \vec{x})$. A non-relativistic diffeomorphism is a time-dependent change of coordinates $x^i \rightarrow x^i + \xi^i(\vec{x}, t)$ that transforms the metric as $\delta g_{ij} = -g_{ik}\nabla_j \xi^k - g_{kj}\nabla_i \xi^k$.

The generally covariant Navier-Stokes equation is

$$\frac{1}{\sqrt{g}} \frac{\partial}{\partial t} (\sqrt{g} \rho u_i) + \nabla_k \Pi_i^k = 0, \quad (72)$$

where $g = \det(g_{ij})$ and ∇_k is the covariant derivative associated with the metric g_{ij} . The stress tensor is $\Pi_{ij} = \Pi_{ij}^0 + \delta \Pi_{ij}$, where $\Pi_{ij}^0 = \rho u_i u_j + P g_{ij}$ is the ideal fluid part, and $\delta \Pi_{ij}$ is the viscous correction. At one-derivative order we have $\delta \Pi_{ij} = -\eta \sigma_{ij} - \zeta g_{ij} \langle \sigma \rangle$ with [86]

$$\sigma_{ij} = \nabla_i u_j + \nabla_j u_i + \dot{g}_{ij} - \frac{2}{3} g_{ij} \langle \sigma \rangle, \quad (73)$$

$$\langle \sigma \rangle = \nabla \cdot u + \frac{\dot{g}}{2g}. \quad (74)$$

The structure of the extra terms involving time derivatives of the metric is dictated by diffeomorphism invariance [20].

Consider a ‘‘pure shear’’ perturbation $g_{ij}(\vec{x}, t) = \delta_{ij} + h_{ij}(\vec{x}, t)$ where the only non-vanishing component of h_{ij} is $h_{xy}(z, t)$. From the linearized Euler equation we can see that this perturbation does not induce a shift in the density, temperature, or velocity. This means that we can directly read off $\delta \Pi_{ij}$ from equ. (73) and (46). The induced stress determined the retarded correlation function via the linear response relation

$$\delta \Pi^{ij} = -\frac{1}{2} G_R^{ijkl} h_{kl}. \quad (75)$$

We find

$$G_R^{xyxy}(\omega, k) = P - i\eta\omega + \tau_R \eta \omega^2 - \frac{\kappa_R}{2} k^2 + O(\omega^3, \omega k^2), \quad (76)$$

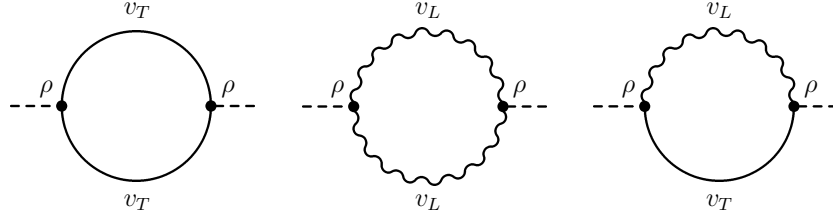


Figure 5: Diagrammatic representation of the leading contribution of thermal fluctuations to the stress tensor correlation function. Solid lines labeled v_T denote the transverse velocity correlator, dominated by the shear pole, and wavy lines labeled v_L denote the longitudinal velocity correlator, governed by the sound pole and the diffusive heat mode.

which is the Kubo relation quoted in the text. The analogous result in the relativistic theory is [38, 19]

$$G_R^{xyxy}(\omega, k) = P - i\eta\omega + \tau_R\eta\omega^2 - \frac{\kappa_R}{2}(k^2 - \omega^2) + O(\omega^3, \omega k^2), \quad (77)$$

The expansion in powers of ω and k maps onto the derivative expansion in hydrodynamics. We note, however, that the two point function G_R^{xyxy} only describes higher derivative terms that are linear in the hydrodynamic variables. There are a number of second order terms that encode non-linearities in the relation between stress and strain, in particular the coefficients $\lambda_{1,2,3}$ in equ. (46,49). Kubo relations for these transport coefficients can be derived by considering higher order terms in the response, which are related to retarded three point functions [176].

The idea of embedding the theory in curved space is also useful for computing the spectral function in kinetic theory. The Boltzmann equation in a four-dimensional curved space is [177]

$$\frac{1}{p^0} \left(p^\mu \frac{\partial}{\partial x^\mu} - \Gamma_{\alpha\beta}^i p^\alpha p^\beta \frac{\partial}{\partial p^i} \right) f(t, x, p) = C[f], \quad (78)$$

where $\Gamma_{\mu\nu}^\alpha$ is the Christoffel symbol associated with the four-dimensional covariant derivative ∇_μ , i, j, k are three-dimensional indices and μ, α, β are four-dimensional indices. In the non-relativistic limit this equation reduces to

$$\left(\frac{\partial}{\partial t} + \frac{p^k}{m} \frac{\partial}{\partial x^k} - \frac{\Gamma_{jk}^i p^j p^k}{m} \frac{\partial}{\partial p^i} - g^{il} \dot{g}_{lk} p^k \frac{\partial}{\partial p^i} \right) f(t, x, p) = C[f]. \quad (79)$$

The term involving \dot{g}_{ij} carries the information about the leading response to a time dependent shear strain. Using the BGK approximation to the collision operator gives the simple result for δf_p quoted in equ. (17). Together with the linear response relation (75) we obtain the spectral function

$$\eta(\omega) = -\frac{1}{\omega} \text{Im} G_R(\omega, 0) = \frac{\eta(0)}{1 + \omega^2 \tau_0^2}, \quad (80)$$

with $\eta(0) = \tau_0 n T$. A more detailed calculation that takes into account the momentum dependence can be found in [75], and a calculation using a T-matrix approximation can be found in [74]. A study of the QCD shear spectral function in kinetic theory is presented in [178].

10. *Fluctuations and the “breakdown” of second order fluid dynamics:* Non-analytic terms in the low energy expansion can be found by computing the low frequency behavior of the retarded correlator in fluid dynamics. In practice it is convenient to begin with the symmetrized correlation function

$$G_S^{xyxy}(\omega, \vec{k}) = \int d^3x \int dt e^{i(\omega t - \vec{k} \cdot \vec{x})} \left\langle \frac{1}{2} \{ \Pi_{xy}(t, \vec{x}), \Pi_{xy}(0, 0) \} \right\rangle, \quad (81)$$

and use the fluctuation-dissipation theorem. In the limit $\omega \rightarrow 0$ we have

$$G_S(\omega, \vec{k}) \simeq -\frac{2T}{\omega} \text{Im} G_R(\omega, \vec{k}). \quad (82)$$

At leading order in the gradient expansion $\Pi_{xy} = \rho u_x u_y$. We expand the hydrodynamic variables around their mean values, $\rho = \rho_0 + \delta\rho$ etc., and use the Gaussian approximation to write expectation values of products of fluctuating fields as products of two point functions. The leading contribution is

$$G_S^{xyxy}(\omega, 0) = \rho_0^2 \int \frac{d\omega'}{2\pi} \int \frac{d^3k}{(2\pi)^3} \left[\Delta_S^{xy}(\omega', \vec{k}) \Delta_S^{yx}(\omega - \omega', \vec{k}) + \Delta_S^{xx}(\omega', \vec{k}) \Delta_S^{yy}(\omega - \omega', \vec{k}) \right]. \quad (83)$$

where Δ_S^{ij} is the symmetrized velocity correlation function

$$\Delta_S^{ij}(\omega, \vec{k}) = \int d^3x \int dt e^{i(\omega t - \vec{k} \cdot \vec{x})} \left\langle \frac{1}{2} \{ u^i(t, \vec{x}), u^j(0, 0) \} \right\rangle. \quad (84)$$

We can view equ. (83) as a one-loop diagram composed of two propagators of hydrodynamic modes, see Fig. 5. Using the low frequency limit of the fluctuation-dissipation relation we can write the one-loop contribution to the retarded correlation function as

$$G_R^{xyxy}(\omega, 0) = \rho_0^2 \int \frac{d\omega'}{2\pi} \int \frac{d^3k}{(2\pi)^3} \left[\Delta_R^{xy}(\omega', \vec{k}) \Delta_S^{yx}(\omega - \omega', \vec{k}) + \Delta_S^{xy}(\omega', \vec{k}) \Delta_R^{yx}(\omega - \omega', \vec{k}) \right. \\ \left. + \Delta_R^{xx}(\omega', \vec{k}) \Delta_S^{yy}(\omega - \omega', \vec{k}) + \Delta_S^{xx}(\omega', \vec{k}) \Delta_R^{yy}(\omega - \omega', \vec{k}) \right]. \quad (85)$$

This result can be generalized. Retarded correlation functions of hydrodynamic variables have diagrammatic expansions in terms of retarded and symmetrized correlation functions, see [160, 152, 161, 162]. The velocity correlation function can be decomposed into longitudinal and transverse parts

$$\Delta_{S,R}^{ij}(\omega, \vec{k}) = \left(\delta^{ij} - \hat{k}^i \hat{k}^j \right) \Delta_{S,R}^T(\omega, \vec{k}) + \hat{k}^i \hat{k}^j \Delta_{S,R}^L(\omega, \vec{k}). \quad (86)$$

The transverse part is purely diffusive. The symmetrized correlation function is given by [179]

$$\Delta_S^T(\omega, \vec{k}) = \frac{2T}{\rho} \frac{D_\eta k^2}{\omega^2 + (D_\eta k^2)^2}, \quad (87)$$

$$\Delta_R^T(\omega, \vec{k}) = \frac{1}{\rho} \frac{-D_\eta k^2}{-i\omega + D_\eta k^2}, \quad (88)$$

where $k = |\vec{k}|$ and $D_\eta = \eta/\rho$ is the momentum diffusion constant. The longitudinal part describes propagating sound modes and diffusive heat modes. The complete calculation of the one-loop diagram is described in [22]. Here, we briefly outline the computation of the contribution due to

shear modes. We use the propagators given in equ. (87,88) and perform the integral over ω' by contour integration. We get

$$G_R^{xyxy}(\omega, 0)|_{shear} = -\frac{7T}{30\pi^2} \int dk \frac{k^4}{k^2 - i\omega/(2D_\eta)}. \quad (89)$$

This integral is divergent in the UV. We regulate the divergence by introducing a momentum cutoff Λ_K . We then expand the retarded correlation function in the limit $\omega \rightarrow 0$. We find

$$G_R^{xyxy}(\omega, 0)|_{shear} = -\frac{7}{90\pi^2} T \Lambda_K^3 - i\omega \frac{7T\Lambda_K}{60\pi^2 D_\eta} + (1+i)\omega^{3/2} \frac{7T}{240\pi D_\eta^{3/2}} + O(\omega^{5/2}). \quad (90)$$

Including the contribution of sound modes changes the coefficient of the $i\omega$ term to $17/120$, and the coefficient of the $\omega^{2/3}$ term to $(7 + (\frac{3}{2})^{3/2})/240$. Comparing equ. (90) to the Kubo formula we observe that the first term is a contribution to the pressure, the second renormalizes the viscosity, and the third is a non-analytic term not captured by the classical linear response formula.

Equation (90) has a number of interesting aspects. First, we note that the fluctuation contribution to the shear viscosity scales inversely with the bare shear viscosity. This leads to the bound on the shear viscosity discussed in the text, see equ. (27). The fluctuation contribution depends on the cutoff. This is consistent with the idea that fluid dynamics is renormalizable in the effective theory sense, because the dependence on Λ_K can be absorbed into the cutoff dependence of the bare viscosity. We also note that the non-analytic term is independent of the cutoff. This is important because there are no bare parameters in the hydrodynamic description that could be used to absorb the cutoff dependence of the $\omega^{3/2}$ term. Finally, we emphasize that the presence of a non-analytic term does not imply a breakdown of hydrodynamics. It only implies that beyond the Navier-Stokes order in three dimensions, and beyond ideal hydrodynamics in two dimensions, fluctuations have to be included.

The structure of the retarded correlation function also implies a low energy theorem for the spectral function. Taking into account both shear and sound modes we get

$$\eta(\omega) = \eta(0) - \sqrt{\omega} T \frac{7 + (\frac{3}{2})^{3/2}}{240\pi D_\eta^{3/2}}. \quad (91)$$

This prediction is reliable in the regime of validity of fluid dynamics, which implies $\omega \ll nT/\eta$. A similar non-analytic structure also appears in the relativistic theory, see [21].

1.4 Models of fluids: Holography

11. Strong coupling results: The leading correction to the infinite coupling limit of η/s in $\mathcal{N} = 4$ SUSY Yang Mills theory is [180, 181, 182, 183]

$$\frac{\eta}{s} = \frac{1}{4\pi} \left\{ 1 + \frac{15\zeta(3)}{\lambda^{3/2}} + \dots \right\}. \quad (92)$$

where $\lambda = g^2 N_c$ is the 't Hooft coupling. We observe that the $\lambda^{-2/3}$ correction is positive, consistent with the idea that η/s evolves smoothly from strong to weak coupling. At weak coupling $\eta/s \sim 1/[\lambda^2 \log(\lambda)]$, see [184]. It is not clear how λ should be chosen in order to make predictions for the

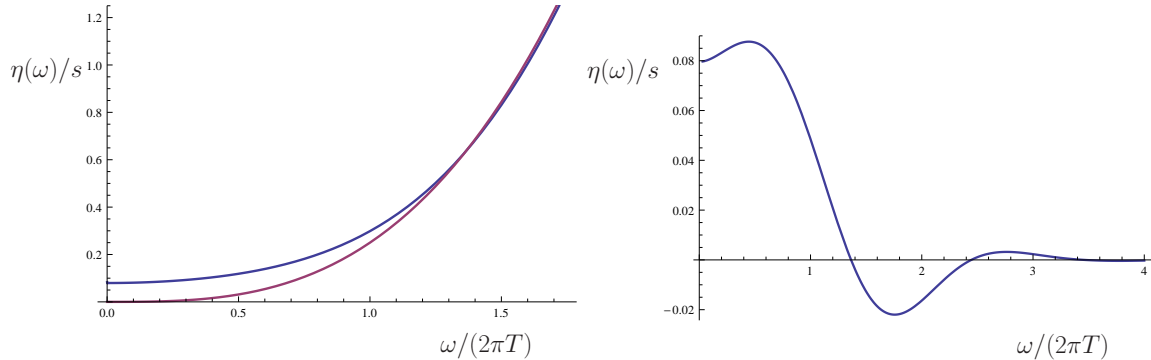


Figure 6: Viscosity spectral function in the large N_c limit of strongly coupled $\mathcal{N} = 4$ SUSY Yang Mills theory, computed using the AdS/CFT correspondence. The left panel shows $\eta(\omega)/s$ (blue) and $\eta_{T=0}(\omega)/s$ (red) as a function of ω . The right panel shows the finite temperature contribution $[\eta(\omega) - \eta_{T=0}(\omega)]/s$.

quark gluon plasma in the vicinity of T_c . For $\alpha_{SYM} \sim 0.3$ and $N_c = 3$ we get $\lambda \sim 10$ and the next order term increases η/s by about 50%.

The AdS/CFT correspondence has been used to compute the second order hydrodynamic coefficients defined in equ. (49). The result is [19, 51, 185]

$$\tau_R = \frac{2 - \log 2}{2\pi T}, \quad \lambda_1 = \frac{\eta}{2\pi T}, \quad \lambda_2 = -\frac{\eta \log 2}{\pi T}, \quad \lambda_3 = 0, \quad \kappa_R = \frac{\eta}{\pi T}, \quad (93)$$

The coefficients τ_R and κ_R can be determined from the retarded two-point function, see equ. (101). The remaining coefficients have been computed using the fluid-gravity correspondence [51], as well as using the Kubo formula combined with the three-point function for the stress tensor in AdS/CFT [185].

The relaxation time is very short, $\tau_R \sim 1/T$, but $(\tau_R T)/(\eta/s)$ is not very different from the result in perturbative QCD, see equ. (134). The coefficient λ_3 corresponds to the vorticity squared term in the stress tensor. In kinetic theory this term does not appear because the second order terms are induced by the first order stresses $\delta\Pi_{\mu\nu} \sim \sigma_{\mu\nu}$. As a result, we can get $D\sigma_{\mu\nu}$, $\sigma_{\mu\lambda}\sigma_{\nu}^{\lambda}$ and $\sigma_{\mu\lambda}\Omega_{\nu}^{\lambda}$, but not $\Omega_{\mu\lambda}\Omega_{\nu}^{\lambda}$. The sign of λ_1 and λ_2 can also be understood in kinetic theory [186]. In AdS/CFT there is no obvious reason why $\lambda_1 > 0$, $\lambda_2 < 0$ and $\lambda_3 = 0$.

$\mathcal{N} = 4$ SUSY Yang Mills theory has a conserved gauge invariant density called R-charge. Son and Starinets computed the shear viscosity and entropy density as a function of the R-charge chemical potential μ . They find that both η and s depend on μ , but the ratio η/s does not [187]. They also determine the thermal conductivity

$$\kappa = \frac{8\pi^2 T}{\mu^2} \eta. \quad (94)$$

The scaling $\kappa \sim 1/\mu^2$ is related to the definition of κ in the Landau frame and also appears in kinetic theory. The diffusion constant of a heavy test quark in the SUSY Yang Mills plasma was calculated in [58, 59, 60]. The result is

$$D = \frac{2}{\pi T} \frac{1}{\sqrt{\lambda}}, \quad (95)$$

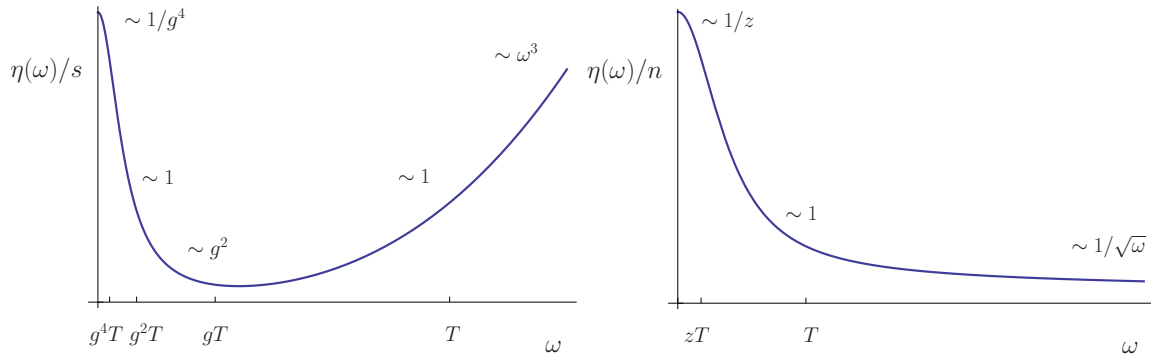


Figure 7: Schematic behavior of the viscosity spectral function in QCD (left panel) and a dilute Fermi gas (right panel). In QCD we plot $\eta(\omega)/s$ as a function of ω . The relevant scales are g^4T (momentum relaxation) $\ll g^2T$ (magnetic screening) $\ll gT$ (electric screening) $\ll T$, where g is the coupling constant. In the dilute Fermi gas η is normalized to the density n , and the momentum relaxation scale $zT \ll T$ involve powers of the fugacity z .

which depends on the value of the coupling λ , and goes to zero in the strong coupling limit. The functional dependence on λ is unusual from the point of view of perturbation theory, which would suggest that D scales as $1/\lambda^2$, and that D is proportional to the momentum diffusion constant $\eta/(sT)$.

$\mathcal{N} = 4$ SUSY Yang Mills theory is scale invariant and the bulk viscosity of the SUSY plasma vanishes. Non-conformal generalizations of the AdS/CFT correspondence have been studied. Buchel proposed that in holographic models there is a lower bound on the bulk viscosity, $\zeta \geq 2(\frac{1}{3} - c_s^2)\eta$, where c_s is the speed of sound [188]. This is in contrast to the weak coupling result $\zeta \sim (\frac{1}{3} - c_s^2)^2\eta$ [175]. Gubser and collaborators considered a number of holographic models tuned to reproduce the QCD equation of state, and find that ζ/s has a maximum near the critical temperature where $\zeta/s \simeq 0.05$ [189, 190].

12. Spectral function and quasi-normal modes: The viscosity spectral function in the strong coupling limit of $\mathcal{N} = 4$ SUSY Yang Mills theory can be computed from the solution of wave equation AdS_5 , see equ. (24). We have defined $\delta g_x^y = \phi_k(u)e^{ikx-i\omega t}$. The infalling solution can be written as

$$\phi_k(u) = (1-u)^{-i\mathfrak{w}/2} F_k(u) \quad (96)$$

where $\mathfrak{w} = \omega/(2\pi T)$ and we have factored out the near horizon behavior. The function $F_k(u)$ can be determined as an expansion in \mathfrak{w} and $\mathfrak{k} = k/(2\pi T)$. At order $O(\mathfrak{w}^2, \mathfrak{k}^2)$ the solution is [42]

$$F_k(u) = 1 - \frac{i\mathfrak{w}}{2} \log\left(\frac{1+u}{2}\right) + \frac{\mathfrak{w}^2}{8} \left\{ \left[8 - \frac{8\mathfrak{k}^2}{\mathfrak{w}^2} + \log\left(\frac{1+u}{2}\right) \right] \log\left(\frac{1+u}{2}\right) - 4Li_2\left(\frac{1-u}{2}\right) \right\}. \quad (97)$$

The wave equation can also be solved analytically in the limit of large $\mathfrak{w}, \mathfrak{k}$ [43]. For $\mathfrak{k} = 0$ we get

$$\phi_k(u) = \pi\mathfrak{w}^2 \frac{u}{\sqrt{1-u^2}} [iJ_2(2\mathfrak{w}\sqrt{u}) - Y_2(2\mathfrak{w}\sqrt{u})]. \quad (98)$$

For intermediate values of \mathfrak{w} and \mathfrak{k} the wave equation can be solved numerically, for example by

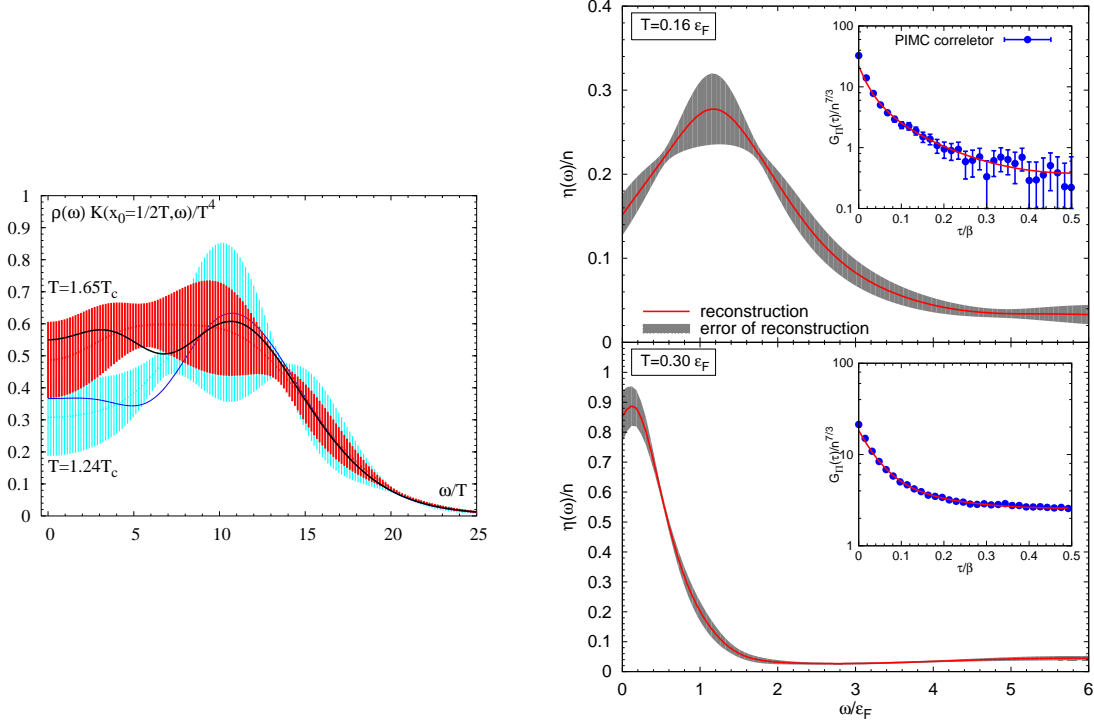


Figure 8: Numerical determination of the viscosity spectral function in QCD [31] (left panel) and a dilute Fermi gas [35] (right panel). In the QCD case the plot shows $\rho(\omega)/[\sinh(\beta\omega/2)T^4]$ with $\rho(\omega) = \omega\eta(\omega)$. The method for determining the error band is explained in [31]. The intercept at $\omega = 0$ corresponds to the values of η/s quoted in Sect. 3. The spectral function $\eta(\omega)$ of the unitary gas is normalized to the density n and computed at two different temperatures $T = 0.16\epsilon_F$ and $T = 0.3\epsilon_F$, where $\epsilon_F = k_F^2/(2m)$ with $k_F = (3\pi^2n)^{1/3}$ is the Fermi energy. See [35] for a discussion of the error bands shown in gray. The insets show the underlying imaginary time correlation function.

starting from the near horizon behavior given in equ. (96) and integrating outwards towards the boundary. The retarded correlation function is determined by the variation of the boundary action with respect to the field. The relevant term in the action is

$$S = -\frac{\pi^2 N^2 T^4}{8} \int du \int d^4x \frac{f(u)}{u} (\partial_u \phi)^2 + \dots \quad (99)$$

This is the quadratic part of the Einstein-Hilbert action, where we have used the AdS/CFT correspondence to express Newton's constant in terms of gauge theory parameters. The boundary action can be derived by integrating by parts. The retarded Green function is given by the second variational derivative with respect to the boundary value of the field [42, 187],

$$G_R(\mathbf{w}, \mathbf{k}) = -\frac{\pi^2 N^2 T^4}{4} \left[\frac{f(u) \partial_u \phi_k(u)}{u \phi_k(u)} \right]_{u \rightarrow 0}. \quad (100)$$

In the low frequency, low momentum limit [19]

$$G_R(\mathbf{w}, \mathbf{k}) = -\frac{\pi^2 N^2 T^4}{4} \left[-\frac{1}{2} + i\mathbf{w} - \mathbf{w}^2 (1 - \log(2)) + \mathbf{k}^2 \right] + \dots \quad (101)$$

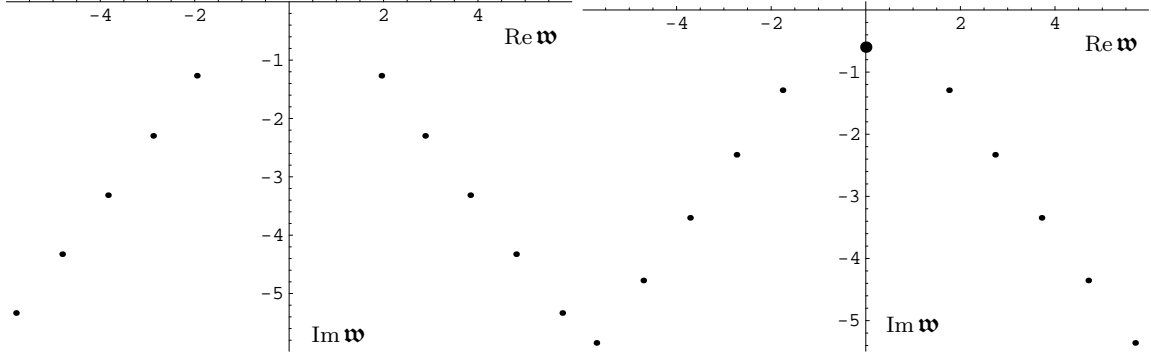


Figure 9: Quasi-Normal modes of gravitational fluctuations around the AdS_5 black hole solution, from [191]. The left panel shows the correlator in the scalar channel G_R^{xyxy} (for $\vec{k} = k\hat{z}$), and the right panel shows G_R^{zzzz} . The plots show the location of poles in the complex \mathfrak{w} plane for $\mathfrak{k} = 1$. Note that G_R^{zzzz} has a hydrodynamic pole at $\mathfrak{w} \simeq -i\bar{\gamma}\mathfrak{k}^2$ with $\bar{\gamma} = 2\pi\eta/s$.

Comparing to the Kubo relation (77) we obtain the relaxation time in equ. (93). The spectral function $\eta(\omega) = -\omega^{-1}Im G_R(\omega, k=0)$ is shown in the left panel of Fig. 6. In the right panel we show the finite temperature contribution $\eta(\omega) - \eta_{T=0}(\omega)$, and in the left panel of Fig. 7 we show the qualitative behavior of the spectral function in the weak coupling limit. The AdS/CFT result has a number of interesting features:

1. The spectral function does not have a quasi-particle peak. The low energy limit $\eta(0) = s/(4\pi)$ is smoothly connected to the high energy limit $\eta(\omega) \sim T^3$.
2. The tail of the finite temperature part of the spectral function oscillates in sign. The result is consistent with the sum rule given in equ. (36), and there is no fundamental requirement that $\eta(\omega) - \eta_{T=0}(\omega)$ has to be positive.
3. The curvature of the spectral function near the origin is positive. This is different from the result in kinetic theory. Note that in kinetic theory the downward curvature is determined by the viscous relaxation time τ_R . In particular, the decrease in $\eta(\omega)$ can be understood as resulting from the lag between the strain σ_{xy} and the viscous stress $\delta\Pi_{xy}$. However, in general there is no direct relation between τ_R and the curvature of $\eta(\omega)$. The Kubo formula relates τ_R to the ω^2 term in $Re G_R$, whereas the curvature is determined by the ω^3 term in $Im G_R$.

Whether these features are present in the QCD spectral function near T_c is unclear. The stress tensor spectral function is not directly accessible in experiment, and the determination of $\eta(\omega)$ on the lattice is difficult because of the finite resolution of the lattice and the need for analytic continuation. The spectral function extracted in [31] is shown in the left panel of Fig. 8. There is no quasi-particle peak, but the resolution is not very good, and the continuum is strongly modified by cutoff effects.

We can also study the location of the poles of $G_R(\omega)$ in the complex plane. Poles of the retarded correlator that approach the origin as $k \rightarrow 0$ are related to hydrodynamic modes, and poles that remain at a finite distance from the origin determine corrections to hydrodynamic behavior. Near

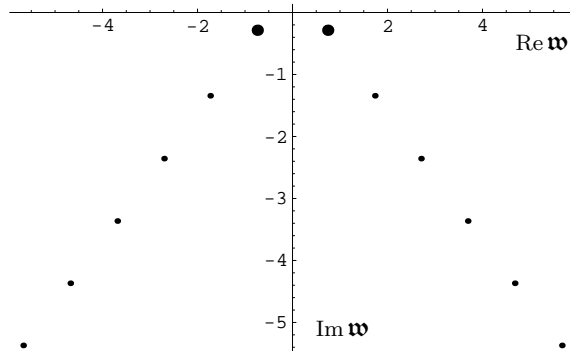


Figure 10: Quasi-Normal modes of gravitational fluctuations around the AdS_5 black hole solution. This figure shows the correlation function G_R^{zzzz} (for $\vec{k} = k\hat{z}$). The plots show the location of poles in the complex w plane for $\mathfrak{k} = 1$. The correlator has a hydrodynamic pole at $w \simeq \pm c_s \mathfrak{k} - i\bar{\gamma}_s \mathfrak{k}^2$ with $\bar{\gamma}_s = \frac{2}{3}\bar{\gamma}$.

the boundary $u = 0$ the function $\phi_k(u)$ can be written as

$$\phi_k(u) = \mathcal{A}(\omega, k)[1 + \dots] + \mathcal{B}(\omega, k)[u^2 + \dots]. \quad (102)$$

Equ. (100) implies that $G_R(\omega, k) \sim \mathcal{B}(\omega, k)/\mathcal{A}(\omega, k)$, and poles of $G_R(\omega, k)$ correspond to zeros of $\mathcal{A}(\omega, k)$. In this case $\phi_k(u)$ satisfies a Dirichlet problem on the boundary, and infalling conditions on the horizon. The corresponding frequencies ω are known as quasi-normal modes.

The quasi-normal mode spectrum of the AdS_5 black hole was determined in [46, 192, 191]. We show some of the results in Fig. 9 and 10. Poles of $G_R^{xyxy}(\omega, k)$ are shown in the left panel of Fig. 9. We observe that quasi-normal modes occur in pairs. Asymptotically, the position of the poles in the limit $\mathfrak{k} = 0$ is given by

$$w_n^\pm = (\pm 0.607 - 0.389i) \pm n(1 \mp i), \quad (103)$$

for integer n [46]. This implies that the regime of validity of the hydrodynamic expansion is indeed given by $\omega \lesssim \pi T$. The right panel of Fig. 9 and Fig. 10 also show the hydrodynamic modes

$$w \simeq -i\bar{\gamma}\mathfrak{k}^2, \quad w \simeq \pm c_s \mathfrak{k} - i\bar{\gamma}_s \mathfrak{k}^2, \quad (104)$$

with $\bar{\gamma} = 2\pi\eta/s$ and $\bar{\gamma}_s = \frac{2}{3}\bar{\gamma}$. The first mode is a diffusive shear mode, and the second is a sound wave. The AdS/CFT correspondence can be used to follow the sound mode beyond the hydrodynamic regime. For large $\mathfrak{k} \gg 1$ the speed of sound goes to one, and sound attenuation is small, see Fig. 11 [191].

1.5 Viscosity bounds

13. Dimensionless ratios: η/s or η/n ? It is not immediately obvious which dimensionless ratio we should consider in connection with possible bounds for the shear viscosity [7, 193]. The kinetic theory argument establishes a possible bound for η/n , but the AdS/CFT correspondence and the theory of hydrodynamic fluctuations establish limits on η/s . We cannot resolve this question here, as none of the proposed bounds have been rigorously proven. We note, however, that the ratio

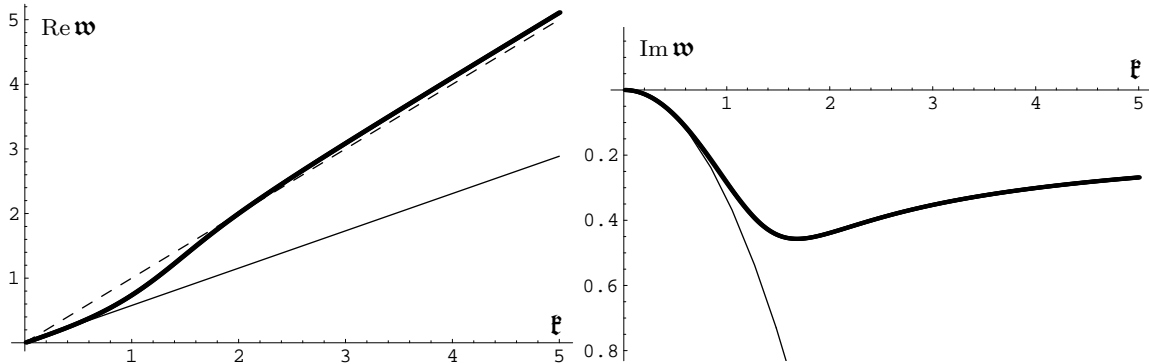


Figure 11: Real and imaginary parts of the sound wave frequency as a function of the sound wave momentum in the strong coupling limit of $\mathcal{N} = 4$ SUSY Yang Mills theory, computed using the AdS/CFT correspondence. Light curves correspond to the hydrodynamic approximation for small k . The dashed line is $\omega = k$. Note that in the regime where the imaginary part is large there is a range of momenta for which $\partial \text{Re}(\omega)/\partial k > 1$.

η/s is well defined for all fluids, whereas η/n can only be defined for fluids with a conserved particle number. Even though η/s was initially introduced for relativistic fluids, it has a smooth non-relativistic limit. Indeed, holographic dualities provide examples of non-relativistic fluids with $\eta/s = 1/(4\pi)$ [194, 195].

If we accept the idea that the basic measure of fluidity is η/s , then we have to address the possibility of driving η/s to zero by increasing the entropy per particle. This can be done, for example, by considering a dilute gas composed of a large number of different species [6, 53, 196]. We first note that in practice it is quite difficult to reduce η/s in this way, because increasing s/n by a factor ξ requires the number of species to grow by a factor e^ξ [197]. We also note that a dilute gas composed of an exponentially large number of species is a very unusual fluid [198], as the time to reach mechanical equilibrium via diffusion of momentum is much shorter than the time required to reach thermal equilibrium. In particular, it takes an exponentially long time for the system to reach the equilibrium entropy starting from a generic non-equilibrium state.

Despite these caveats there is no obstacle that prevents us from constructing a fluid with e^ξ degrees of freedom in non-relativistic quantum mechanics. Whether these models can be embedded in a relativistic field theory is not clear. An ingenious construction was suggested in [53], but the proposed system is not stable on time scales required to observe the large mixing entropy [198].

2 Nonrelativistic fluids

2.1 The unitary Fermi gas

14. Transport properties of the dilute Fermi gas: In kinetic theory we can not only compute the shear viscosity of the dilute Fermi gas at unitarity, but also other transport properties like the thermal conductivity, the spin diffusion constant, and the bulk viscosity. Suitable ratios of these quantities provide additional information on quasi-particle properties. The thermal conductivity is

[199]

$$\kappa = \frac{225}{128\sqrt{\pi}} m^{1/2} T^{3/2}. \quad (105)$$

The relative magnitude of thermal and momentum diffusion is characterized by the Prandtl number $Pr = c_P \eta / (\rho \kappa)$, where c_P is the specific heat at constant pressure. The Prandtl number determines, for example, the relative importance of shear viscosity and thermal conductivity in sound attenuation. In the high temperature limit we find $Pr = 2/3$, which is equal to the Prandtl ratio of a weakly interacting gas. If the shear viscosity of the gas is known the thermal conductivity can be extracted from the sound attenuation length. The speed of sound has been measured by a number of groups [200], but the sound attenuation length has not been measured.

The spin diffusion constant is defined by Fick's law,

$$\vec{j}_s = -D_s \vec{\nabla} M, \quad (106)$$

where \vec{j}_s is the spin current, and $M = n_\uparrow - n_\downarrow$ is the polarization. A calculation of the diffusion constant in kinetic theory gives [201]

$$D_s = \frac{3}{16\sqrt{\pi}} \frac{(mT)^{3/2}}{mn}. \quad (107)$$

The spin diffusion constant decreases as the temperature is lowered. Near the critical temperature D_s is expected to approach the universal value $D_s \sim \hbar/m$, where we have reinstated Planck's constant. Quantum limited spin diffusion was observed experimentally in [202], see also [203]. The experiment is based on observing the late time relaxation of two colliding clouds of spin up and down fermions. It is interesting to compare the result $D_s \sim \hbar/m$ to the observed shear viscosity near T_c . The momentum diffusion constant is $D_\eta = \eta/(mn)$. In the vicinity of T_c we have $\eta/s \simeq 0.5\hbar/k_B$ and $s/n \simeq k_B$. These numbers imply $D_\eta \simeq 0.5\hbar/m$, and we conclude that the spin and momentum diffusion constants are comparable. A similar correlation between the heavy quark and momentum diffusion constants can be studied in the quark gluon plasma, see below.

The dilute Fermi gas at unitarity is scale invariant and the bulk viscosity vanishes [86]. The leading contribution to the bulk viscosity near $a = \infty$ can be computed systematically in the high temperature limit. The result is [69]

$$\zeta = \frac{1}{96\pi^{5/2}} (mT)^{3/2} \left(\frac{z\lambda_{dB}}{a} \right)^2, \quad (108)$$

where z is the fugacity and λ_{dB} is the de Broglie wave length. This result is consistent with the assumption that the bulk viscosity scales as the shear viscosity multiplied by the square of the departure from scale invariance in the equation of state, $\zeta \sim \eta(P - \frac{2}{3}\mathcal{E})^2$.

The physical mechanism for generating bulk viscosity is somewhat subtle. Bulk viscosity can arise in elastic two-body collisions provided the quasi-particle self energy has a momentum dependent contribution that violates scale invariance. In this case the equilibrium distribution function is not only a function of $p^2/(mT)$. As the gas expands two-body collisions are needed to reestablish the correct equilibrium distribution. Since the collisions rate is finite the resulting lag will lead to a non-equilibrium contribution to the pressure and a non-zero bulk viscosity.

Second order transport coefficients are given by [204]

$$\eta\tau_R = \frac{\eta^2}{P}, \quad \lambda_1 = \frac{15\eta^2}{14P}, \quad \lambda_2 = -\frac{\eta^2}{P}, \quad \lambda_3 = 0, \quad (109)$$

where τ_R is the viscous relaxation time, and λ_{123} are the coefficients of non-linear terms defined in equ. (46). The result for τ_R shows that the expansion parameter of the gradient expansion is indeed ω/ω_{fl} with $\omega_{fl} = P/\eta$. The expressions for the second order coefficients can be compared to the analogous results for a quark gluon plasma, see equ. (134). We observe that, in units of η^2/P , the results are very similar.

15. Spectral function: The schematic behavior of the shear viscosity spectral function in the high temperature limit is shown in the right panel of Fig. 7. The low frequency behavior is obtained in kinetic theory, see equ. (80). The high frequency behavior $\eta(\omega) \sim 1/\sqrt{\omega}$ was first determined, up to an overall factor, using the high frequency behavior of the f-sum rule [76]. The correct prefactor was computed in [74] based on a T-matrix approach.

A more general method for studying the high frequency behavior of spectral functions is based on the operator product expansion (OPE) [205, 78] (see [101] for an OPE study of the viscosity spectral function in QCD). The basic idea can be explained using the current correlation function as an example. Indeed, since the transverse current correlator has a diffusive pole, it is possible to extract $\eta(\omega)$ from the current correlation function. Consider the operator product

$$A_{ij}^{\sigma\sigma'}(\omega, \vec{q}) = \int dt \int d^3r \int d^3R e^{i(\omega t - \vec{q} \cdot \vec{r})} T \left[j_i^\sigma \left(\vec{R} + \frac{\vec{r}}{2}, t \right) j_{i'}^{\sigma'} \left(\vec{R} - \frac{\vec{r}}{2}, 0 \right) \right], \quad (110)$$

where $j_i^\sigma = -i/(2m)\psi_\sigma^\dagger \overleftrightarrow{\nabla}_i \psi_\sigma$ is the current operator and T is the time ordering symbol. The OPE proceeds by expanding the operator product in a series of local operators [78],

$$A_{ij}^{\sigma\sigma'}(\omega, \vec{q}) = \sum_{k,\alpha} \frac{1}{\omega^{\Delta_k/2-3/2}} c_{ij\alpha}^{(k)} \left(\frac{q^2}{2m\omega}, \frac{a^{-1}}{\sqrt{m\omega}} \right) \int d^3R \mathcal{O}_\alpha^{(k)}(\vec{R}) \quad (111)$$

where $\mathcal{O}_\alpha^{(k)}$ is an operator labeled by k , and α is a set of indices that the operator may carry. Δ_k denotes the scaling dimension of the operator defined by $\mathcal{O}_\alpha^{(k)}(\lambda\vec{x}, \lambda^2 t) = \lambda^{-\Delta_k} \mathcal{O}_\alpha^{(k)}(\vec{x}, t)$. Current correlation functions are determined by taking thermal averages of equ. (111). This implies that the frequency and momentum dependence is determined by the coefficient functions $c_{ij\alpha}^{(k)}$, and the density and temperature dependence is carried by the expectation values of the local operators $\mathcal{O}_\alpha^{(k)}$. The simplest local operator is the density $n(\vec{x}, t)$ with $\Delta_n = 3$. Other one-body operators are the current j_i and the stress tensor $\pi_{ij} = 1/(2m)\psi_\sigma^\dagger \overleftrightarrow{\nabla}_i \overleftrightarrow{\nabla}_j \psi_\sigma$.

Short range correlations are described by two-body operators. The simplest operator is the contact density [77]

$$\hat{\mathcal{C}} = m^2 C_0^2 \psi_\uparrow^\dagger \psi_\downarrow^\dagger \psi_\downarrow \psi_\uparrow. \quad (112)$$

The contact density has scaling dimension $\Delta_C = 4$, which agrees with naive dimensional analysis. The crucial observation is that \mathcal{C} as defined in equ. (112) has UV finite matrix elements even though C_0 and $\psi_\uparrow^\dagger \psi_\downarrow^\dagger \psi_\downarrow \psi_\uparrow$ are divergent. This can be seen, for example, using the effective lagrangian give in equ. (28). This lagrangian can be written in a partially bosonized form as

$$\mathcal{L} = \psi^\dagger \left(i\partial_0 + \frac{\vec{\nabla}^2}{2m} \right) \psi + [\psi_\uparrow \psi_\downarrow \Phi^\dagger + h.c.] + \frac{1}{C_0} (\Phi \Phi^\dagger). \quad (113)$$

We note that the equation of motion for the bosonic field is $\Phi = -C_0 \psi_\uparrow \psi_\downarrow$, so the contact density is $\hat{\mathcal{C}} = m^2 \Phi^\dagger \Phi$. At zero chemical potential we can compute the propagator for Φ exactly, see for

example [69]. We get

$$D(\omega, \vec{q}) = \frac{4\pi}{m^{3/2}} \frac{i}{\sqrt{\omega - \frac{q^2}{4m} + i\epsilon}}. \quad (114)$$

The scaling dimension of \mathcal{C} can be extracted from the Fourier transform of this result. We find $\Delta_{\mathcal{C}} = 4$.

Having identified the relevant operators we can now study the OPE for the current correlation function

$$G_{ij}(\omega, \vec{q}) = \frac{i}{2} \sum_{\sigma\sigma'} \langle A_{ij}^{\sigma\sigma'}(\omega, \vec{q}) \rangle. \quad (115)$$

Using the equation of motion for the momentum density, $\partial_t \pi_i = -\nabla_j \Pi_{ij}$, we can relate the shear viscosity to the retarded transverse correlation function,

$$\eta(\omega) = m^2 \lim_{q \rightarrow 0} \frac{\omega}{q^2} \text{Im} G_T(\omega, \vec{q}), \quad (116)$$

where G_T is defined as in equ. (86). The behavior of G_T at large ω is determined by the lowest dimension operator in the OPE. We note, however, that one-body operators like the density lead to diagrams in which all the momentum flows through a single fermion line. This means that the imaginary part is a delta-function. The tail of the spectral function is therefore dominated by the leading two-body operator, which is the contact density. Using $\Delta_{\mathcal{C}} = 4$ we get

$$\eta(\omega) \sim \frac{\mathcal{C}}{\sqrt{m\omega}}, \quad (117)$$

where $\mathcal{C} = \langle \hat{\mathcal{C}} \rangle$. The appearance of a non-analytic dependence on ω is interesting. The numerical coefficient in equ. (117) is $1/(15\pi)$, see [74, 78]. The expectation value \mathcal{C} is a non-perturbative quantity that can be measured experimentally [206], or extracted from quantum Monte Carlo calculations [207]. In the high temperature limit \mathcal{C} can be computed using the virial expansion, $\mathcal{C} = 4\pi n^2 \lambda_{dB}^2$ [208].

Knowledge of the large frequency behavior of $\eta(\omega)$ is important for quantum Monte Carlo studies of the shear viscosity, and for identifying consistent many-body approaches to transport theory. It is not clear how the large frequency behavior of $\eta(\omega)$ can be measured. However, the analogous tail in the dynamic structure factor can be studied experimentally, see [209].

16. Nonrelativistic AdS/CFT correspondence: There have been a number of attempts to extend the AdS/CFT correspondence to non-relativistic fluids. The idea proposed in [210,211] is to embed a $d+1$ non-relativistic theory into a $d+2$ dimensional relativistic theory. Consider the Minkowski metric in light cone coordinates (x^+, x^-, x^i) with $x^\pm = (x^0 \pm x^{d+1})/\sqrt{2}$ for $i = 1, \dots, d$. We have

$$ds^2 = \eta_{\mu\nu} dx^\mu dx^\nu = -2dx^+ dx^- + dx^i dx^i. \quad (118)$$

The equation of motion of a massless scalar field is given by

$$\left(-2 \frac{\partial}{\partial x^-} \frac{\partial}{\partial x^+} + \frac{\partial^2}{\partial x_i^2} \right) \phi(x) = 0. \quad (119)$$

We now compactify the theory on a light-like circle, $\phi(x^-) = \phi(x^- + 2\pi/m)$. The winding number one mode is given by $\phi(x) \sim e^{-imx^-} \psi(x^+, x_i)$ where ψ satisfies the Schrödinger equation

$$\left(i \frac{\partial}{\partial x^+} + \frac{\vec{\nabla}^2}{2m} \right) \psi(x^+, x_i) = 0. \quad (120)$$

In terms of symmetries this construction shows that the non-relativistic conformal group in $d + 1$ dimensions, the Schrödinger group $Sch(d)$ [212,213], can be embedded in $SO(d+2, 2)$, the conformal group in $d + 2$ dimensions.

This idea can be applied to spaces that are asymptotically AdS. The specific proposal described in [210,211] is that the $Schr(d)$ symmetry of a non-relativistic $d + 1$ dimensional conformal field theory can be mapped onto the isometries of the $d + 3$ dimensional metric

$$ds^2 = r^2 \left(-2dx^+ dx^- - \beta^2 r^2 (dx^+)^2 + (dx^i)^2 \right) + \frac{dr^2}{r^2}, \quad (121)$$

which reduces to the metric of AdS_{d+3} in the limit $\beta \rightarrow 0$. This metric can be obtained in type IIB string theory starting from geometries of the form $AdS_{d+3} \times \mathcal{X}$, where \mathcal{X} is a compact manifold [195,194,214]. The construction can be extended to AdS Schwarzschild black holes. If we start from AdS_5 we obtain a strongly coupled $2 + 1$ dimensional conformal field theory. This theory has an unusual equation of state, $P \sim T^4/\mu^2$ [194], but it can be shown that the fluid saturates the KSS bound, $\eta/s = 1/(4\pi)$ [195,194]. The method of light-like compactifications can also be used to establish a non-relativistic version of the fluid gravity correspondence [215]. The equations of conformal fluid dynamics obtained in this way obey constraints that go beyond those that follow from Galilean invariance and conformal symmetry alone [20], which suggest that the light cone method is too restrictive.

A new idea for constructing non-relativistic holographic theories is based on Horava-Lifshitz gravity, see [216,217]. Another proposal is based on Vasiliev theory, a gravitational theory with higher spin gauge fields [218]. These theories are very interesting, but it remains to be seen whether they provide more realistic models of non-relativistic fluids. We should note that it may be difficult to realize a holographic dual of the dilute Fermi gas at unitarity. One reason is that the unitary gas does not have a smooth limit as the number of internal degrees of freedom is taken to infinity. Unitary Fermi gases with three or more spin states are thermodynamically unstable because of the existence of deeply bound three-body states, although it is possible to construct $1/N$ expansions for thermodynamics observables based on a $Sp(2N)$ invariant interaction [219,220]. Another reason is that the unitary gas is just one member of a family of non-relativistic conformal field theories. For example, one can construct conformal fluids with different thermodynamic and transport properties by varying the mass ratio m_\uparrow/m_\downarrow of the two spin states [221]. This means that the value of η/s at unitarity is not completely fixed by the symmetries of the unitary gas.

2.2 Viscosity and flow

17. Nonrelativistic scaling flows: There are two types of experiments that have been used to estimate the shear viscosity of an ultracold Fermi gas. The first is based on collective oscillations, and the second studies the expansion after release from a harmonic trap. Both of these involve

approximate scaling flows. Consider a time dependent density profile of the form

$$n(x, t) = \frac{1}{b_x(t)b_y(t)b_z(t)} F\left(\frac{x^2}{b_x^2(t)} + \frac{y^2}{b_y^2(t)} + \frac{\lambda^2 z^2}{b_z^2(t)}\right), \quad (122)$$

where $\lambda = \omega_z/\omega_\perp$ is the trap deformation, $F(x)$ is an arbitrary function and the scale parameters $b_i(t)$ satisfy the initial condition $b_i(0) = 1$. At $t = 0$ equ. (122) is consistent with hydrostatic equilibrium, which requires that the density is only a function of the local chemical potential $\mu(\vec{x}) = \mu - V(\vec{x})$.

For time dependent solutions this ansatz satisfies the continuity equation provided the velocity field is given by $u_i(x, t) = \alpha_i(t)x_i$ with $\alpha_i = \dot{b}_i/b_i$. It is fairly straightforward to find solutions to the equations of ideal hydrodynamics. In that case entropy is conserved and we only have to solve the Euler equation, which can be written as a coupled set of differential equations for $b_i(t)$. In the case of free expansion We find [80]

$$\ddot{b}_i = \frac{\omega_i^2}{(\prod_i b_i)^{2/3}} \frac{1}{b_i}. \quad (123)$$

In a strongly deformed trap the transverse and axial motion approximately decouple. For $t \gtrsim \omega_\perp^{-1}$ the transverse scale parameter is $b_\perp \sim \sqrt{3/2}\omega_\perp t$. The cloud becomes spherical after a time of order $\sqrt{2/3}\omega_z^{-1}$, and then continues to expand in the transverse direction.

It is more difficult to find solutions to the equation of dissipative fluid dynamics. In the case of collective oscillations we can, as a first approximation, ignore the increase in entropy. The increase in entropy is due to viscous heating which converts the kinetic energy of the collective mode to heat, and leads to a slow increase in the temperature and mean radius of the cloud. The change in the mean radius does not directly back-react on the damping rate, which can be computed from the viscous force in the Navier-Stokes equation. The result is equivalent to the calculation of the damping rate from the rate of energy dissipation, see equ. (32).

In the case of an expanding system we cannot ignore the increase in entropy, because viscous heating increases the thermal energy and therefore also the pressure of the cloud. Pressure drives the expansion of the cloud, and viscous heating partially compensates for the effects of viscous friction. Semi-analytical solutions to the hydrodynamic equations can be found if the viscosity scales like the density of the system, $\eta(x) = \alpha_n n(x)$, and the equation of state is that of a free gas, $P = nT$. For a scaling solution to exist the force $f_i = (\nabla_i P)/n$ must be linear in the coordinates. We use the ansatz $f_i = a_i x_i$ together with the velocity field $u_i = \alpha_i x_i$ introduced above. The continuity equation requires $\alpha_i = \dot{b}_i/b_i$. The Navier-Stokes equation and conservation of energy give a set of coupled equations for the scale parameters a_i and b_i ,

$$\frac{\ddot{b}_\perp}{b_\perp} = a_\perp - \frac{2\beta\omega_\perp}{b_\perp^2} \left(\frac{\dot{b}_\perp}{b_\perp} - \frac{\dot{b}_x}{b_x} \right), \quad (124)$$

$$\frac{\ddot{b}_z}{b_z} = a_z + \frac{4\beta\lambda^2\omega_\perp}{b_z^2} \left(\frac{\dot{b}_\perp}{b_\perp} - \frac{\dot{b}_z}{b_z} \right), \quad (125)$$

$$\dot{a}_\perp = -\frac{2}{3}a_\perp \left(5\frac{\dot{b}_\perp}{b_\perp} + \frac{\dot{b}_z}{b_z} \right) + \frac{8\beta\omega_\perp^2}{3b_\perp} \left(\frac{\dot{b}_\perp}{b_\perp} - \frac{\dot{b}_z}{b_z} \right)^2, \quad (126)$$

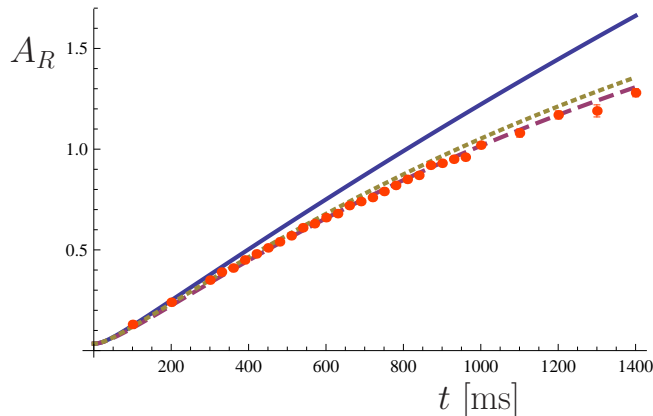


Figure 12: This figure shows the matching between kinetic theory and Navier-Stokes hydrodynamics. We show the evolution of the aspect ratio $A_R = R_z/R_\perp$, where R_z and R_\perp are the longitudinal and transverse radii, as a function of time. The solid points are data taken at an initial energy $E/E_F = 3.61$ [81]. The solid line shows a solution of the Euler equation, the long dashed line is a solution of the Navier-Stokes equation where the viscosity coefficient $\alpha_n = 22.1$ ($\eta = \alpha_n n$) was adjusted to reproduce the data, and the short-dashed line is a solution to the Boltzmann equation in the relaxation time approximation with $\tau = \alpha_n/T$.

$$\dot{a}_z = -\frac{2}{3}a_z \left(4\frac{\dot{b}_z}{b_z} + 2\frac{\dot{b}_\perp}{b_\perp} \right) + \frac{8\beta\lambda^2\omega_\perp^2}{3b_z^2} \left(\frac{\dot{b}_\perp}{b_\perp} - \frac{\dot{b}_z}{b_z} \right)^2, \quad (127)$$

where $\beta = \alpha_n N \omega_\perp / E_0$ and E_0 is the total (internal and potential) energy of the gas cloud. The initial conditions are $b_\perp(0) = b_z(0) = 1$, $\dot{b}_\perp(0) = \dot{b}_z(0) = 0$ as before, and $a_\perp(0) = \omega_\perp^2$, $a_z(0) = \omega_z^2$. Terms proportional to β in eqns. (124,125) are linear in \dot{b}_i and correspond to viscous friction, whereas dissipative terms in eqns. (126,127) are quadratic in \dot{b}_i and are related to viscous heating. The effect of the viscous terms is to slow down the transverse expansion of the cloud. We find, in particular, that the delay in the time at which the cloud becomes spherical is $(\Delta t)/t \sim \beta$.

The scaling solution described by eqns. (124-127) was compared to numerical solutions in [222], and it forms the basis of the experimental measurements presented in [81, 87, 140]. These experiments address, in the order listed, the high temperature behavior of the shear viscosity, exact scale invariance at unitarity, and the dependence of the shear viscosity on $1/a$ near the unitary limit.

18. Corona and ballistic limit: The regime of validity of the hydrodynamic expansion can be established by computing the Knudsen number $Kn = l_{mfp}/L$ of the trapped atomic gas. Consider a deformed trap containing N atoms. We use $l_{mfp} = 1/(n\sigma)$, where σ is a thermal average of the cross section. We also take L to be the short axis of the cloud, and use the density at the center of the cloud. We find

$$Kn = \frac{3\pi^{1/2}}{4(3\lambda N)^{1/3}} \left(\frac{T}{T_F} \right)^2, \quad (128)$$

where T_F is the Fermi temperature of the cloud. The Fermi temperature is defined by $k_B T_F = \epsilon_F$, where $\epsilon_F = (3N)^{1/3} \bar{\omega}$ with $\bar{\omega} = (\omega_z \omega_\perp^2)^{1/3}$ is the Fermi energy of N non-interacting fermions in a harmonic trap. For the conditions probed in experiments $Kn \ll 1$ corresponds to $T \lesssim 5T_F$ [8].

In this regime the center of the cloud is hydrodynamic. Note that because of scale invariance any dimensionless scale describing the gas is only a function of T/μ . For an ideal scaling expansion T/μ is constant in a comoving fluid element. This means that the center of the cloud remains hydrodynamic even as the gas is expanding.

In the dilute corona the cloud the mean free path is large and hydrodynamics is not applicable. In this regime we can study the expansion of the cloud using kinetic theory and the Boltzmann equation. In order to understand the connection to hydrodynamics we consider the case that the whole cloud is in the kinetic regime. For simplicity we consider solutions of the Boltzmann equation (12) with the BGK collision term given in equ. (14). We follow [223,224,225,226] and use a scaling ansatz for the distribution function

$$f(\vec{x}, \vec{v}, t) = \Gamma(t) f_0\left(\vec{R}(t), \vec{U}(t)\right), \quad R_i = \frac{x_i}{b_i}, \quad U_i = \frac{v_i - \frac{\dot{b}_i}{b_i} x_i}{\theta_i^{1/2}}, \quad \Gamma = \prod_j \frac{1}{b_j \theta_j^{1/2}}, \quad (129)$$

where b_i, θ_i are functions of t and $f_0(r, v)$ is a solution of the Boltzmann equation in equilibrium. In the present case f_0 is a Maxwell-Boltzmann distribution at temperature T and chemical potential $\mu = \mu_0 - V(x)$.

The scaling ansatz (129) breaks local thermal equilibrium only through the anisotropy of the temperature parameters θ_i . The corresponding local equilibrium distribution f_{le} can be found by replacing $\theta_i \rightarrow \bar{\theta} = (\sum_i \theta_i)/3$. This distribution function is characterized by having the same mean kinetic energy as the non-equilibrium distribution f .

We can obtain a differential equation for the parameters $b_i(t)$ and $\theta_i(t)$ by taking moments of the Boltzmann equation. Integrating the Boltzmann equation over $\int d^3U d^3R U_j R_j$ (no sum over j) gives [224]

$$\ddot{b}_j + \omega_j^2 b_j - \omega_j^2 \frac{\theta_j}{b_j} = 0. \quad (130)$$

Note that the second term is due to the external potential and is not present if we consider free expansion. Integrating over $\int d^3U d^3R U_j U_j$ gives

$$\dot{\theta}_j + 2 \frac{\dot{b}_j}{b_j} \theta_j = -\frac{1}{\tau_0} (\theta_j - \bar{\theta}). \quad (131)$$

Moments of the Boltzmann equation weighted with $R_j R_j$ do not provide additional constraints. Together with the initial conditions $b_j(0) = \theta_j(0) = 1$ and $\dot{b}_j(0) = 0$ the two equations (130) and (131) describe the evolution of an expanding cloud.

In the free streaming limit $\tau_0 \rightarrow \infty$ equ. (130) provides an exact solution of the Boltzmann equation. We get $\theta_i = 1/b_i^2$ and $b_i = (1 + \omega_i^2 t^2)^{1/2}$. In the opposite limit, $\tau_0 \rightarrow 0$, we get $\theta_i = \bar{\theta}$ with $\bar{\theta} = (\prod_i b_i)^{-2/3}$ and equ. (130) is equivalent to the Euler equation. Keeping leading order corrections in $1/\tau_0$ leads to a solution of the Navier-Stokes equation with $\zeta = 0$ and $\eta = n\tau_0 T_{le}$ [226], see Fig. 12. We have therefore obtained a kinetic model that interpolates between the ballistic and Navier-Stokes limits. The shortcoming of the model is that we have assumed that τ_0 is a constant which is independent of the density and temperature. From the matching condition between τ_0 and η we observe that this implies that the shear viscosity is proportional to density, which is at variance with the expected behavior in the low density limit.

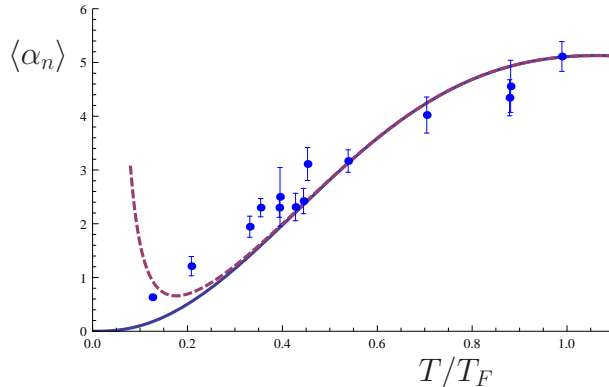


Figure 13: Trap averaged shear viscosity to density ratio $\langle \alpha_n \rangle$. We show $\langle \alpha_n \rangle$ as a function of T/T_F^{trap} , where $T_F^{trap} = (3\lambda N)^{1/3}\omega_\perp$ is the Fermi temperature of the trap. We have chosen $N = 2 \cdot 10^5$ and $\lambda = 0.045$ as in [227]. The solid line shows the kinetic theory result, the dashed line includes fluctuation corrections to the shear viscosity. The data are from [228], which is a reanalysis of the results reported in [227].

It is possible to consider a more general behavior for τ_0 , for example by allowing τ_0 to be a functional of the distribution function. In order to obtain $\eta \sim const$ we have to assume that $1/\tau \sim \int d^3v f(\vec{x}, \vec{v}, t)$ [226]. Matching quadratic moments of the Boltzmann equation to the Navier-Stokes equation gives an effective density dependent shear viscosity $\eta(x) = \lambda^3 n(x)/\bar{n}$, where \bar{n} is the average density. The problem is that this solution does not automatically reduce to the free streaming limit in the dilute part of the cloud.

19. Transient fluid dynamics and the kinetic limit: In the case of collective oscillations an improved matching to kinetic theory can be obtained by considering transient hydrodynamics as in equ. (8). For a system with harmonic time dependence the relaxation time equation is solved by $\delta\Pi_{ij} = -\eta(\omega)\sigma_{ij}$ with a frequency dependent shear viscosity $\eta(\omega) = \eta/(1 + i\omega\tau_R)$. The trap integrated shear viscosity is

$$\langle \eta \rangle = \int d^3x \frac{\eta(\vec{x})}{1 + \omega^2 \tau_R(\vec{x})^2}. \quad (132)$$

Using $\tau_R(\vec{x}) = \eta(\vec{x})/(n(\vec{x})T)$ we observe that the trap average is well defined even in the dilute corona. In this regime the relaxation time is large, and the viscous stresses never reach the Navier-Stokes value. We can now use the method described in Sect. 2.2 to compute the damping rate of collective modes. For the transverse breathing mode the velocity profile is $\vec{u} \sim (x, y, 0)$ and the damping constant is given by

$$\Gamma = \frac{\langle \alpha_n \rangle}{(3N\lambda)^{1/3}} \frac{\omega_\perp}{(E_0/[N\epsilon_F])}. \quad (133)$$

Here, E_0 is the total (potential and internal) energy of the trapped gas, $\epsilon_F = (3N\lambda)^{1/3}\omega_\perp$ is the Fermi energy of the trapped system, and $\langle \alpha_n \rangle = \langle \eta \rangle/N$. A typical result is shown in Fig. 13.

The advantage of this formalism is that it reproduces the hydrodynamic and kinetic theory results in certain limits. For a density dependent shear viscosity of the form $\eta \sim n$ it reduces, up to corrections of second order in the gradient expansion, to the Navier-Stokes result. For $\eta \sim \lambda_{dB}^{-3}$

the result reproduces, in the high temperature limit, the damping rate obtained from solutions of the Boltzmann equation in the Knudsen limit [90].

An analysis of the collective mode data reported in [227] using this method can be found in [80]. For $\eta \sim \lambda_{dB}^{-3} \sim (mT)^{3/2}$ we find that $\Gamma \sim T^3$ at low temperature, and $\Gamma \sim 1/T$ at high temperature. The fact that the damping rate decreases in the high temperature limit even though the viscosity is growing is related to the increase in the relaxation time $\tau_R \simeq \eta/(nT)$. As the relaxation time grows the strain σ_{ij} and the induced stress π_{ij} are increasingly out of phase, and the dissipated energy is reduced. This implies that careful measurements of the damping rate in the regime where the T^3 behavior starts to break down can be used to measure τ_R . A similar transition from hydrodynamic to kinetic behavior is also seen in the dependence of Γ on the particle number. At low temperature the damping rate scales as $\Gamma \sim N^{-1/3}$, and at high temperature the scaling law changes to $\Gamma \sim N^{1/3}$.

3 Relativistic fluids

3.1 The quark gluon plasma

20. Transport properties of the QGP: Comparing the shear viscosity to other transport properties of the quark gluon plasma provides additional information on the existence and properties of quasi-particles, and on the mechanism for charge and momentum transport in the plasma. In the high temperature limit the full set of transport coefficients has been computed in kinetic theory, and there are exploratory measurements of shear and bulk viscosity, heavy quark diffusion as well as electric conductivity on the lattice [34].

Weak coupling results for transport coefficients at second order in the hydrodynamic expansion are given by [186]

$$\eta\tau_R = (5 \cdots 5.9) \frac{\eta^2}{sT}, \quad \lambda_1 = (4.1 \cdots 5.2) \frac{\eta^2}{sT}, \quad \lambda_2 = -2\eta\tau_R, \quad \lambda_3 = 0, \quad \kappa_R = \frac{5s}{8\pi^2 T}, \quad (134)$$

where the numerical ranges correspond to the variation of the numerical coefficients with the coupling constant. The coefficients τ_R and λ_i scale inversely with g and were determined using kinetic theory [186]. The quantity κ_R , which governs the curvature term in the stress tensor is independent of g , and was determined using the Kubo relation [101]. Kubo relations also show that, in general, λ_3 is not zero [176]. The results given in equ. (134) can be compared to the AdS/CFT predictions in equ. (93), and to the non-relativistic results in equ. (109).

The bulk viscosity of the quark gluon plasma was calculated by Arnold, Dogan, and Moore [229]. The result is

$$\zeta = \frac{A\alpha_s^2 T^3}{\log(\mu^*/m_D)}, \quad (135)$$

where $A = 0.443$ and $\mu^* = 7.14T$ in pure gauge QCD, and $A = 0.657$, $\mu^* = 7.77T$ in QCD with $N_f = 3$ light quark flavors. The dependence of ζ on α_s can be understood from the simple estimate $\zeta \sim (\mathcal{E} - 3P)^2 \eta$ with $\mathcal{E} - 3P \sim \alpha_s^2$ and $\eta \sim 1/\alpha_s^2$. The thermal conductivity of a quark gluon plasma is a somewhat subtle quantity. At zero chemical potential one cannot distinguish between energy and particle transport, and the thermal conductivity is not defined. In the limit of small chemical potential, $T \gg \mu$, the relaxation time approximation gives $\kappa \sim T^4/(\alpha_s^2 \mu^2)$ [5]. This result

appears to be singular in the limit $\mu \rightarrow 0$, but the dissipative contribution to the energy and baryon currents are finite. The behavior of η , ζ and κ in the limit $\mu \gg T$ is reviewed in [230].

The heavy quark diffusion constant is [231, 232]

$$D = \frac{36\pi}{C_F g^4 T} \left[N_c \left(\log \left(\frac{2T}{m_D} \right) + c \right) + \frac{N_f}{2} \left(\log \left(\frac{4T}{m_D} \right) + c \right) \right]^{-1}, \quad (136)$$

where $C_F = (N_c^2 - 1)/(2N_c)$ and $c = 0.5 - \gamma_E + \zeta'(2)/\zeta(2)$. Comparing this result with the shear viscosity given in equ. (35) we observe that heavy quark and momentum diffusion are related. In the relevant range of coupling constants one finds $DT \simeq 6(\eta/s)$ [232]. This relation provides a test whether transport is dominated by quasi-particles, because in the strong coupling limit of the AdS/CFT correspondence we find $DT \ll (\eta/s)$.

3.2 Flow, higher moments of flow, and viscosity

21. Scaling flows, from Bjorken to Gubser: The Bjorken flow discussed in Sect. 3.2 is an exact solution of the Navier-Stokes solution with longitudinal boost invariance and no dependence on the transverse coordinates. The Bjorken solution is most easily described using a set of coordinates (τ, η, r, ϕ) , where $\tau = (t^2 - z^2)^{1/2}$ is proper time, $\eta = (1/2) \log[(t+z)/(t-z)]$ is rapidity, and (r, ϕ) are polar coordinates. The metric is

$$ds^2 = -d\tau^2 + \tau^2 d\eta^2 + dr^2 + r^2 d\phi^2. \quad (137)$$

Bjorken flow corresponds to a velocity field $u^\mu = (1, 0, 0, 0)$. Energy density and pressure are functions of τ only and scale invariance requires $\epsilon(\tau) = P(\tau)/3$. In ideal fluid dynamics $\mathcal{E}(\tau) \sim 1/\tau^{4/3}$. If dissipation is included $\mathcal{E}(\tau)$ is determined by equ. (38).

Gubser discovered a generalization of Bjorken flow that includes transverse expansion, and therefore serves as a much more realistic model of a heavy ion collision [233, 119]. The solution was inspired by the fluid-gravity correspondence, but it can be described purely as a solution to the relativistic Euler and Navier-Stokes equations for a scale invariant fluid. Scale invariance implies that $\mathcal{E} = 3P$ and $\eta = H_0 T^3$. The velocity profile is

$$u_\mu = (\cosh(\kappa), 0, \sinh(\kappa), 0), \quad \kappa = \operatorname{arctanh} \left(\frac{2q^2 \tau r}{1 + q^2 \tau^2 + q^2 r^2} \right), \quad (138)$$

where q is a parameter. This solution has a hidden $SO(3)$ symmetry that can be made manifest by switching to another set of coordinates, see [233]. Consider first the ideal case. The energy density can be written as

$$\mathcal{E} = \frac{\hat{\mathcal{E}}(g)}{\tau^\alpha}, \quad \alpha = 4, \quad g = \frac{1 - q^2 \tau^2 + q^2 r^2}{2q\tau}. \quad (139)$$

The solution of the Euler equation is $\hat{\mathcal{E}} = \hat{\mathcal{E}}_0/(1 + g^2)^{4/3}$, which corresponds to

$$\mathcal{E} = \frac{\hat{\mathcal{E}}_0}{\tau^{4/3}} \frac{(2q)^{8/3}}{[1 + 2q^2(\tau^2 + r^2) + q^4(\tau^2 - r^2)^2]^{4/3}}. \quad (140)$$

Taking $q \rightarrow 0$ with $\hat{\mathcal{E}}_0 q^{8/3}$ constant we recover the Bjorken solution. As in the Bjorken case the flow profile is not modified by dissipative effects. The evolution of the energy density is most easily

described in terms of $\hat{T} = \hat{\mathcal{E}}^{1/4}$. We get

$$\hat{T} = \frac{\hat{T}_0}{(1+g^2)^{1/3}} + \frac{H_0 g}{(1+g^2)^{1/2}} \left[1 - (1+g^2)^{1/6} {}_2F_1\left(\frac{1}{2}, \frac{1}{6}; \frac{3}{2}; -g^2\right) \right], \quad (141)$$

where ${}_2F_1(\alpha, \beta; \gamma; \delta)$ is a hypergeometric function. Gubser also studied the evolution of small fluctuations around this solution [119], see also [234, 235, 236, 237]. He finds that modes with wave number k are suppressed by

$$P_k = \exp\left(-\frac{2\eta k^2 t}{3sT}\right). \quad (142)$$

The Glauber model gives an approximately flat spectrum of initial perturbations [238], so this formula predicts that higher flow harmonics are exponentially damped. This is in rough agreement with the data [239], although the details are more complicated. In particular, lower moments of the initial energy deposition depend on the geometry and the initial state model, and there is some amount of mode mixing in the hydrodynamic response [240, 241, 242].

Bjorken flow arises naturally in weak coupling approaches to thermalization [243, 244]. In strong coupling calculations, based on the collision of shock waves in AdS_5 , more complicated flow profiles are obtained [245]. An interesting parameterization, termed “complex deformation of Bjorken flow”, of these flow profiles was recently suggested in [246]. Consider cartesian coordinates (t, \vec{x}) and

$$\begin{aligned} u_\mu^{\mathbb{C}} &= \frac{1}{\sqrt{(t + \mathfrak{t}_3)^2 - x_3^2}} (- (t + \mathfrak{t}_3), 0, 0, x_3), \\ \mathcal{E}^{\mathbb{C}} &= \frac{\mathcal{E}_0^{\mathbb{C}}}{[(t + \mathfrak{t}_3)^2 - x_3^2]^{2/3}}, \\ \Pi_{\mu\nu}^{\mathbb{C}} &= \mathcal{E}^{\mathbb{C}} u_\mu^{\mathbb{C}} u_\nu^{\mathbb{C}} + \frac{\mathcal{E}^{\mathbb{C}}}{3} (g_{\mu\nu} + u_\mu^{\mathbb{C}} u_\nu^{\mathbb{C}}). \end{aligned} \quad (143)$$

If \mathfrak{t}_3 is a real parameter then this flow profile is just a time translation of the Bjorken solution. However, if \mathfrak{t}_3 is a complex parameter then we obtain something new. Note that $\Pi_{\mu\nu}^{\mathbb{C}} \equiv \text{Re} \Pi_{\mu\nu}^{\mathbb{C}}$ satisfies the conservation laws, but $u_\mu \equiv \text{Re} u_\mu^{\mathbb{C}}$ and $\mathcal{E} \equiv \text{Re} \mathcal{E}^{\mathbb{C}}$ are not solutions of the Euler equation, because they do not satisfy the constitutive equation. Nevertheless, for suitable choices of the phases, in particular for $\arg \mathfrak{t}_3 = \pi/2$ and $\arg \mathcal{E}^{\mathbb{C}} = \pi/3$, interesting flow profiles are obtained. These flows are Landau-like at early time, glasma-like ($P_L \simeq -\mathcal{E}$) near the light cone, and Bjorken-like at late time and in the central rapidity slice.

22. From kinetics to hydrodynamics in relativistic heavy ion collisions: The transition from kinetic theory to hydrodynamic behavior in relativistic heavy ion collisions has been studied by a number of authors. Kolb et al. compared scaling relations in the ballistic and hydrodynamic limits to the data at the SPS and RHIC [247]. They found clear indications for hydrodynamic behavior at RHIC. The conditions for achieving the hydrodynamic limit in a kinetic model of the quark gluon plasma were studied by Molnar and Gyulassy [248]. They find that obtaining hydrodynamic behavior in a model that includes elastic $2 \leftrightarrow 2$ scattering only requires rather extreme assumptions concerning the initial parton density or the parton cross section. More recently, it was shown that the inclusion of $2 \leftrightarrow 3$ processes leads to a more rapid approach to hydrodynamics [249, 250]. We

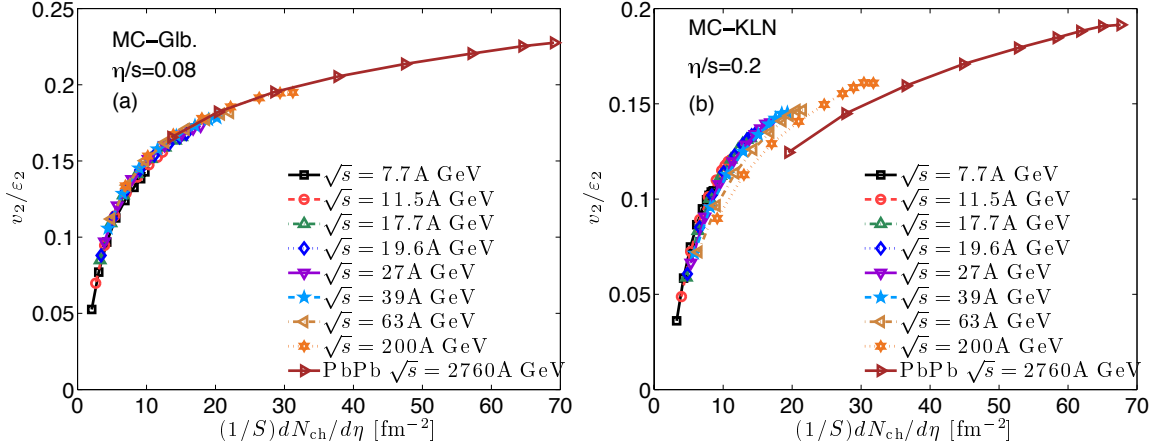


Figure 14: Eccentricity scaled elliptic flow v_2 plotted as a function of the charged hadron multiplicity density dN/dy divided by the overlap area S for different collision energies, from [257]. The left panel shows results from a hydrodynamic simulation for MC-Glauber initial conditions with $\eta/s = 0.08$, and the right panel shows a calculation with MC-KLN initial conditions and $\eta/s = 0.2$.

should note, however, that the correct implementation of $2 \leftrightarrow 3$ scattering is still being discussed [251, 252].

In the case of expanding Fermi gases we emphasized the need to find a transport model that smoothly interpolates between hydrodynamics in the center of the cloud and free streaming in the dilute corona. In the case of a heavy ion collision we would like to make contact with longitudinal free streaming at early times, and with both longitudinal and transverse free streaming at late times. This can be accomplished by using a kinetic framework in which the longitudinal and transverse temperatures are allowed to differ [253, 254]. Using moments of the Boltzmann equation one can derive a set of fluid dynamic equations that involve additional, non-hydrodynamic, modes. If the mean free path is short these modes relax quickly and one recovers the usual Navier-Stokes equation. In the opposite limit the equations reproduce the free streaming limit.

A very different approach that has many of the same features is the lattice Boltzmann equation (LBE) [255, 256]. The LBE is a kinetic equation that acts on a very simple, discrete, velocity space. The LBE provides a very robust and efficient implementation of the Navier-Stokes equation in the limit of a short mean free path, and reduces to free streaming in the limit $l_{mfp} \rightarrow \infty$.

23. Knudsen number scaling: In Sect. 3.2 we argued that the local expansion parameter for the hydrodynamic gradient expansion in a heavy ion collision is given by $\eta/(s\tau T)$. In order to compare experimental data from collisions at different beam energies, impact parameters, and nuclear mass numbers it is also important to identify global variables that control the validity of hydrodynamics. An important step in this direction was taken by Heiselberg and Levy, who studied elliptic flow in the dilute limit [258]. The contribution from single elastic scattering events is

$$v_2(p_{1,T}) = \frac{\delta}{16S} \frac{dN}{dy} \frac{v_{1,T}^2}{\langle v_{12}^2 \rangle} \langle v_{12,T} \sigma_{tr} \rangle, \quad \delta = \frac{\langle R_y^2 - R_x^2 \rangle}{\langle R_y^2 + R_x^2 \rangle}, \quad (144)$$

where dN/dy is the multiplicity per unit of rapidity, S is the transverse overlap area, and $v_{1,T}$ is

the transverse velocity. The symbol $\langle \cdot \rangle$ denotes an average over the distribution of particle 2, and v_{12} is the relative velocity of particles 1 and 2. We have also defined the transport cross section σ_{tr} , the cross section weighted by $(1 - \cos \theta)$, where $\cos \theta$ is the scattering angle. Finally, R_x and R_y are the radii of the overlap region, and δ is the elliptic deformation. It is standard to characterize the elliptic deformation not in terms of δ , but using the quantity ϵ_2 defined by

$$\epsilon_2 = \frac{\langle y^2 - x^2 \rangle}{\langle y^2 + x^2 \rangle}, \quad (145)$$

where the average is carried out using the energy density as a weight function. Based on equ. (144) we predict

$$\frac{v_2}{\epsilon_2} \sim \frac{1}{S} \frac{dN}{dy} \langle \sigma \rangle. \quad (146)$$

Following the arguments in Sect. 1.2 we expect that the parameter $(1/S)(dN/dy)\langle\sigma\rangle$ also appears in fluid dynamics. This is indeed the case, as we can see using the following argument [259]. Consider a fireball of size $\bar{R} \simeq \sqrt{R_x^2 + R_y^2}$ which is undergoing Bjorken expansion in the longitudinal direction. The time scale for transverse expansion is $\tau = \bar{R}/c_s$, and the density at this time is $n \sim 1/(c\tau S)(dN/dy)$. This implies that the inverse Knudsen number is

$$\frac{1}{Kn} = \frac{\bar{R}}{l_{mfp}} = \bar{R}n\langle\sigma\rangle = \frac{c_s}{c} \frac{1}{S} \frac{dN}{dy} \langle\sigma\rangle. \quad (147)$$

Knudsen number scaling of v_2/ϵ_2 was first studied by Voloshin and Poskanzer, see [260, 261]. The results compiled in [261] demonstrate nice data collapse if different systems, centralities, and beam energies are plotted as a function of $(1/S)(dN/dy)$. The compilation also shows that v_2/ϵ_2 rises almost linearly with $(1/S)(dN/dy)$, and that the RHIC data at 200 GeV per nucleon saturate the flow predicted by ideal hydrodynamics. A more recent analysis of data from the RHIC beam energy scan and $Pb + Pb$ collisions at the LHC is shown in Fig. 14 [257]. There is some uncertainty related to different models for ϵ_2 , which is reflected in the difference between the left and right panels. The main result is that there is data collapse, which is excellent for the Monte Carlo Glauber model, and not quite as good in the case of the KLN model. We also observe some curvature in v_2/ϵ_2 . This means that there are viscous effects at high energy, and that there is no saturation of flow even at the LHC.

An important assumption in Fig. 14 is that the effective cross section is not a function of the collision parameters. At high temperature the quark gluon plasma is scale invariant and we expect $\langle\sigma\rangle \sim s^{-2/3}$. Then

$$\frac{1}{Kn} \sim \left(\frac{c_s}{c} \frac{dN}{dy} \right)^{1/3}, \quad (148)$$

and the overlap area does not appear in the estimate for the Knudsen number. This makes a significant difference when comparing pA and AA collisions, and there is some evidence that dN/dy scaling is preferred by the data [262].

24. Sensitivity to the relaxation time: We have seen that an important consistency check for the hydrodynamic description is to show that the dependence on second order coefficients, like the relaxation time, is weak. On the other hand, we have also argued that second order hydrodynamics

can be used to regularize instabilities and acausal behavior of the Navier-Stokes equation. How can both of these statements be correct? In particular, if second order terms serve as regulators then the $\tau_R \rightarrow 0$ limit cannot be smooth.

It is straightforward to compute the limiting speed of a shear wave in transient fluid dynamics [13]

$$v_{max} = \lim_{q \rightarrow \infty} \frac{\partial \omega}{\partial q} = \left[\frac{\eta}{(\mathcal{E} + P)\tau_R} \right]^{1/2}. \quad (149)$$

We observe that $v_{max} \leq 1$ is satisfied if $(\eta/s) < (\tau_R T)$. For $\eta/s \ll 1$ this implies that there is indeed a large window for $\tau_R T$ in which both causality and the constraint from the validity of the gradient expansion, $\tau_R T < 1$, are satisfied. We also note that if acausal modes are excluded by incorporating an explicit cutoff then the limit $\tau_R \rightarrow 0$ is smooth.

4 Frontiers

25. The role of the AdS/CFT correspondence: The successful hydrodynamic description of heavy ion collisions outlined in Sect. 3.2 does not rely on the AdS/CFT correspondence. Indeed, as we have emphasized, hydrodynamics is an effective theory of the long distance behavior of non-equilibrium systems that does not depend on specific features of the underlying microscopic theory. Nevertheless, the success of nearly perfect fluid dynamics in describing heavy ion collisions at RHIC and the LHC is frequently mentioned as one of the principal success stories of string theory and the AdS/CFT correspondence. This is indeed justified for several reasons:

1. *The possibility of nearly perfect fluidity:* The idea that η/s could be as small as 0.1 was first discussed in the important work of Danielewicz and Gyulassy [5]. It should be noted, however, that this work can be interpreted as showing that i) the applicability of hydrodynamics in relativistic heavy ion collisions requires $\eta/s \ll 1$, ii) a value of η/s this small requires rather extreme assumptions about kinetic theory. It is then reasonable to conclude that these assumptions are not likely to be realized in practice, and the focus in the years following the publication of [5] shifted from dissipative fluid dynamics to parton cascades [263, 264] (see [265, 266] for rare exceptions). Interest in nearly perfect fluid dynamics was revived because of the experimental discoveries at RHIC, combined with the almost contemporaneous result that the strongly coupled fluid described by AdS/CFT satisfies $\eta/s = 1/(4\pi)$.
2. *Second order conformal fluid dynamics:* The general structure of the equations of relativistic conformal fluid dynamics can be established purely based on symmetry arguments, but in practice the equations were first found with the help of the AdS/CFT correspondence [19]. In principle the Israel-Stewart equations form a consistent subset of the most general second order equations. However, in practice some studies employed truncations of the Israel-Stewart equations that are not consistent with conformal symmetry [267]. The truncated equations exhibit significant dependence on the relaxation time [268], which becomes much weaker once the full Israel-Stewart equations are considered [269]. These differences could have been resolved without AdS/CFT, but historically the holographic flows found by Heller and Janik [270], and the subsequent matching to second hydrodynamics provided by Baier et al. [19] played a central role in explaining the relation between different approaches. More

recently, anomalous transport coefficients were discovered using the AdS/CFT correspondence [146]. These transport coefficients can be understood based on the general properties of fluid dynamics [147], but in the literature the presence of these terms had been missed.

3. *Rapid hydrodynamization:* The hydrodynamic description of elliptic flow in relativistic heavy ion collisions requires a very short equilibration time $\tau_{eq} \sim 1$ fm/c. Equilibration can be understood in kinetic theories based on $2 \rightarrow 2$ and $2 \rightarrow 3$ scattering, and equilibration times are known to be further reduced by collective plasma effects. However, quantitative estimates give $\tau_{eq} \gtrsim (2-3)$ fm/c, see for example [271]. On the other hand, fast equilibration is natural in holographic theories [47]. In addition to that, AdS/CFT shows that the Navier-Stokes description can be reliable even if non-equilibrium contributions to the pressure are large [47, 48], as is the case in the early stages of a heavy ion collision.
4. *Absence of quasi-particles:* AdS/CFT provides an explicit example of a fluid in which hydrodynamic behavior does not emerge from an underlying kinetic theory. While we still do not know whether this is the correct picture for the quark gluon plasma produced at RHIC and the LHC, the existence of an alternative to the quasi-particle paradigm has been very useful for studying the role of various assumptions in analyzing the data.

Despite this impressive list we should emphasize that a lot of important work on relativistic fluid dynamics has little or no relation to AdS/CFT. A variety of schemes for transient higher order fluid dynamics were developed [272, 273, 174], and these schemes provided the tools to test the sensitivity of the analysis of the RHIC data to poorly constrained high order transport coefficients, see [134, 135, 274]. We note, in particular, that even those implementations of higher order fluid dynamics that are based on the conformal, AdS/CFT inspired, second order equations make use of the idea of transient fluid dynamics, see equ. (8). This approach emerges naturally in kinetic theory, but it is not a systematic approximation to fluid dynamics in AdS/CFT.

26. Puzzles and challenges: As noted in Sect. 4 there are number of puzzles related to the hydrodynamic description of heavy ion collisions at RHIC and LHC.

1. Approximate beam energy independence of the charged particle elliptic flow $v_2(p_T)$: The elliptic flow of charged particles has been measured over a large range of beam energies, from the low end of the RHIC beam energy scan, $\sqrt{s_{NN}} = 7.7$ GeV, to the current LHC energy $\sqrt{s_{NN}} = 2.76$ TeV [115, 275, 276]. In a given centrality class the results are essentially beam energy independent. Within hydrodynamics this is somewhat surprising because many variables, such as the lifetime of the system and η/s are obviously changing. The result may be somewhat of an accident, because the v_2 of identified particles, and the p_T integrated v_2 do show beam energy dependence.
2. Large photon elliptic flow: The photon $v_2(p_T)$ has been measured at RHIC and LHC [277, 278], and the result is comparable (within sizable errors) to the elliptic flow of light hadrons. This is surprising, because photon emission is expected to be dominated by the early stages of the quark gluon plasma evolution before a significant collective flow can develop [279].
3. Hydrodynamic flow in p+Pb collisions: Significant elliptic and triangular flow has been observed in high multiplicity p+Pb collisions at the LHC [280, 281, 282]. A particularly striking

discovery is the mass ordering of $v_2(p_T)$ [282], which is usually regarded as strong evidence for collective expansion [105]. The result is surprising, because the proton nucleus collisions have generally been regarded as a control experiment in which dissipative corrections are too large for collective flow to develop. We should note, however, that the collective response to initial state fluctuations in nucleus-nucleus collisions already indicates that the mean free path is very short, and that hydrodynamic response can be seen on small scales. A simple scaling analysis of hydrodynamic behavior in p+Pb collisions was recently presented in [262], but we should note that initial state effects may well be important [283, 284].

LITERATURE CITED

1. L. P. Kadanoff, P. C. Martin, "Hydrodynamic equations and correlation functions," *Ann. Phys.* **24**, 419 (1963).
2. D. Forster, "Hydrodynamic Fluctuations, Broken Symmetry, and Correlation Functions", Addison Wesley (1995).
3. M. Reiner, "The Deborah Number," *Phys. Today* 17(1), 62 (1964).
4. E. M. Purcell, "Life at Low Reynolds Number," *Am. J. of Phys.* **45**, 3 (1977).
5. P. Danielewicz and M. Gyulassy, "Dissipative Phenomena in Quark Gluon Plasmas," *Phys. Rev. D* **31**, 53 (1985).
6. P. Kovtun, D. T. Son and A. O. Starinets, "Viscosity in strongly interacting quantum field theories from black hole physics," *Phys. Rev. Lett.* **94**, 111601 (2005) [arXiv:hep-th/0405231].
7. T. Schäfer and D. Teaney, "Nearly Perfect Fluidity: From Cold Atomic Gases to Hot Quark Gluon Plasmas," *Rept. Prog. Phys.* **72**, 126001 (2009) [arXiv:0904.3107 [hep-ph]].
8. A. Adams, L. D. Carr, T. Schäfer, P. Steinberg and J. E. Thomas, "Strongly Correlated Quantum Fluids: Ultracold Quantum Gases, Quantum Chromodynamic Plasmas, and Holographic Duality," *New J. Phys.* **14**, 115009 (2012) [arXiv:1205.5180 [hep-th]].
9. D. Burnett, "The distribution of velocities in a slightly non-uniform gas," *Proc. Lond. Math. Soc.* **39** 385 (1935).
10. L. S. Garcia-Colina, R. M. Velasco, F. J. Uribea, "Beyond the Navier-Stokes equations: Burnett hydrodynamics" *Phys. Rep.* **465** 149 (2008).
11. H. Grad, "On the kinetic theory of rarefied gases," *Comm. Pure and Appl. Math.* **2** 331 (1949).
12. W. Israel and J. M. Stewart, "Transient relativistic thermodynamics and kinetic theory," *Annals Phys.* **118**, 341 (1979).
13. P. Romatschke, "New Developments in Relativistic Viscous Hydrodynamics," *Int. J. Mod. Phys. E* **19**, 1 (2010) [arXiv:0902.3663 [hep-ph]].
14. L. D. Landau, E. M. Lifshitz, "Theory of Elasticity", *Course of Theoretical Physics, Vol. VII*, Pergamon Press (1959).
15. C. Cattaneo, "Sulla conduzione del calore," *Atti Sem. Mat. Fis. Univ. Modena* **3** (1948) 3.
16. I. Müller, "A History of Thermodynamics," Springer, Heidelberg (2006).
17. I. Müller, "Zum Paradoxon der Wärmeleitungstheorie," *Z. Phys.* **198** (1967) 329.

18. W. Israel, J. M. Stewart, “Thermodynamics of nonstationary and transient effects in a relativistic gas,” *Phys. Lett. A* **58**, 213 (1967).
19. R. Baier, P. Romatschke, D. T. Son, A. O. Starinets and M. A. Stephanov, “Relativistic viscous hydrodynamics, conformal invariance, and holography,” *JHEP* **0804**, 100 (2008) [arXiv:0712.2451 [hep-th]].
20. J. Chao and T. Schäfer, “Conformal symmetry and non-relativistic second order fluid dynamics,” *Annals Phys.* **327**, 1852 (2012) [arXiv:1108.4979 [hep-th]].
21. P. Kovtun, G. D. Moore and P. Romatschke, “The stickiness of sound: An absolute lower limit on viscosity and the breakdown of second order relativistic hydrodynamics,” *Phys. Rev. D* **84**, 025006 (2011) [arXiv:1104.1586 [hep-ph]].
22. C. Chafin and T. Schäfer, “Hydrodynamic fluctuations and the minimum shear viscosity of the dilute Fermi gas at unitarity,” *Phys. Rev. A* **87**, 023629 (2013) [arXiv:1209.1006 [cond-mat.quant-gas]].
23. R. Adhikari, M. E. Cates, K. Stratford, A. J. Wagner, “Fluctuating lattice Boltzmann,” *Europhys. Lett.* **71**, 473 (2205) [arXiv:cond-mat/0402598 [cond-mat.stat-mech]].
24. K. Murase and T. Hirano, “Relativistic fluctuating hydrodynamics with memory functions and colored noises,” arXiv:1304.3243 [nucl-th].
25. P. L. Bhatnagar, E. P. Gross, M. Krook, “A Model for Collision Processes in Gases,” *Phys. Rev.* **94**, 511 (1954).
26. S. Chapman and T. G. Cowling, “The Mathematical Theory of Non-Uniform Gases”, Cambridge University Press, 3rd ed. (1970).
27. L. P. Kadanoff, G. Baym, “Quantum statistical mechanics: Green’s function methods in equilibrium and nonequilibrium problems,” W. A. Benjamin, New York (1962).
28. J. C. Maxwell, E. Garber, S. G. Brush, C. W. F. Everitt, “Maxwell on Molecules and Gases,” MIT Press (1986).
29. S. G. Brush, “The kind of motion we call heat,” North Holland (1986).
30. F. Karsch and H. W. Wyld, “Thermal Green’s Functions And Transport Coefficients On The Lattice,” *Phys. Rev. D* **35**, 2518 (1987).
31. H. B. Meyer, “A calculation of the shear viscosity in SU(3) gluodynamics,” *Phys. Rev. D* **76**, 101701 (2007) [arXiv:0704.1801 [hep-lat]].
32. S. Sakai and A. Nakamura, “Lattice calculation of the QGP viscosities - Present results and next project,” *PoS LAT2007*, 221 (2007) [arXiv:0710.3625 [hep-lat]].
33. G. Aarts, C. Allton, J. Foley, S. Hands and S. Kim, “Spectral functions at small energies and the electrical conductivity in hot, quenched lattice QCD,” *Phys. Rev. Lett.* **99**, 022002 (2007) [arXiv:hep-lat/0703008].
34. H. B. Meyer, “Transport Properties of the Quark-Gluon Plasma: A Lattice QCD Perspective,” *Eur. Phys. J. A* **47**, 86 (2011) [arXiv:1104.3708 [hep-lat]].
35. G. Wlazlowski, P. Magierski, A. Bulgac and K. J. Roche, “The temperature evolution of the shear viscosity in a unitary Fermi gas,” *Phys. Rev. A* **88**, 013639 (2013) [arXiv:1304.2283 [cond-mat.quant-gas]].
36. K. S. Thorne, R. H. Price, D. A. MacDonald, “Black Holes: The Membrane Paradigm”, Yale University Press, 1986.
37. J. M. Maldacena, “The large N limit of superconformal field theories and supergrav-

- ity,” *Adv. Theor. Math. Phys.* **2**, 231 (1998) [*Int. J. Theor. Phys.* **38**, 1113 (1999)] [arXiv:hep-th/9711200].
38. D. T. Son and A. O. Starinets, “Viscosity, Black Holes, and Quantum Field Theory,” *Ann. Rev. Nucl. Part. Sci.* **57**, 95 (2007) [arXiv:0704.0240 [hep-th]].
 39. S. S. Gubser and A. Karch, “From gauge string duality to strong interactions: A Pedestrian’s Guide,” *Ann. Rev. Nucl. Part. Sci.* **59**, 145 (2009) [arXiv:0901.0935 [hep-th]].
 40. J. Casalderrey-Solana, H. Liu, D. Mateos, K. Rajagopal and U. A. Wiedemann, “Gauge/String Duality, Hot QCD and Heavy Ion Collisions,” arXiv:1101.0618 [hep-th].
 41. O. DeWolfe, S. S. Gubser, C. Rosen and D. Teaney, “Heavy ions and string theory,” arXiv:1304.7794 [hep-th].
 42. G. Policastro, D. T. Son and A. O. Starinets, “From AdS / CFT correspondence to hydrodynamics,” *JHEP* **0209**, 043 (2002) [hep-th/0205052].
 43. D. Teaney, “Finite temperature spectral densities of momentum and R-charge correlators in $N = 4$ Yang Mills theory,” *Phys. Rev. D* **74**, 045025 (2006) [arXiv:hep-ph/0602044].
 44. G. Policastro, D. T. Son and A. O. Starinets, “The shear viscosity of strongly coupled $N = 4$ supersymmetric Yang-Mills plasma,” *Phys. Rev. Lett.* **87**, 081601 (2001) [arXiv:hep-th/0104066].
 45. P. Kovtun and A. Starinets, “Thermal spectral functions of strongly coupled $N = 4$ supersymmetric Yang-Mills theory,” *Phys. Rev. Lett.* **96**, 131601 (2006) [arXiv:hep-th/0602059].
 46. A. O. Starinets, “Quasinormal modes of near extremal black branes,” *Phys. Rev. D* **66**, 124013 (2002) [hep-th/0207133].
 47. P. M. Chesler and L. G. Yaffe, “Holography and colliding gravitational shock waves in asymptotically AdS_5 spacetime,” *Phys. Rev. Lett.* **106**, 021601 (2011) [arXiv:1011.3562 [hep-th]].
 48. M. P. Heller, R. A. Janik and P. Witaszczyk, “The characteristics of thermalization of boost-invariant plasma from holography,” *Phys. Rev. Lett.* **108**, 201602 (2012) [arXiv:1103.3452 [hep-th]].
 49. M. P. Heller, R. A. Janik and P. Witaszczyk, “On the character of hydrodynamic gradient expansion in gauge theory plasma,” *Phys. Rev. Lett.* **110**, 211602 (2013) [arXiv:1302.0697 [hep-th]].
 50. P. Kovtun and L. G. Yaffe, “Hydrodynamic fluctuations, long time tails, and supersymmetry,” *Phys. Rev. D* **68**, 025007 (2003) [hep-th/0303010].
 51. S. Bhattacharyya, V. E. Hubeny, S. Minwalla and M. Rangamani, “Nonlinear Fluid Dynamics from Gravity,” *JHEP* **0802**, 045 (2008) [arXiv:0712.2456 [hep-th]].
 52. M. Rangamani, “Gravity and Hydrodynamics: Lectures on the fluid-gravity correspondence,” *Class. Quant. Grav.* **26**, 224003 (2009) [arXiv:0905.4352 [hep-th]].
 53. T. D. Cohen, “Is there a most perfect fluid consistent with quantum field theory?,” *Phys. Rev. Lett.* **99**, 021602 (2007) [arXiv:hep-th/0702136].
 54. N. F. Mott, “Conduction in non-crystalline systems IX: The minimum metallic conductivity,” *Phil. Magazine* **26**, 1015 (1972).
 55. M. A. Paalanen, T. F. Rosenbaum, G. A. Thomas, and R. N. Bhatt, “Stress Tuning of the Metal-Insulator Transition at Millikelvin Temperatures,” *Phys. Rev. Lett.* **48**, 1284 (1982).
 56. A. Buchel and J. T. Liu, “Universality of the shear viscosity in supergravity,” *Phys. Rev. Lett.* **93**, 090602 (2004) [arXiv:hep-th/0311175].

57. N. Iqbal and H. Liu, “Universality of the hydrodynamic limit in AdS/CFT and the membrane paradigm,” *Phys. Rev. D* **79**, 025023 (2009) [arXiv:0809.3808 [hep-th]].
58. C. P. Herzog, A. Karch, P. Kovtun, C. Kozcaz and L. G. Yaffe, “Energy loss of a heavy quark moving through $N = 4$ supersymmetric Yang-Mills plasma,” *JHEP* **0607**, 013 (2006) [arXiv:hep-th/0605158].
59. J. Casalderrey-Solana and D. Teaney, “Heavy quark diffusion in strongly coupled $N = 4$ Yang Mills,” *Phys. Rev. D* **74**, 085012 (2006) [arXiv:hep-ph/0605199].
60. S. S. Gubser, “Drag force in AdS/CFT,” *Phys. Rev. D* **74**, 126005 (2006) [arXiv:hep-th/0605182].
61. Y. Kats and P. Petrov, “Effect of curvature squared corrections in AdS on the viscosity of the dual gauge theory,” *JHEP* **0901**, 044 (2009) [arXiv:0712.0743 [hep-th]].
62. S. Cremonini, “The Shear Viscosity to Entropy Ratio: A Status Report,” *Mod. Phys. Lett. B* **25**, 1867 (2011) [arXiv:1108.0677 [hep-th]].
63. M. Brigante, H. Liu, R. C. Myers, S. Shenker and S. Yaida, “Viscosity Bound Violation in Higher Derivative Gravity,” *Phys. Rev. D* **77**, 126006 (2008) [arXiv:0712.0805 [hep-th]].
64. A. Buchel and R. C. Myers, “Causality of Holographic Hydrodynamics,” *JHEP* **0908**, 016 (2009) [arXiv:0906.2922 [hep-th]].
65. X. O. Camanho, J. D. Edelstein and M. F. Paulos, “Lovelock theories, holography and the fate of the viscosity bound,” *JHEP* **1105**, 127 (2011) [arXiv:1010.1682 [hep-th]].
66. Y. Castin and F. Werner, “The Unitary Gas and its Symmetry Properties,” in: Springer Lecture Notes in Physics “BEC-BCS Crossover and the Unitary Fermi gas. Wilhelm Zwerger (editor) [arXiv:1103.2851 [cond-mat.quant-gas]].
67. I. Bloch, J. Dalibard, W. Zwerger, “Many-Body Physics with Ultracold Gases” *Rev. Mod. Phys.* **80**, 885 (2008) [arXiv:0704.3011].
68. S. Giorgini, L. P. Pitaevskii, S. Stringari, “Theory of ultracold atomic Fermi gases” *Rev. Mod. Phys.* **80** 1215 (2008) [arXiv:0706.3360].
69. T. Schäfer and K. Dusling, “Bulk viscosity and conformal symmetry breaking in the dilute Fermi gas near unitarity,” *Phys. Rev. Lett.* **111**, 120603 (2013) [arXiv:1305.4688 [cond-mat.quant-gas]].
70. P. Massignan, G. M. Bruun, H. Smith, “Viscous relaxation and collective oscillations in a trapped Fermi gas near the unitarity limit”, *Phys. Rev. A* **71**, 033607 (2005) [cond-mat/0409660].
71. G. M. Bruun, H. Smith, “Viscosity and thermal relaxation for a resonantly interacting Fermi gas”, *Phys. Rev. A* **72**, 043605 (2005) [cond-mat/0504734].
72. M. J. H. Ku, A. T. Sommer, L. W. Cheuk, M. W. Zwierlein, “Revealing the Superfluid Lambda Transition in the Universal Thermodynamics of a Unitary Fermi Gas,” *Science* **335**, 563 (2012) [arXiv:1110.3309 [cond-mat.quant-gas]].
73. G. Rupak and T. Schäfer, “Shear viscosity of a superfluid Fermi gas in the unitarity limit,” *Phys. Rev. A* **76**, 053607 (2007) [arXiv:0707.1520 [cond-mat.other]].
74. T. Enss, R. Haussmann, and W. Zwerger, “Viscosity and scale invariance in the unitary Fermi gas,” *Annals Phys.* **326**, 770-796 (2011). [arXiv:1008.0007 [cond-mat.quant-gas]].
75. M. Braby, J. Chao and T. Schäfer, “Viscosity spectral functions of the dilute Fermi gas in kinetic theory,” *New J. Phys.* **13**, 035014 (2011) [arXiv:1012.0219 [cond-mat.quant-gas]].

76. E. Taylor and M. Randeria, “Viscosity of strongly interacting quantum fluids: spectral functions and sum rules,” *Phys. Rev.* **A81**, 053610 (2010). [arXiv:1002.0869 [cond-mat.quant-gas]].
77. S. Tan, “Large momentum part of fermions with large scattering length,” *Ann. Phys.* **323**, 2971 (2008).
78. J. Hofmann, “Current response, structure factor and hydrodynamic quantities of a two- and three-dimensional Fermi gas from the operator product expansion,” *Phys. Rev. A* **84**, 043603 (2011) [arXiv:1106.6035 [cond-mat.quant-gas]].
79. K. M. O’Hara, S. L. Hemmer, M. E. Gehm, S. R. Granade, J. E. Thomas, “Observation of a Strongly-Interacting Degenerate Fermi Gas of Atoms,” *Science* **298**, 2179 (2002) [cond-mat/0212463].
80. T. Schäfer and C. Chafin, “Scaling Flows and Dissipation in the Dilute Fermi Gas at Unitarity,” *Lect. Notes Phys.* **836**, 375 (2012) [arXiv:0912.4236 [cond-mat.quant-gas]].
81. C. Cao, E. Elliott, J. Joseph, H. Wu, J. Petricka, T. Schäfer and J. E. Thomas, “Universal Quantum Viscosity in a Unitary Fermi Gas,” *Science* **331**, 58 (2011) [arXiv:1007.2625 [cond-mat.quant-gas]].
82. “Collective oscillations of a trapped superfluid Fermi gas near a Feshbach resonance” S. Stringari, *Europhys. Lett.* **65**, 749 (2004) [cond-mat/0312614].
83. A. Bulgac and G. F. Bertsch, “Collective Oscillations of a Trapped Fermi Gas near the Unitary Limit,” *Phys. Rev. Lett.* **94**, 070401 (2005) [cond-mat/0404687].
84. J. Kinast, A. Turlapov, J. E. Thomas, “Breakdown of Hydrodynamics in the Radial Breathing Mode of a Strongly-Interacting Fermi Gas,” *Phys. Rev. A* **70**, 051401(R) (2004) [arXiv:cond-mat/0408634 [cond-mat.soft]].
85. M. Bartenstein, A. Altmeyer, S. Riedl, S. Jochim, C. Chin, J. Hecker Denschlag, and R. Grimm, “Collective Excitations of a Degenerate Gas at the BEC-BCS Crossover,” *Phys. Rev. Lett.* **92**, 203201 (2004) [cond-mat/0412712];
86. D. T. Son, “Vanishing bulk viscosities and conformal invariance of unitary Fermi gas,” *Phys. Rev. Lett.* **98**, 020604 (2007) [arXiv:cond-mat/0511721].
87. E. Elliott, J. A. Joseph, J. E. Thomas, “Observation of conformal symmetry breaking and scale invariance in expanding Fermi gases,” arXiv:1308.3162 [cond-mat.quant-gas].
88. T. Schäfer, “The Shear Viscosity to Entropy Density Ratio of Trapped Fermions in the Unitarity Limit,” *Phys. Rev. A* **76**, 063618 (2007) [arXiv:cond-mat/0701251].
89. A. Turlapov, J. Kinast, B. Clancy, L. Luo, J. Joseph, J. E. Thomas, “Is a Gas of Strongly Interacting Atomic Fermions a Nearly Perfect Fluid” *J. Low Temp. Phys.* **150**, 567 (2008) [arXiv:0707.2574].
90. G. M. Bruun, H. Smith, “Frequency and damping of the Scissors Mode of a Fermi gas”, *Phys. Rev. A* **76**, 045602 (2007) [arXiv:0709.1617].
91. K. Kajantie, M. Laine, K. Rummukainen and Y. Schroder, “The Pressure of hot QCD up to $g^6 \ln(1/g)$,” *Phys. Rev. D* **67**, 105008 (2003) [hep-ph/0211321].
92. J. P. Blaizot, E. Iancu and A. Rebhan, “Thermodynamics of the high-temperature quark gluon plasma”, in *Quark Gluon Plasma 3*, R. Hwa, X.-N. Wang, eds., (2003) [hep-ph/0303185].
93. E. Braaten and R. D. Pisarski, “Calculation of the gluon damping rate in hot QCD,” *Phys. Rev. D* **42**, 2156 (1990).
94. J. P. Blaizot and E. Iancu, “Ultrasoft amplitudes in hot QCD,” *Nucl. Phys. B* **570**, 326 (2000)

- [hep-ph/9906485].
95. G. Baym, H. Monien, C. J. Pethick and D. G. Ravenhall, “Transverse interactions and transport in relativistic quark - gluon and electromagnetic plasmas,” *Phys. Rev. Lett.* **64**, 1867 (1990).
 96. P. Arnold, G. D. Moore and L. G. Yaffe, “Transport coefficients in high temperature gauge theories. I: Leading-log results,” *JHEP* **0011**, 001 (2000) [arXiv:hep-ph/0010177].
 97. P. Arnold, G. D. Moore and L. G. Yaffe, “Transport coefficients in high temperature gauge theories. II: Beyond leading log,” *JHEP* **0305**, 051 (2003) [arXiv:hep-ph/0302165].
 98. Y. Aoki, Z. Fodor, S. D. Katz and K. K. Szabo, “The QCD transition temperature: Results with physical masses in the continuum limit,” *Phys. Lett. B* **643**, 46 (2006) [arXiv:hep-lat/0609068].
 99. A. Bazavov, T. Bhattacharya, M. Cheng, C. DeTar, H. T. Ding, S. Gottlieb, R. Gupta and P. Hegde *et al.*, “The chiral and deconfinement aspects of the QCD transition,” *Phys. Rev. D* **85**, 054503 (2012) [arXiv:1111.1710 [hep-lat]].
 100. M. Prakash, M. Prakash, R. Venugopalan and G. Welke, “Nonequilibrium properties of hadronic mixtures,” *Phys. Rept.* **227**, 321 (1993).
 101. P. Romatschke and D. T. Son, “Spectral sum rules for the quark-gluon plasma,” *Phys. Rev. D* **80**, 065021 (2009) [arXiv:0903.3946 [hep-ph]].
 102. G. Aarts and J. M. Martinez Resco, “Transport coefficients, spectral functions and the lattice,” *JHEP* **0204**, 053 (2002) [arXiv:hep-ph/0203177].
 103. Y. Zhu and A. Vuorinen, “The shear channel spectral function in hot Yang-Mills theory,” *JHEP* **1303**, 002 (2013) [arXiv:1212.3818 [hep-ph]].
 104. H. T. Ding, A. Francis, O. Kaczmarek, F. Karsch, E. Laermann and W. Soeldner, “Thermal dilepton rate and electrical conductivity: An analysis of vector current correlation functions in quenched lattice QCD,” *Phys. Rev. D* **83**, 034504 (2011) [arXiv:1012.4963 [hep-lat]].
 105. U. W. Heinz, “Early collective expansion: Relativistic hydrodynamics and the transport properties of QCD matter,” arXiv:0901.4355 [nucl-th].
 106. D. A. Teaney, “Viscous Hydrodynamics and the Quark Gluon Plasma,” arXiv:0905.2433 [nucl-th].
 107. J. Cleymans and H. Satz, “Thermal hadron production in high-energy heavy ion collisions,” *Z. Phys. C* **57**, 135 (1993) [hep-ph/9207204].
 108. P. Braun-Munzinger, J. Wambach, “Colloquium: Phase diagram of strongly interacting matter,” *Rev. Mod. Phys.* **81**, 1031-1050 (2009).
 109. E. Schnedermann, J. Sollfrank and U. W. Heinz, “Thermal phenomenology of hadrons from 200-A/GeV S+S collisions,” *Phys. Rev. C* **48**, 2462 (1993) [arXiv:nucl-th/9307020].
 110. J. -Y. Ollitrault, “Anisotropy as a signature of transverse collective flow,” *Phys. Rev. D* **46**, 229 (1992).
 111. B. Schenke, P. Tribedy and R. Venugopalan, “Fluctuating Glasma initial conditions and flow in heavy ion collisions,” *Phys. Rev. Lett.* **108**, 252301 (2012) [arXiv:1202.6646 [nucl-th]].
 112. D. Kharzeev and M. Nardi, “Hadron production in nuclear collisions at RHIC and high density QCD,” *Phys. Lett. B* **507**, 121 (2001) [nucl-th/0012025].
 113. S. S. Adler *et al.* [PHENIX Collaboration], “Elliptic flow of identified hadrons in Au + Au collisions at $s_{NN}^{1/2} = 200$ GeV,” *Phys. Rev. Lett.* **91**, 182301 (2003). [arXiv:nucl-ex/0305013].

114. J. Adams *et al.* [STAR Collaboration], “Azimuthal anisotropy in Au + Au collisions at $s_{NN}^{1/2} = 200\text{-GeV}$,” *Phys. Rev. C* **72**, 014904 (2005). [arXiv:nucl-ex/0409033].
115. K. Aamodt *et al.* [ALICE Collaboration], “Elliptic flow of charged particles in Pb-Pb collisions at 2.76 TeV,” *Phys. Rev. Lett.* **105**, 252302 (2010). [arXiv:1011.3914 [nucl-ex]].
116. B. Alver, G. Roland, “Collision geometry fluctuations and triangular flow in heavy-ion collisions,” *Phys. Rev. C* **81**, 054905 (2010) [arXiv:1003.0194 [nucl-th]].
117. B. Alver *et al.*, “Importance of correlations and fluctuations on the initial source eccentricity in high-energy nucleus-nucleus collisions,” *Phys. Rev. C* **77**, 014906 (2008) [arXiv:0711.3724 [nucl-ex]].
118. J. D. Bjorken, “Highly relativistic nucleus-nucleus collisions: The central rapidity region *Phys. Rev. D* **27**, 140 (1983).
119. S. S. Gubser and A. Yarom, “Conformal hydrodynamics in Minkowski and de Sitter spacetimes,” *Nucl. Phys. B* **846**, 469 (2011) [arXiv:1012.1314 [hep-th]].
120. G. Aad *et al.* [ATLAS Collaboration], “Measurement of the azimuthal anisotropy for charged particle production in $\sqrt{s_{NN}} = 2.76\text{ TeV}$ lead-lead collisions with the ATLAS detector,” *Phys. Rev. C* **86**, 014907 (2012) [arXiv:1203.3087 [hep-ex]].
121. C. Gale, S. Jeon, B. Schenke, P. Tribedy and R. Venugopalan, “Event-by-event anisotropic flow in heavy-ion collisions from combined Yang-Mills and viscous fluid dynamics,” *Phys. Rev. Lett.* **110**, 012302 (2013) [arXiv:1209.6330 [nucl-th]].
122. F. Cooper and G. Frye, “Comment on the Single Particle Distribution in the Hydrodynamic and Statistical Thermodynamic Models of Multiparticle Production,” *Phys. Rev. D* **10**, 186 (1974).
123. D. Teaney, “Effect of shear viscosity on spectra, elliptic flow, and Hanbury Brown-Twiss radii,” *Phys. Rev. C* **68**, 034913 (2003) [nucl-th/0301099].
124. U. Heinz and R. Snellings, “Collective flow and viscosity in relativistic heavy-ion collisions,” *Ann. Rev. Nucl. Part. Sci.* **63**, 123 (2013) [arXiv:1301.2826 [nucl-th]].
125. C. Gale, S. Jeon and B. Schenke, “Hydrodynamic Modeling of Heavy-Ion Collisions,” *Int. J. Mod. Phys. A* **28**, 1340011 (2013) [arXiv:1301.5893 [nucl-th]].
126. M. L. Miller, K. Reygers, S. J. Sanders and P. Steinberg, “Glauber modeling in high energy nuclear collisions,” *Ann. Rev. Nucl. Part. Sci.* **57**, 205 (2007) [arXiv:nucl-ex/0701025].
127. M. Martinez and M. Strickland, “Dissipative Dynamics of Highly Anisotropic Systems,” *Nucl. Phys. A* **848**, 183 (2010) [arXiv:1007.0889 [nucl-th]].
128. H. Petersen, J. Steinheimer, G. Burau, M. Bleicher and H. Stoecker, “A Fully Integrated Transport Approach to Heavy Ion Reactions with an Intermediate Hydrodynamic Stage,” *Phys. Rev. C* **78**, 044901 (2008) [arXiv:0806.1695 [nucl-th]].
129. W. van der Schee, P. Romatschke and S. Pratt, “A fully dynamical simulation of central nuclear collisions,” *Phys. Rev. Lett.* **111**, 222302 (2013) [arXiv:1307.2539 [nucl-th]].
130. P. Huovinen and P. Petreczky, “QCD Equation of State and Hadron Resonance Gas,” *Nucl. Phys. A* **837**, 26 (2010) [arXiv:0912.2541 [hep-ph]].
131. S. A. Bass and A. Dumitru, “Dynamics of hot bulk QCD matter: From the quark gluon plasma to hadronic freezeout,” *Phys. Rev. C* **61**, 064909 (2000) [nucl-th/0001033].
132. T. Hirano, U. W. Heinz, D. Kharzeev, R. Lacey and Y. Nara, “Hadronic dissipative ef-

- fects on elliptic flow in ultrarelativistic heavy-ion collisions,” *Phys. Lett. B* **636**, 299 (2006) [arXiv:nucl-th/0511046].
133. P. Romatschke and U. Romatschke, “Viscosity Information from Relativistic Nuclear Collisions: How Perfect is the Fluid Observed at RHIC?,” *Phys. Rev. Lett.* **99**, 172301 (2007) [arXiv:0706.1522 [nucl-th]].
134. K. Dusling and D. Teaney, “Simulating elliptic flow with viscous hydrodynamics,” *Phys. Rev. C* **77**, 034905 (2008) [arXiv:0710.5932 [nucl-th]].
135. H. Song and U. W. Heinz, “Causal viscous hydrodynamics in 2+1 dimensions for relativistic heavy-ion collisions,” *Phys. Rev. C* **77**, 064901 (2008) [arXiv:0712.3715 [nucl-th]].
136. H. Song, S. A. Bass and U. Heinz, “Elliptic flow in 200 A GeV Au+Au collisions and 2.76 A TeV Pb+Pb collisions: insights from viscous hydrodynamics + hadron cascade hybrid model,” *Phys. Rev. C* **83**, 054912 (2011) [Erratum-ibid. *C* **87**, 019902 (2013)] [arXiv:1103.2380 [nucl-th]].
137. M. Luzum and J. -Y. Ollitrault, “Extracting the shear viscosity of the quark-gluon plasma from flow in ultra-central heavy-ion collisions,” *Nucl. Phys. A* **904-905**, 377c (2013) [arXiv:1210.6010 [nucl-th]].
138. H. Song and U. W. Heinz, “Extracting the QGP viscosity from RHIC data – a status report from viscous hydrodynamics,” *J. Phys. G* **36**, 064033 (2009) [arXiv:0812.4274 [nucl-th]].
139. P. Huovinen, “Hydrodynamics at RHIC and LHC: What have we learned?,” *Int. J. Mod. Phys. E* **22**, 1330029 (2013) [arXiv:1311.1849 [nucl-th]].
140. E. Elliott, J. A. Joseph, J. E. Thomas, “Anomalous minimum in the shear viscosity of a Fermi gas,” arXiv:1311.2049 [cond-mat.quant-gas].
141. M. Mueller, J. Schmalian, L. Fritz, “Graphene - a nearly perfect fluid,” *Phys. Rev. Lett.* **103**, 025301 (2009) [arXiv:0903.4178 [cond-mat.mes-hall]].
142. H. Guo, D. Wulin, C.-C. Chien, K. Levin, “Perfect Fluids and Bad Metals: Transport Analogies Between Ultracold Fermi Gases and High T_c Superconductors,” *New J. Phys.* **13**, 075011 (2011) [arXiv:1009.4678 [cond-mat.supr-con]].
143. A. Kurkela and G. D. Moore, “Thermalization in Weakly Coupled Nonabelian Plasmas,” *JHEP* **1112**, 044 (2011) [arXiv:1107.5050 [hep-ph]].
144. D. E. Kharzeev, L. D. McLerran and H. J. Warringa, “The Effects of topological charge change in heavy ion collisions: Event by event P and CP violation,” *Nucl. Phys. A* **803**, 227 (2008) [arXiv:0711.0950 [hep-ph]].
145. D. E. Kharzeev and D. T. Son, “Testing the chiral magnetic and chiral vortical effects in heavy ion collisions,” *Phys. Rev. Lett.* **106**, 062301 (2011) [arXiv:1010.0038 [hep-ph]].
146. J. Erdmenger, M. Haack, M. Kaminski and A. Yarom, “Fluid dynamics of R-charged black holes,” *JHEP* **0901**, 055 (2009) [arXiv:0809.2488 [hep-th]].
147. D. T. Son and P. Surowka. Hydrodynamics with Triangle Anomalies. *Phys. Rev. Lett.* **103**, 191601 (2009) [arXiv:0906.5044 [hep-th]].
148. I. M. Khalatnikov, “Introduction to the Theory of Superfluidity”, W. A. Benjamin, Inc. (1965).
149. I. E. Dzyaloshinskii, G. E. Volovik, “Poisson brackets in condensed matter physics,” *Ann. Phys.* **125**, 67 (1980).
150. D. T. Son, “Hydrodynamics of nuclear matter in the chiral limit,” *Phys. Rev. Lett.* **84**, 3771 (2000) [hep-ph/9912267].

151. D. T. Son and M. A. Stephanov, “Real time pion propagation in finite temperature QCD,” *Phys. Rev. D* **66**, 076011 (2002) [hep-ph/0204226].
152. P. C. Hohenberg and B. I. Halperin, “Theory Of Dynamic Critical Phenomena,” *Rev. Mod. Phys.* **49**, 435 (1977).
153. D. T. Son and M. A. Stephanov, “Dynamic universality class of the QCD critical point,” *Phys. Rev. D* **70**, 056001 (2004) [arXiv:hep-ph/0401052].
154. L. D. Landau, E. M. Lifshitz, “Fluid Dynamics”, *Course of Theoretical Physics, Vol.VI*, Pergamon Press (1959).
155. H. Leutwyler, “Nonrelativistic effective Lagrangians,” *Phys. Rev. D* **49**, 3033 (1994) [hep-ph/9311264].
156. M. Greiter, F. Wilczek and E. Witten, “Hydrodynamic Relations in Superconductivity,” *Mod. Phys. Lett. B* **3**, 903 (1989).
157. D. T. Son, “Low-energy quantum effective action for relativistic superfluids,” hep-ph/0204199.
158. D. T. Son and M. Wingate, “General coordinate invariance and conformal invariance in non-relativistic physics: Unitary Fermi gas,” *Annals Phys.* **321**, 197 (2006) [cond-mat/0509786].
159. G. Rupak and T. Schäfer, “Density Functional Theory for non-relativistic Fermions in the Unitarity Limit,” *Nucl. Phys. A* **816**, 52 (2009) [arXiv:0804.2678 [nucl-th]].
160. P. C. Martin, E. D. Siggia and H. A. Rose, “Statistical Dynamics of Classical Systems,” *Phys. Rev. A* **8**, 423 (1973).
161. C. De Dominicis and L. Peliti, “Field Theory Renormalization and Critical Dynamics Above T_c : Helium, Antiferromagnets and Liquid Gas Systems,” *Phys. Rev. B* **18**, 353 (1978).
162. I. M. Khalatnikov, V. V. Lebedev and A. I. Sukhorukov, “Diagram Technique For Calculating Long Wave Fluctuation Effects,” *Phys. Lett. A* **94**, 271 (1983).
163. P. Kovtun, “Lectures on hydrodynamic fluctuations in relativistic theories,” *J. Phys. A* **45**, 473001 (2012) [arXiv:1205.5040 [hep-th]].
164. P. Kovtun, G. D. Moore and P. Romatschke, “Towards an effective action for relativistic dissipative hydrodynamics,” arXiv:1405.3967 [hep-ph].
165. K. Jensen, M. Kaminski, P. Kovtun, R. Meyer, A. Ritz and A. Yarom, “Towards hydrodynamics without an entropy current,” *Phys. Rev. Lett.* **109**, 101601 (2012) [arXiv:1203.3556 [hep-th]].
166. S. Dubovsky, L. Hui, A. Nicolis and D. T. Son, “Effective field theory for hydrodynamics: thermodynamics, and the derivative expansion,” *Phys. Rev. D* **85**, 085029 (2012) [arXiv:1107.0731 [hep-th]].
167. G. Torrieri, “Viscosity of An Ideal Relativistic Quantum Fluid: A Perturbative study,” *Phys. Rev. D* **85**, 065006 (2012) [arXiv:1112.4086 [hep-th]].
168. Y. He, K. Levin, “Establishing Conservation Laws in Pair Correlated Many Body theories: T matrix Approaches,” arXiv:1308.6793 [cond-mat.quant-gas].
169. S. Jeon and L. G. Yaffe, “From quantum field theory to hydrodynamics: Transport coefficients and effective kinetic theory,” *Phys. Rev. D* **53**, 5799 (1996) [hep-ph/9512263].
170. L. D. Landau, E. M. Lifshitz, “Physical Kinetics”, *Course of Theoretical Physics, Vol.X*, Pergamon Press (1981).
171. G. M. Bruun, H. Smith, “Shear viscosity and damping for a Fermi gas in the unitarity limit” *Phys. Rev. A* **75**, 043612 (2007) [cond-mat/0612460].

172. M. H. Ernst, “Bogoliubov Choh Uhlenbeck theory: Cradle of modern kinetic theory,” in: Progress in Statistical Physics, Proc. Int. Conf. on Statistical Physics in Memory of Prof. Soon-Tahk Choh, Seoul, Korea, World Scientific Publ. Co., Singapore, 1998. Eds. W. Sung et al. [arXiv:cond-mat/9707146 [cond-mat.stat-mech]].
173. S. Caron-Huot and G. D. Moore, “Heavy quark diffusion in QCD and N=4 SYM at next-to-leading order,” JHEP **0802**, 081 (2008) [arXiv:0801.2173 [hep-ph]].
174. G. S. Denicol, H. Niemi, E. Molnar and D. H. Rischke, “Derivation of transient relativistic fluid dynamics from the Boltzmann equation,” Phys. Rev. D **85**, 114047 (2012) [arXiv:1202.4551 [nucl-th]].
175. S. Weinberg, “Gravitation and Cosmology”, Wiley & Sons (1972).
176. G. D. Moore and K. A. Sohrabi, “Kubo Formulae for Second-Order Hydrodynamic Coefficients,” Phys. Rev. Lett. **106**, 122302 (2011) [arXiv:1007.5333 [hep-ph]].
177. C. Cercignani, G. M. Kremer, “The Relativistic Boltzmann Equation: Theory and Applications”, Birkhäuser Verlag (2002).
178. J. Hong and D. Teaney, “Spectral densities for hot QCD plasmas in a leading log approximation,” Phys. Rev. C **82**, 044908 (2010) [arXiv:1003.0699 [nucl-th]].
179. L. D. Landau, E. M. Lifshitz, “Statistical Mechanics, Part II”, Course of Theoretical Physics, Vol.IX, Pergamon Press (1981).
180. A. Buchel, J. T. Liu and A. O. Starinets, “Coupling constant dependence of the shear viscosity in N=4 supersymmetric Yang-Mills theory,” Nucl. Phys. B **707**, 56 (2005) [arXiv:hep-th/0406264].
181. A. Buchel, “Shear viscosity of boost invariant plasma at finite coupling,” Nucl. Phys. B **802**, 281 (2008) [arXiv:0801.4421 [hep-th]].
182. A. Buchel, “Resolving disagreement for η/s in a CFT plasma at finite coupling,” Nucl. Phys. B **803**, 166 (2008) [arXiv:0805.2683 [hep-th]].
183. R. C. Myers, M. F. Paulos and A. Sinha, “Quantum corrections to η/s ,” Phys. Rev. D **79**, 041901 (2009) [arXiv:0806.2156 [hep-th]].
184. S. C. Huot, S. Jeon and G. D. Moore, “Shear viscosity in weakly coupled N = 4 super Yang-Mills theory compared to QCD,” Phys. Rev. Lett. **98**, 172303 (2007) [arXiv:hep-ph/0608062].
185. P. Arnold, D. Vaman, C. Wu and W. Xiao, “Second order hydrodynamic coefficients from 3-point stress tensor correlators via AdS/CFT,” JHEP **1110**, 033 (2011) [arXiv:1105.4645 [hep-th]].
186. M. A. York and G. D. Moore, “Second order hydrodynamic coefficients from kinetic theory,” Phys. Rev. D **79**, 054011 (2009) [arXiv:0811.0729 [hep-ph]].
187. D. T. Son and A. O. Starinets, “Hydrodynamics of R-charged black holes,” JHEP **0603**, 052 (2006) [arXiv:hep-th/0601157].
188. A. Buchel, “Bulk viscosity of gauge theory plasma at strong coupling,” Phys. Lett. B **663**, 286 (2008) [arXiv:0708.3459 [hep-th]].
189. S. S. Gubser, S. S. Pufu and F. D. Rocha, “Bulk viscosity of strongly coupled plasmas with holographic duals,” JHEP **0808**, 085 (2008) [arXiv:0806.0407 [hep-th]].
190. O. DeWolfe, S. S. Gubser and C. Rosen, “Dynamic critical phenomena at a holographic critical point,” Phys. Rev. D **84**, 126014 (2011) [arXiv:1108.2029 [hep-th]].
191. P. K. Kovtun and A. O. Starinets, “Quasinormal modes and holography,” Phys. Rev. D **72**,

- 086009 (2005) [hep-th/0506184].
192. A. Nunez and A. O. Starinets, “AdS / CFT correspondence, quasinormal modes, and thermal correlators in N=4 SYM,” *Phys. Rev. D* **67**, 124013 (2003) [hep-th/0302026].
 193. J. Liao and V. Koch, “On the Fluidity and Super-Criticality of the QCD matter at RHIC,” *Phys. Rev. C* **81**, 014902 (2010) [arXiv:0909.3105 [hep-ph]].
 194. A. Adams, K. Balasubramanian and J. McGreevy, “Hot Spacetimes for Cold Atoms,” *JHEP* **0811**, 059 (2008) [arXiv:0807.1111 [hep-th]].
 195. C. P. Herzog, M. Rangamani and S. F. Ross, “Heating up Galilean holography,” *JHEP* **0811**, 080 (2008) [arXiv:0807.1099 [hep-th]].
 196. A. Cherman, T. D. Cohen and P. M. Hohler, “A Sticky business: The Status of the conjectured viscosity/entropy density bound,” *JHEP* **0802**, 026 (2008) [arXiv:0708.4201 [hep-th]].
 197. A. Dobado and F. J. Llanes-Estrada, “On the violation of the holographic viscosity versus entropy KSS bound in non relativistic systems,” *Eur. Phys. J. C* **51**, 913 (2007) [hep-th/0703132].
 198. D. T. Son, “Comment on ‘Is There a ‘Most Perfect Fluid’ Consistent with Quantum Field Theory?’,” *Phys. Rev. Lett.* **100**, 029101 (2008) [arXiv:0709.4651 [hep-th]].
 199. M. Braby, J. Chao and T. Schäfer, “Thermal Conductivity and Sound Attenuation in Dilute Atomic Fermi Gases,” *Phys. Rev. A* **82**, 033619 (2010) [arXiv:1003.2601 [cond-mat.quant-gas]].
 200. J. Joseph, B. Clancy, L. Luo, J. Kinast, A. Turlapov, J. E. Thomas, “Sound propagation in a Fermi gas near a Feshbach resonance,” *Phys. Rev. Lett.* **98**, 170401 (2007) [cond-mat/0612567].
 201. G. M. Bruun, “Spin diffusion in Fermi gases,” *New J. Phys.* **13**, 035005, (2011) [arXiv:1012.1607 [cond-mat.quant-gas]].
 202. A. Sommer, M. Ku, G. Roati, and M. W. Zwierlein. “Universal spin transport in a strongly interacting Fermi gas,” *Nature* **472**, 201 (2011) [arXiv:1103.2337v1 [cond-mat.quant-gas]]
 203. G. M. Bruun, C. J. Pethick, “Spin diffusion in trapped clouds of strongly interacting cold atoms,” *Phys. Rev. Lett.* **107**, 255302 (2011) [arXiv:1109.5709 [cond-mat.quant-gas]].
 204. T. Schäfer, “Second order fluid dynamics for the unitary Fermi gas from kinetic theory,” arXiv:1404.6843 [cond-mat.quant-gas].
 205. E. Braaten and L. Platter, “Exact Relations for a Strongly Interacting Fermi Gas from the Operator Product Expansion,” *Phys. Rev. Lett.* **100**, 205301 (2008) [arXiv:0803.1125 [cond-mat.other]].
 206. Y. Sagi, T. E. Drake, R. Paudel, D. S. Jin, “Measurement of the Homogeneous Contact of a Unitary Fermi Gas,” *Phys. Rev. Lett.* **109**, 220402 (2012) [arXiv:1208.2067 [cond-mat.quant-gas]].
 207. J. E. Drut, T. A. Lahde and T. Ten, “Momentum Distribution and Contact of the Unitary Fermi gas,” *Phys. Rev. Lett.* **106**, 205302 (2011) [arXiv:1012.5474 [cond-mat.stat-mech]].
 208. Z. Yu, G. M. Bruun, G. Baym, “Short-range correlations and entropy in ultracold atomic Fermi gases,” *Phys. Rev. A* **80**, 023615 (2009) [arXiv:0905.1836].
 209. E. Braaten, “Universal Relations for Fermions with Large Scattering Length,” *Lect. Notes Phys.* **836**, 193 (2012) [arXiv:1008.2922 [cond-mat.quant-gas]].
 210. D. T. Son, “Toward an AdS/cold atoms correspondence: a geometric realization of the Schroedinger symmetry,” *Phys. Rev. D* **78**, 046003 (2008) [arXiv:0804.3972 [hep-th]].

211. K. Balasubramanian and J. McGreevy, “Gravity duals for non-relativistic CFTs,” *Phys. Rev. Lett.* **101**, 061601 (2008) [arXiv:0804.4053 [hep-th]].
212. C. R. Hagen, “Scale and conformal transformations in galilean-covariant field theory,” *Phys. Rev. D* **5**, 377 (1972).
213. Y. Nishida and D. T. Son, “Nonrelativistic conformal field theories,” *Phys. Rev. D* **76**, 086004 (2007) [arXiv:0706.3746 [hep-th]].
214. J. Maldacena, D. Martelli and Y. Tachikawa, “Comments on string theory backgrounds with non-relativistic conformal symmetry,” *JHEP* **0810**, 072 (2008) [arXiv:0807.1100 [hep-th]].
215. M. Rangamani, S. F. Ross, D. T. Son and E. G. Thompson, “Conformal non-relativistic hydrodynamics from gravity,” *JHEP* **0901**, 075 (2009) [arXiv:0811.2049 [hep-th]].
216. S. Janiszewski and A. Karch, “String Theory Embeddings of Nonrelativistic Field Theories and Their Holographic Horava Gravity Duals,” *Phys. Rev. Lett.* **110**, 081601 (2013) [arXiv:1211.0010 [hep-th]].
217. S. Janiszewski, A. Karch, B. Robinson and D. Sommer, “Charged black holes in Horava gravity,” arXiv:1401.6479 [hep-th].
218. X. Bekaert, E. Meunier and S. Moroz, “Towards a gravity dual of the unitary Fermi gas,” *Phys. Rev. D* **85**, 106001 (2012) [arXiv:1111.1082 [hep-th]].
219. P. Nikolic and S. Sachdev, “Renormalization-group fixed points, universal phase diagram, and $1/N$ expansion for quantum liquids with interactions near the unitarity limit,” *Phys. Rev. A* **75**, 033608 (2007) [cond-mat/0609106 [cond-mat.supr-con]].
220. M. Y. Veillette, D. E. Sheehy, L. Radzihovsky, “Large- N expansion for unitary superfluid Fermi gases,” *Phys. Rev. A* **75**, 043614 (2007) [arXiv:cond-mat/0610798 [cond-mat.other]].
221. Y. Nishida, D. T. Son and S. Tan, “Universal Fermi Gas with Two- and Three-Body Resonances,” *Phys. Rev. Lett.* **100**, 090405 (2008) [arXiv:0711.1562 [cond-mat.other]].
222. T. Schäfer, “Dissipative fluid dynamics for the dilute Fermi gas at unitarity: Free expansion and rotation,” *Phys. Rev. A* **82**, 063629 (2010) [arXiv:1008.3876 [cond-mat.quant-gas]].
223. D. Guery-Odelin, F. Zambelli, J. Dalibard, and S. Stringari, “Collective oscillations of a classical gas confined in harmonic traps” *Phys. Rev. A* **60** 4851 (1999).
224. P. Pedri, D. Guery-Odelin and S. Stringari, “Dynamics of a classical gas including dissipative and mean-field effects” *Phys. Rev. A* **68** 043608 (2003) [cond-mat/0305624].
225. C. Menotti, P. Pedri, S. Stringari, “Expansion of an interacting Fermi gas,” *Phys. Rev. Lett.* **89**, 250402 (2002) [cond-mat/0208150].
226. K. Dusling and T. Schäfer, “Elliptic flow of the dilute Fermi gas: From kinetics to hydrodynamics,” *Phys. Rev. A* **84**, 013622 (2011) [arXiv:1103.4869 [cond-mat.stat-mech]].
227. J. Kinast, A. Turlapov, J. E. Thomas, “Two Transitions in the Damping of a Unitary Fermi Gas,” *Phys. Rev. Lett.* **94**, 170404 (2005) [cond-mat/0502507].
228. C. Cao, E. Elliott, H. Wu and J. E. Thomas, “Searching for Perfect Fluids: Quantum Viscosity in a Universal Fermi Gas,” *New J. Phys.* **13** (2011) 075007 [arXiv:1105.2496 [cond-mat.quant-gas]].
229. P. Arnold, C. Dogan and G. D. Moore, “The bulk viscosity of high-temperature QCD,” *Phys. Rev. D* **74**, 085021 (2006) [arXiv:hep-ph/0608012].
230. M. G. Alford, A. Schmitt, K. Rajagopal and T. Schäfer, “Color superconductivity in dense quark matter,” *Rev. Mod. Phys.* **80**, 1455 (2008) [arXiv:0709.4635 [hep-ph]].

231. B. Svetitsky, “Diffusion of charmed quark in the quark - gluon plasma,” *Phys. Rev. D* **37**, 2484 (1988).
232. G. D. Moore and D. Teaney, “How much do heavy quarks thermalize in a heavy ion collision?,” *Phys. Rev. C* **71**, 064904 (2005) [arXiv:hep-ph/0412346].
233. S. S. Gubser, “Symmetry constraints on generalizations of Bjorken flow,” *Phys. Rev. D* **82**, 085027 (2010) [arXiv:1006.0006 [hep-th]].
234. E. Shuryak, “The Cone, the Ridge and the Fate of the Initial State Fluctuations in Heavy Ion Collisions,” *Phys. Rev. C* **80**, 054908 (2009) [Erratum-ibid. *C* **80**, 069902 (2009)] arXiv:0903.3734 [nucl-th].
235. P. Staig, E. Shuryak, “The Fate of the Initial State Fluctuations in Heavy Ion Collisions: II. The Fluctuations and Sounds,” *Phys. Rev. C* **84**, 034908 (2011) [arXiv:1008.3139 [nucl-th]].
236. P. Staig and E. Shuryak, “The Fate of the Initial State Fluctuations in Heavy Ion Collisions: III. The Second Act of Hydrodynamics,” *Phys. Rev. C* **84**, 044912 (2011) [arXiv:1105.0676 [nucl-th]].
237. J. I. Kapusta, B. Muller and M. Stephanov, “Relativistic Theory of Hydrodynamic Fluctuations with Applications to Heavy Ion Collisions,” *Phys. Rev. C* **85**, 054906 (2012) [arXiv:1112.6405 [nucl-th]].
238. A. Mocsy and P. Sorensen, “Analyzing the Power Spectrum of the Little Bangs,” *Nucl. Phys. A* **855**, 241 (2011) [arXiv:1101.1926 [hep-ph]].
239. R. A. Lacey, A. Taranenko, J. Jia, D. Reynolds, N. N. Ajitanand, J. M. Alexander, Y. Gu and A. Mwai, “Beam energy dependence of the viscous damping of anisotropic flow,” arXiv:1305.3341 [nucl-ex].
240. F. G. Gardim, F. Grassi, M. Luzum and J. -Y. Ollitrault, “Mapping the hydrodynamic response to the initial geometry in heavy-ion collisions,” *Phys. Rev. C* **85**, 024908 (2012) [arXiv:1111.6538 [nucl-th]].
241. D. Teaney and L. Yan, “Non linearities in the harmonic spectrum of heavy ion collisions with ideal and viscous hydrodynamics,” *Phys. Rev. C* **86**, 044908 (2012) [arXiv:1206.1905 [nucl-th]].
242. S. Floerchinger, U. A. Wiedemann, A. Beraudo, L. Del Zanna, G. Inghirami and V. Rolando, “How (non-) linear is the hydrodynamics of heavy ion collisions?,” arXiv:1312.5482 [hep-ph].
243. J. P. Blaizot and A. H. Mueller, “The Early Stage of Ultrarelativistic Heavy Ion Collisions,” *Nucl. Phys. B* **289**, 847 (1987).
244. R. Baier, A. H. Mueller, D. Schiff and D. T. Son, “‘Bottom up’ thermalization in heavy ion collisions,” *Phys. Lett. B* **502**, 51 (2001) [hep-ph/0009237].
245. J. Casalderrey-Solana, M. P. Heller, D. Mateos and W. van der Schee, “From full stopping to transparency in a holographic model of heavy ion collisions,” *Phys. Rev. Lett.* **111**, 181601 (2013) [arXiv:1305.4919 [hep-th]].
246. S. S. Gubser, “Complex deformations of Bjorken flow,” *Phys. Rev. C* **87**, 014909 (2013) [arXiv:1210.4181 [hep-th]].
247. P. F. Kolb, P. Huovinen, U. W. Heinz and H. Heiselberg, “Elliptic flow at SPS and RHIC: From kinetic transport to hydrodynamics,” *Phys. Lett. B* **500**, 232 (2001) [arXiv:hep-ph/0012137].
248. D. Molnar and M. Gyulassy, “Saturation of elliptic flow and the transport opacity of the gluon plasma at RHIC,” *Nucl. Phys. A* **697**, 495 (2002) [Erratum-ibid. *A* **703**, 893 (2002)]

- [nucl-th/0104073].
249. Z. Xu and C. Greiner, “Thermalization of gluons in ultrarelativistic heavy ion collisions by including three-body interactions in a parton cascade,” *Phys. Rev. C* **71**, 064901 (2005) [hep-ph/0406278].
250. Z. Xu, C. Greiner and H. Stoecker, “PQCD calculations of elliptic flow and shear viscosity at RHIC,” *Phys. Rev. Lett.* **101**, 082302 (2008) [arXiv:0711.0961 [nucl-th]].
251. J.-W. Chen, J. Deng, H. Dong and Q. Wang, “Shear and Bulk Viscosities of a Gluon Plasma in Perturbative QCD: Comparison of Different Treatments for the $gg \leftrightarrow ggg$ Process,” *Phys. Rev. C* **87**, 024910 (2013) [arXiv:1107.0522 [hep-ph]].
252. O. Fochler, J. Uphoff, Z. Xu and C. Greiner, “Radiative parton processes in perturbative QCD: An improved version of the Gunion and Bertsch cross section from comparisons to the exact result,” *Phys. Rev. D* **88**, 014018 (2013) [arXiv:1302.5250 [hep-ph]].
253. W. Florkowski and R. Ryblewski, “Highly-anisotropic and strongly-dissipative hydrodynamics for early stages of relativistic heavy-ion collisions,” *Phys. Rev. C* **83**, 034907 (2011) [arXiv:1007.0130 [nucl-th]].
254. M. Martinez and M. Strickland, “Dissipative Dynamics of Highly Anisotropic Systems,” *Nucl. Phys. A* **848**, 183 (2010) [arXiv:1007.0889 [nucl-th]].
255. P. Romatschke, M. Mendoza and S. Succi, “A fully relativistic lattice Boltzmann algorithm,” *Phys. Rev. C* **84**, 034903 (2011) [arXiv:1106.1093 [nucl-th]].
256. P. Romatschke, “Relativistic (Lattice) Boltzmann Equation with Non-Ideal Equation of State,” *Phys. Rev. D* **85**, 065012 (2012) [arXiv:1108.5561 [gr-qc]].
257. C. Shen and U. Heinz, “Collision Energy Dependence of Viscous Hydrodynamic Flow in Relativistic Heavy-Ion Collisions,” *Phys. Rev. C* **85**, 054902 (2012) [Erratum-ibid. *C* **86**, 049903 (2012)] [arXiv:1202.6620 [nucl-th]].
258. H. Heiselberg and A.-M. Levy, “Elliptic flow and HBT in noncentral nuclear collisions,” *Phys. Rev. C* **59**, 2716 (1999) [nucl-th/9812034].
259. R. S. Bhalerao, J.-P. Blaizot, N. Borghini and J.-Y. Ollitrault, “Elliptic flow and incomplete equilibration at RHIC,” *Phys. Lett. B* **627**, 49 (2005) [nucl-th/0508009].
260. S. A. Voloshin and A. M. Poskanzer, “The Physics of the centrality dependence of elliptic flow,” *Phys. Lett. B* **474**, 27 (2000) [nucl-th/9906075].
261. C. Alt *et al.* [NA49 Collaboration], “Directed and elliptic flow of charged pions and protons in Pb + Pb collisions at 40-A-GeV and 158-A-GeV,” *Phys. Rev. C* **68**, 034903 (2003) [nucl-ex/0303001].
262. G. Basar and D. Teaney, “A scaling relation between pA and AA collisions,” arXiv:1312.6770 [nucl-th].
263. X.-N. Wang and M. Gyulassy, “HIJING: A Monte Carlo model for multiple jet production in pp, pA and AA collisions,” *Phys. Rev. D* **44**, 3501 (1991).
264. K. Geiger and B. Muller, “Dynamics of parton cascades in highly relativistic nuclear collisions,” *Nucl. Phys. B* **369**, 600 (1992).
265. D. H. Rischke, “Fluid dynamics for relativistic nuclear collisions,” In “Cape Town 1998, Hadrons in dense matter and hadrosynthesis” 21-70 [nucl-th/9809044].
266. A. Muronga, “Second order dissipative fluid dynamics for ultrarelativistic nuclear collisions,” *Phys. Rev. Lett.* **88**, 062302 (2002) [Erratum-ibid. **89**, 159901 (2002)] [nucl-th/0104064].

267. U. W. Heinz, H. Song and A. K. Chaudhuri, “Dissipative hydrodynamics for viscous relativistic fluids,” *Phys. Rev. C* **73**, 034904 (2006) [nucl-th/0510014].
268. H. Song and U. W. Heinz, “Suppression of elliptic flow in a minimally viscous quark-gluon plasma,” *Phys. Lett. B* **658**, 279 (2008) [arXiv:0709.0742 [nucl-th]].
269. H. Song and U. W. Heinz, “Multiplicity scaling in ideal and viscous hydrodynamics,” *Phys. Rev. C* **78**, 024902 (2008) [arXiv:0805.1756 [nucl-th]].
270. M. P. Heller and R. A. Janik, “Viscous hydrodynamics relaxation time from AdS/CFT,” *Phys. Rev. D* **76**, 025027 (2007) [hep-th/0703243 [HEP-TH]].
271. R. Baier, A. H. Mueller, D. Schiff and D. T. Son, “Does parton saturation at high density explain hadron multiplicities at LHC?,” arXiv:1103.1259 [nucl-th].
272. R. P. Geroch and L. Lindblom, “Dissipative relativistic fluid theories of divergence type,” *Phys. Rev. D* **41**, 1855 (1990).
273. H. C. Öttinger, “Relativistic and nonrelativistic description of fluids with anisotropic heat conduction,” *Physica A* **254** 433 (1998).
274. M. Luzum and P. Romatschke, “Conformal Relativistic Viscous Hydrodynamics: Applications to RHIC results at $s_{NN}^{1/2} = 200$ GeV,” *Phys. Rev. C* **78**, 034915 (2008) [arXiv:0804.4015 [nucl-th]].
275. S. Chatrchyan *et al.* [CMS Collaboration], “Measurement of the elliptic anisotropy of charged particles produced in PbPb collisions at nucleon-nucleon center-of-mass energy = 2.76 TeV,” *Phys. Rev. C* **87**, 014902 (2013) [arXiv:1204.1409 [nucl-ex]].
276. L. Adamczyk *et al.* [STAR Collaboration], “Inclusive charged hadron elliptic flow in Au + Au collisions at $\sqrt{s_{NN}} = 7.7 - 39$ GeV,” *Phys. Rev. C* **86**, 054908 (2012) [arXiv:1206.5528 [nucl-ex]].
277. A. Adare *et al.* [PHENIX Collaboration], “Observation of direct-photon collective flow in $\sqrt{s_{NN}} = 200$ GeV Au+Au collisions,” *Phys. Rev. Lett.* **109**, 122302 (2012) [arXiv:1105.4126 [nucl-ex]].
278. D. Lohner [ALICE Collaboration], “Measurement of Direct-Photon Elliptic Flow in Pb-Pb Collisions at $\sqrt{s_{NN}} = 2.76$ TeV,” *J. Phys. Conf. Ser.* **446**, 012028 (2013) [arXiv:1212.3995 [hep-ex]].
279. R. Chatterjee, E. S. Frodermann, U. W. Heinz and D. K. Srivastava, “Elliptic flow of thermal photons in relativistic nuclear collisions,” *Phys. Rev. Lett.* **96**, 202302 (2006) [nucl-th/0511079].
280. S. Chatrchyan *et al.* [CMS Collaboration], “Multiplicity and transverse momentum dependence of two- and four-particle correlations in pPb and PbPb collisions,” *Phys. Lett. B* **724**, 213 (2013) [arXiv:1305.0609 [nucl-ex]].
281. G. Aad *et al.* [ATLAS Collaboration], “Measurement with the ATLAS detector of multi-particle azimuthal correlations in p+Pb collisions at $\sqrt{s_{NN}}=5.02$ TeV,” *Phys. Lett. B* **725**, 60 (2013) [arXiv:1303.2084 [hep-ex]].
282. B. B. Abelev *et al.* [ALICE Collaboration], “Long-range angular correlations of pi, K and p in p-Pb collisions at $\sqrt{s_{NN}} = 5.02$ TeV,” *Phys. Lett. B* **726**, 164 (2013) [arXiv:1307.3237 [nucl-ex]].
283. K. Dusling and R. Venugopalan, “Comparison of the color glass condensate to dihadron correlations in proton-proton and proton-nucleus collisions,” *Phys. Rev. D* **87**, 094034 (2013)

[arXiv:1302.7018 [hep-ph]].

284. L. McLerran, M. Praszalowicz and B. Schenke, “Transverse Momentum of Protons, Pions and Kaons in High Multiplicity pp and pA Collisions: Evidence for the Color Glass Condensate?,” Nucl. Phys. A **916**, 210 (2013) [arXiv:1306.2350 [hep-ph]].